Understanding the Inflammatory Mechanisms That Predispose to Emphysema In Mouse Models

Chuan En Eric Lam

B.BioMed Sc (Hons)

Submitted for the degree of

DOCTOR of PHILOSOPHY

Discipline of Immunology and Microbiology
School of Biomedical Sciences and Pharmacy
Faculty of Health
Priority Research Centre for Asthma and Respiratory Disease
The University of Newcastle
Australia

April 2011

Statement of Originality

This thesis contains no material which has been accepted for the award of any other degree or diploma in any university or other tertiary institution and, to the best of my knowledge and belief, contains no material previously published or written by another person, except where due reference has been made in the text. I give consent to this copy of my thesis, when deposited in the University Library, being made available for loan and photocopying subject to the provisions of the Copyright Act 1968.

I hereby certify that the work embodied in this thesis has been done in collaboration with other researchers, or carried out in other institutions. I have included as part of the thesis a statement clearly outlining the extent of collaboration, with whom and under what auspices. This statement can be found on Page III.

Eric Chuan En Lam

_____

April 2011

List of Collaborative Work

This section officially acknowledges the contribution from our collaborators.

Collaborator	Collaboration
A/Prof Philip Hansbro (UoN)	Supply of Non-Typeable *Haemophilus influenzae* for the investigations carried out in Chapters 3 and 4
Ms. Ama-Tawiah Essilfie (UoN)	Preparation of stock *Haemophilus influenzae* for infection of mice and bacterial recovery.
Dr. Jodie Simpson (HMRI)	Determining chemerin levels in sputum (comparing between Health and COPD subjects) and anaylsying results for Figure 4-23 in Chapter 4.

Acknowledgements

I would like to thank my supervisors Dr. Simon Phipps and Prof. Paul Foster for their guidance and support over the last 5 years, as well as the opportunity to undertake this PhD. I would also like to extend my sincere gratitude to Dr. Nicole Hansbro for proofreading the thesis. Special thanks to Adeline for the many great discussions into some of the experimental techniques and great lab mate all round. I would also like to thank all past and present members from the Foster laboratory, who had assisted in one way or another, making this journey a memorable one.

I would like to thank Anne Prins (ANU) and all staff members from the Animal Services Unit (UoN) for the support over the years. I would also like to thank our collaborators A/Prof. Philip Hansbro (UoN) and Ama-Tawiah Essilfie (UoN) for providing the *Haemophilus influenzae* and bacterial recovery work respectively, as well as Dr. Jodie Simpson (HMRI) for supplying the human chemerin data.

I would also like to acknowledge funding support from the University of Newcastle and Cooperative Research Centre for Asthma and Airways for the project.

Last but not least, a huge thank you to my parents, especially my dad for the huge support, encouragement, and funding to see me through this journey. Thank you!

Table of Contents

Abstract

Chronic obstructive pulmonary disease (COPD) is a growing global health problem, and this disorder is projected to rank fifth by 2020 as a worldwide burden of disease (Murray and Lopez., 1996). Remarkably, little is known about the pathogenesis of COPD and current pharmacologic agents fail to halt disease progression. Emphysema is a major inflammatory disorder that falls under the clinical description of COPD. Emphysema can be induced by smoking but can also occur in non-smokers. Emerging data suggests that the loss of alveolar tissue which characterises emphysema may result from increased cell death (apoptosis) of alveolar epithelial cells mediated by the sphingolipid mediator ceramide (Petrache *et al.*, 2005). The cause of COPD exacerbations are commonly bacterial or viral respiratory infections. Under certain conditions, immunity from infection is mediated through the initiation of apoptotic pathways by infected cells to prevent the pathogen from replicating within the host. Toll-like receptors (TLRs) recognise molecular patterns expressed by pathogens such as bacteria and viruses to initiate innate immune responses. Notably, significant amounts of the bacterial wall component lipopolysaccharide (LPS) are found in cigarette smoke. LPS is a TLR4 ligand that increases the level of the apoptotic mediator ceramide and production of proinflammatory cytokines (such as tumour necrosis factor (TNF)–α, interleukin (IL)-1β, and IL-6) implicated in the pathogenesis of emphysema. We hypothesise that chronic inhalation of LPS leads to the dysregulation of TLR4 signalling pathways that increases susceptibility to

respiratory infection, and uncontrolled inflammation that promotes alveolar cell apoptosis and emphysematous-like lesions. We developed mouse models of LPS- and bacterial-induced emphysema to determine if attenuating inflammation can prevent the development of emphysema.

Our results demonstrate that exposure to LPS or infection with Non-typeable *Haemophilus influenzae* (NTHi) (often found in patients with emphysema) can induce hallmark features of emphysema, such as alveolar enlargement (determined by mean linear intercept and percentage alveolar airspace measurements) and inflammation dominated by neutrophils and macrophages. We demonstrated that alveolar enlargement was due to the loss of alveolar parenchyma (from apoptosis), is dependent on TLR4 and myeloid differentiation factor-88 (MyD88), increased proinflammatory cytokines, chemokines, and inflammatory cells (neutrophils and macrophages) in the lung. Prophylactic administration of synthesised chemerin-derived peptide (C15) attenuated LPS- or NTHi-induced inflammation, which resulted in inhibition of the development of emphysematous-like lesions. Notably, specific depletion of alveolar macrophages protects mice from LPS- or NTHi-induced emphysema.

Collectively, we demonstrate that blocking inflammation during the development of emphysema is critical for preventing or attenuating the progression of the disease.

List of Abbreviations

AA	Amino acid
ALF	Australian Lung Foundation
APAAP	Mouse Alkaline-Phosphatase anti-Alkaline-Phosphatase
Apaf-1	Apoptotic protease activating factor-1
APCs	Antigen presenting cells
ASmase	Acid Sphingomyelinase
CAD	Caspase-activated DNAse
CCRL2	Chemokine (CC motif) receptor-like 2
cDNA	complementary DNA
CKRX	Chemokine Receptor X
CMKLR1	Chemokine-like receptor 1
COPD	Chronic obstructive pulmonary disease
2CA	2-Chloroadenosine
ECM	Extracellular matrix
E.coli	Escherichia coli
EtOH	Ethanol
FCS	Fetal Calf Serum
FEV_1	Forced expiratory volume in one second
FVC	Forced vital capacity
GOLD	Global initiative for Chronic Obstructive Lung Disease
GPCR	Protein-coupled receptors
H.influenzae	*Haemophilus influenzae*
HKR	Human chemokine receptor
HMGB-1	High-mobility group protein B1
HMRI	Hunter Medical and Research Institute
IRFs	Interferon regulatory factors
IVC	Individually ventilated cages
LASS	Dihydroceramid Synthases
L-CCR	LPS-inducible C-C chemokine receptor related gene
LOS	Lipooligosaccharides
LPS	Lipopolysaccharide
MAL	MyD88 adaptor-like
MiP-1α	Macrophage inflammatory Protein – 1 -alpha
MLI	Mean linear intercepts
MMP-9	Matrix metallopeptidase 9
MMP-12	Macrophage Elastase
mRNA	messenger RNA
$MyD88^{-/-}$	MyD88-deficient
MyD88	Myeloid-Differentiating factor 88
NADPH	reduced Nicotinamide adenine dinucleotide phosphate
NCdase	Neutral Ceramidase
NGS	Normal Goat Serum
NHLBI	National Heart, Lung, and Blood Institute

NLRs	NOD-like receptors
Nox-3	NADPH oxidase 3
NTHi	Non-typeable Haemophilus influenzae
PAMPs	Pathogen-associated molecular patterns
PBS	Phosphate Buffered Saline
PFA	Paraformaldehyde
% alveolar airspace (%AA)	percentage alveolar airspace
qPCR	quantitative real-time PCR
RARRES2	Retinoic acid receptor responder 2
RSV	Respiratory Syncytial Virus
SARM	Sterile α and armadillo motif-containing protein
SMases	Sphingomyelinases
SMS	Sphingomyelinase Synthase
SP	Scrambled Peptide
S. pneumoniae	*Streptococus pneumoniae*
S1-P	Sphingosine-1-phosphate
Tg	Transgenic
TIG2	tazzarotene induced gene 2
TIR	Toll-IL-1 receptor
TLR	Toll-like receptor
TLR4$^{-/-}$	TLR4 deficient
TNF-α	Tumour necrosis factor-alpha
TRAIL	TNF-related apoptosis inducing ligand
TRAM	TRIF-related adaptor molecule
TRIF	TIR domain-containing adaptor inducing interferon-β
TSANZ	The Thoracic Society of Australia and New Zealand
VEGF	Vascular Endothelial Growth Factor
WHO	World Health Organisation
WT	Wild type

Chapter 1

Introduction

Chapter 1: Introduction

1.1 Chronic Obstructive Pulmonary Disease

Chronic obstructive pulmonary disease (COPD) is a chronic inflammatory disorder characterised by progressive and irreversible airway obstruction (Murray and Lopez., 1996; Saetta *et al.*, 2001). It is a long-term condition and a major cause of death with worldwide prevalence. In 1990, the World Health Organisation (WHO) ranked COPD as the twelfth biggest worldwide burden of disease and predicted that by 2020 it would rank fifth. COPD is already the fourth leading cause of chronic morbidity and mortality in the United States and according to the Australian Lung Foundation (ALF) and The Thoracic Society of Australia and New Zealand (TSANZ), COPD is the fourth largest cause of death in Australia. In a concerted worldwide effort, the Global initiative for Chronic Obstructive Lung Disease (GOLD), a collaboration between the US National Heart, Lung, and Blood Institute (NHLBI) and the World Health Organisation (WHO) was established to increase awareness of COPD and to decrease morbidity and mortality from the disease.

GOLD has classified COPD into four main stages of severity as shown in **Table 1-1** (GOLD, 2005) based on patient lung function. The diagnosis of COPD is considered in any patient showing symptoms of cough, high sputum production, or dyspnea, and/or a history of exposure to the known risk factors for COPD. The diagnosis is confirmed by spirometry, which includes measurements of forced

expiratory volume in one second (FEV_1) and forced vital capacity (FVC). As the severity of COPD increases, FEV_1 falls rapidly, indicating a loss in lung function. In mild cases (lower stages), coughing or breathlessness may be the only symptoms. In most cases, the patient may not even be aware that his or her lung function is compromised. COPD is a progressive and irreversible disease and therefore the severity of disease increases overtime. When the severity reaches stage II, shortness of breath can occur from moderate daily chores, with frequent coughing and recurrent chest infections. At this stage, the quality of life is lowered and individuals start to seek medical advice. In severe cases, breathing becomes so impaired that exacerbations can be fatal.

As a growing global health problem, COPD has become a significant cause of chronic disability, with hospital admissions and loss of time from work, resulting in economical and social burden. COPD patients have an increased susceptibility to exacerbations from bacterial and/or viral infections, leading to systemic inflammation. The loss of skeletal muscles and hence lean body mass through COPD is a cause of functional impairment and thus recognised as a major co-morbidity of COPD (Hansen *et al.*, 2006). Other related co-morbidities stemming from COPD include weight loss and depression (ZuWallack *et al.*, 2005; Hansen *et al.*, 2006). So detrimental are these secondary symptoms that death is frequently associated with their presentation rather than the pathology of COPD.

Risk factors associated with COPD include host factors and exposure to environmental stimuli. Host factors, however, such as genetic predispositions (e.g. hereditary deficiency of alpha-1 antitrypsin (Shapiro and Ingenito, 2005), airway hyperresponsiveness (asthma patients), and abnormal lung growth are rare. The more common risk factors include tobacco smoke, occupational dust and chemicals (particulate matter, irritants and organic dust), indoor and outdoor air pollutants, respiratory infections from bacteria and viruses during childhood, and socioeconomic status (overcrowding and poor nutrition). The single biggest risk factor however, is exposure to cigarette smoke.

Table 1-1: GOLD Classification of severity of chronic obstructive pulmonary disease.

Stage	Characteristics
0: At risk	• Normal spirometry • Chronic symptoms (cough, sputum production)
I: Mild COPD	• $FEV_1/FVC < 70\%$ • $FEV_1 \geq 80\%$ predicted • With or without chronic symptoms (cough, sputum production)
II: Moderate COPD	• $FEV_1/FVC < 70\%$ • $50\% \leq FEV_1 < 80\%$ predicted • With or without chronic symptoms (cough, sputum production)
III: Severe COPD	• $FEV_1/FVC < 70\%$ • $30\% \leq FEV_1 < 50\%$ predicted • With or without chronic symptoms (cough, sputum production)
IV: Very Severe COPD	• $FEV_1/FVC < 70\%$ • $FEV_1 < 30\%$ predicted or $FEV_1 < 50\%$ predicted plus chronic respiratory failure

Table 1 taken from GOLD's 2005 executive summary (http://www.goldcopd.com).

1.1.1 Emphysema

Emphysema is characterised by chronic inflammation and destruction of the respiratory bronchioles and walls of the alveoli (Hogg *et al.*, 2004). The destruction of the alveolar walls results in the honeycomb-like structure of the lung parenchyma being replaced with larger "air sacs" (**Figure 1-0**). The enlargement of the air sacs results in decreased surface area for gaseous exchange in the lungs and gives rise to poor lung function characterised by airflow obstruction and impaired elastic recoil (Daheshia, 2005).

For copyright considerations, this image was not included.
Image was sourced from:
Cross-Sectional analysis of the utility of pulmonary function tests in predicting emphysema in ever-smokers.
Sean E. Hesselbacher *et al.* (2011). Int. J. Environ. Res. Public Health. 8(5):1324-1340
Figure 3 – Images A and B.

Figure 1-0: Aadapted from Sean et al (2011) compares the difference in quantitated alveolar airspace between healthy control (1% airspace) and patient with severe emphysema (40% airspace). (Sean E. Hesselbacher *et al.*, 2011)

Emphysema is progressive, irreversible, and the prognosis is poor. Diagnosis usually occurs in adults over the age of 40, when the disease is moderately advanced and the damage irreparable. Emphysema patients are rendered more susceptible to develop severe secondary symptoms such as smooth muscle hypertrophy, fibrosis and thickening of the airway wall (O'Byrne P and Postma, 1999; Saetta *et al.*, 2001). Greater than 90% of patients with emphysema have a history of smoking.

Current therapies only partially relieve the symptoms for sufferers and are without effect on disease progression. Treatments include the use of bronchodilators, glucocorticosteroids, oxygen treatment, genetic augmentation, antibiotics against secondary infections, or surgical treatments. With no therapy yet able to slow the relentless progression of emphysema, the identification of an early marker(s) of disease to aid diagnosis before it becomes clinically apparent is urgently required, in a bid to increase development of pro-active measures to prevent disease development.

1.1.2 The Inflammatory response

In emphysematous lungs, the accumulation of inflammatory mucous exudates in the airway is significantly higher than those in normal lungs (Hogg *et al.*, 2004). Cellular aggregates in the airway wall i.e. separate from the alveoli (parenchyma) were shown to be composed of polymorphonuclear neutrophils, macrophages, CD4+ T cells, CD8+ T cells and B cells. Increasing numbers of these cells in the parenchyma were associated with disease progression (Jeffery, 1998; Hogg *et al.*, 2004). The volume of the tissue in the airway wall was also observed to increase with increasing severity of disease, which may be the result of localised fibrosis. Intriguingly, organised follicles along the bronchioles were observed in patients in stages III (severe) and IV (very severe) of the disease. These follicles are lymphoid-like structures that contain lymphocytes including B cells, T cells and dendritic cells (Hogg *et al.*, 2004). One possibility is that these

structures are formed in response to the colonisation of various pathogens in the lungs. The presence of these follicles suggests that the adaptive immune response is an active participant in the inflammatory response present in the lungs of emphysema patients, but whether this is beneficial or detrimental to the host has yet to be explored.

1.1.2.1 TNF-α

Activated inflammatory cells in the lungs of COPD patients can release a myriad of mediators that have been implicated in the pathogenesis of emphysema. Activated CD8+ T cells are potent producers of tumour necrosis factor-alpha (TNF-α) which has been associated with emphysema pathology (Keatings *et al.*, 1996), and co-morbidities (Hansen *et al.*, 2006). TNF-α is an inflammatory mediator with a number of diverse effects, which include maturation of dendritic cells, regulation of inflammatory cell influx and induction of cell death. In mice, the over-expression of TNF-α in the T cell compartment has been demonstrated to induce alterations in lymphoid tissue and a lethal wasting syndrome (Hogg *et al.*, 2004; Hansen *et al.*, 2006). The selective over-expression of TNF-α in the mouse lung (using the epithelial promoter surfactant protein C) induced lung neutrophilia, airspace enlargement (increased alveolar diameter) and significantly, the development of new lymphoid tissue populated by B cells (Vuillemenot *et al.*, 2004). Indeed, the Peyer's Patches (lymph node-like structures just beneath the gut epithelium) of mice deficient in the 55 kDa

receptor for TNF-α have also been shown to lack organisation. Thus, TNF-α may be responsible for the formation of the follicles observed in patients with emphysema.

The production and release of TNF-α can be induced from macrophages following exposure to lipopolysaccharide (LPS), a constituent part of the cell wall of gram negative bacteria. Notably, LPS is present in high concentrations in cigarette smoke (120 ng/cigarette) (Hasday *et al.*, 1999) and repeated administration to the lungs of mice induces an inflammatory response with the development of emphysematous-like lesions in hamsters, rats and mice (Vernooy *et al.*, 2002). Significantly, LPS has also been shown to increase the intracellular production of ceramide (Claycombe *et al.*, 2002; Kumar Mangalam *et al.*, 2002), a signalling molecule in the apoptotic pathway. However, while the proinflammatory properties of LPS are well documented, it is only relatively recently that the receptor by which it is recognised has been identified.

1.2 Toll-like receptors

In Drosophila, Toll protein has two known functions. It is responsible for specifying dorsoventral polarity during embryonic development, and providing anti-fungal defense during adulthood (Kambris *et al.*, 2002; Imler and Zheng, 2004). Thus, Toll is known to have a role in innate immunity. In the late 1990s, the understanding of the mammalian innate immune system was significantly advanced through the identification and cloning of the first mammalian homolog

of the gene that encodes drosophila Toll protein, toll-like receptor 4 (TLR). TLR4 was found to activate the NF-κB pathway and initiate an adaptive immune response (Medzhitov *et al.*, 1997). Genetic mapping then identified TLR4 as the receptor for LPS (Poltorak *et al.*, 1998). TLR4 is now known as one of a family of evolutionary conserved receptors that recognise molecular patterns associated with microbes. To date, eleven TLRs have been identified in humans and thirteen in mice, each with different specificities to conserved molecular patterns of microbial products termed pathogen-associated molecular patterns (PAMPs; see Table 1-2) (Nagase *et al.*, 2003; Akira and K., 2004; Diebold SS *et al.*, 2004; West *et al.*, 2006).

The first studies to explore the functional contribution of TLRs focused on whether they acted as a bridge between the innate and adaptive immune response. Consequently, the dendritic cell, as the professional antigen presenting cell was shown to express the majority of TLRs and release proinflammatory mediators such as IL-6, IL-12 and TNF-α after stimulation through these receptors. Later, it was shown that the majority of cells selectively express toll-like receptors, including structural cells such as epithelial cells and fibroblasts. For example, human alveolar and bronchial epithelial cells constitutively express TLR4 and stimulation with LPS has been demonstrated to induce the release of IL-6 and IL-8 (both implicated in emphysema) (Guillot, 2003).

Table 1-2: Toll-Like Receptors (in general), corresponding pathogen associated molecular patterns (PAMPs)/ligand, and origin of PAMPs. (E.M. Pålsson-McDermott and O'Neill., 2007; van de Veerdonk *et al.*, 2008).

Toll – Like Receptor	PAMP/Ligand	Origin of PAMP
TLR-1	Tri-acyl lipopeptides	Bacteria
TLR-2	Peptidoglycan, Lipoteichoic acid	gram +ve bacteria
TLR-3	Double stranded RNA (dsRNA)Polyinosinic:polycytidylic acid (Poly I:C)(synthetic dsRNA)	Virus, ssRNA replicating viruses
TLR-4	Lipopolysaccharide, Fusion protein from Respiratory Syncytial Virus	gram –ve bacteria, RSV
TLR-5	Flagellin	Bacteria
TLR-6	Di-acyl lipopeptides	Bacteria
TLR-7	Single stranded RNA (ssRNA) Imidazoquinoline/Loxoribine	ssRNA virus
TLR-8	Imidazoquinoline/Loxoribine	--
TLR-9	Unmethylated CpG motifs	Microbial DNA
TLR-11	Uropathogenic Escherichia coli (UPEC) Profilin	Bacteria
TLR-10, 12 and 13	Unknown	Unknown

1.2.1 Toll-like receptor signalling

Understanding how the innate immune system discriminates between various infectious organisms so that the appropriate adaptive T cell and humoral responses are generated may aid in the design of new therapeutic agents for the treatment of infections (Schnare M *et al.*, 2000). Thus, unraveling the signalling machinery and the functional responses downstream of TLR ligation is the subject of intense research. Dimerisation of TLRs triggers activation of signalling pathways, which originate from a cytoplasmic Toll-IL-1 receptor (TIR) domain. Of all the known TLRs, TLR4 is unique in that it can signal through four adaptor proteins, myeloid-differentiation factor 88 (MyD88), MyD88 adaptor-like (MAL), Toll/interleukin-1 receptor (TIR) domain-containing adaptor inducing interferon-β (TRIF), and TRIF-related adaptor molecule (TRAM) (O'Neill *et al.*, 2003). It is thought that MAL is associated functionally with MyD88 as a bridging molecule while TRAM combines with TRIF. Both of these pathways lead to the activation and nuclear translocation of the transcription factor NF-κB and the interferon regulatory factors (IRFs). In general, the activation of inflammatory genes (e.g. cytokines/chemokines) is MyD88-dependent whereas the activation of interferon (IFN)-stimulated genes (ISGs) occurs in a TRIF-dependent manner through the production of IFN-β. Both the MyD88-MAL and TRIF-TRAM pathways activate NF-κB albeit with different kinetics. The MAL-MyD88 pathway initiates the early activation of NF-κB, whereas the TRIF-TRAM pathway induces later activation (Kawai *et al.*, 2001; Yamamoto *et al.*, 2002; Hoebe *et al.*, 2003; Yamamoto *et al.*,

2003). The mechanism that underpins this temporal difference is a requirement for TNF-α production downstream of IRF3 activation in the TRIF-TRAM pathway (Yoneyama *et al.*, 2004). TNF-α then acts in an autocrine manner to activate NF-κB (Covert *et al.*, 2005; Werner *et al.*, 2005). Although differences in adaptor protein usage have been proposed to promote specificity of the immune response, both the MyD88 and TRIF pathways are able to induce the production of TNF-α.

1.2.2 Synergies between TLR signalling

To date, nearly all of the studies that have explored the interaction between toll-like receptors and their specific ligands or infectious pathogens have viewed one of the TLRs in isolation. Thus, while respiratory syncytial virus (RSV) can be recognised by TLR-3, -4 and -7, it has only been studied in single-factor deficient mice (mainly because of the lack of availability of multiple TLR gene deficient mice). The importance of studying the effects of activating two or more TLRs within hours of each other was recently demonstrated by Napolitani *et al*. (2005). This study found that selected TLRs act in synergy (Napolitani *et al.*, 2005). IL-23p19 and IL-12p40 subunits were increased more than 40 fold (messenger RNA) when bone marrow derived dendritic cells were treated *in vitro* with a combination of either LPS (TLR4 ligand) and R848 (synthetic TLR7-ligand or LPS and Poly (I:C) (synthetic TLR3-ligand), as compared to cells treated with one of the PAMPs (Nagase et al., 2003). Emerging data suggests that IL-23, a

heterodimer of IL-23p19 and the IL-12 subunit p40, is the critical factor for differentiating naïve T cells into inflammatory T cells capable of secreting large amounts of TNF-α and IL-17 (Cua *et al.*, 2003; Napolitani *et al.*, 2005). This may have important ramifications in the pathogenesis of emphysema given the increased frequency of bacterial colonisation in the lungs of these individuals and the effect of infections on disease exacerbations. However, to date no studies have explored the synergistic effects of TLRs *in vivo*, or the contribution of IL-17 and IL-23 to the development of emphysema.

1.2.3 Non pathogen-associated ligands of toll-like receptors

Emerging evidence has shown that TLRs can also recognise host-derived molecules, in particular those that help form the extracellular matrix such as hyaluronans, fibronectin and byglycan. A recent study has demonstrated that following injury to the lung, these molecules may regulate cell/tissue homeostasis through TLR4-MyD88-dependent pathways (Jiang *et al.*, 2005) (these observations may fit more closely with the developmental role of Toll in drosophila). Thus, TLR4 has been implicated as a central regulator of diverse cell processes such as inflammation, apoptosis and tissue repair/growth.

Other forms of non pathogenic-associated ligands of TLRs are the alarmins which can be categorized as damage associated molecular patterns (DAMPs). Alarmins can be found in various cell types and are in general released via degranulation in response to infection or tissue injury (De Yang *et al.*, 2009).

These alarmins can then interact with specific TLRs which can then recruit and/or activate pro-inflammatory cell types such as leukocytes and antigen-presenting cells.

Given that pathogen-activated cells exist in a state of 'high-alert' in which apoptosis can either be efficiently initiated if the infection progresses or prevented if the infection resolves (Demedts *et al.*, 2006; Pierce *et al.*, 2007), the dysregulation of these two pathways may critically alter the response to respiratory infections, which are a major cause of COPD exacerbations. Thus, the failure to tightly regulate the activation of TLR4 may lead to inappropriate and exaggerated responses such as chronic inflammation and local tissue damage that characterise emphysematous-like lesions. Remarkably, only a handful of studies have explored the role of the innate immune system in the development of emphysema (Bracke *et al.*, 2006; Atochina-Vasserman *et al.*, 2007; Doz *et al.*, 2008).

1.3 Bacterial infections and COPD

COPD exacerbations are commonly associated with bacterial infections in particular colonisation of bacteria in the lower respiratory tract (Moller *et al.*, 1998; Sethi *et al.*, 2006). *Streptococus pneumoniae (S. pneumoniae)* and *Haemophilus influenzae* (*H. influenzae*) are the two most common bacteria isolated from these patients including those suffering from emphysema.

1.3.1 *Haemophilus influenzae* and COPD

H. influenzae is an opportunistic pathogen and exists as two major strains. They are the encapsulated strains and the un-encapsulated strains. The capsulated strains cause invasive disease (e.g. epiglottitis) and can resist phagocytosis with their capsules. In contrast, the un-encapsulated strains (Non-Typeable *Haemophilus influenzae*; NTHi) are commensal and common to the nasopharynx and upper airways in humans (Pang *et al.*, 2008). *H. influenzae* are also Gram-negative bacteria and therefore contain forms of lipopolysacharrides on their cell surfaces.

While NTHi poses no risk to healthy individuals, it can cause acute upper and lower respiratory tract infections, and persists in the lower respiratory tract of COPD or emphysema patients. Furthermore, NTHi is thought to persist *via* host mimicry that may slow immune clearance (Moran *et al.*, 1996).

NTHi infections in the airways of COPD patients may lead to further exacerbations of inflammatory responses from the host. Like most gram negative bacteria, endotoxins such as LPS produced from NTHi can induce host cell responses *via* TLR4 (Lazou *et al.*, 2001). Moreover, other proteins and lipoproteins produced have now been demonstrated to activate a host of other murine TLRs such as TLR2 and TLR9 (Shuto *et al.*, 2001; Galdiero *et al.*, 2004). These inflammatory responses include the increased production of chemokines

(e.g. Macrophage Elastase (MMP-12) and macrophage inflammatory protein (MiP)-1α) and cytokines (TNF-α, IL-1B, IL-6).

Prolonged persistence of the bacterial infection driving a continued inflammatory response eventually leads to detrimental and permanent effects such as structural changes in airways and alveoli, as well as destruction to alveolar walls through apoptosis resulting in the disease phenotypes observed in patients with COPD or emphysema (Moghaddam *et al.*, 2008)).

1.4 Role of apoptosis in emphysema

Apoptosis (programmed cell death) is a naturally occurring process to eliminate unwanted, damaged or infected cells. Apoptosis occurs in four stages, depending on the balance between negative and positive signals, and the alteration of essential survival factors versus factors triggering the apoptotic process. Apoptosis involves well regulated, chronological and distinct processes which can be stimulated by both internal and external mechanisms (Demedts *et al.*, 2006; Pierce *et al.*, 2007). In the initial two phases, the process is still reversible, meaning the cell can still be re-programmed to not commit to apoptosis. When the signalling cascade continues and the cell enters the third and fourth phase, it is now apoptotic. During these last two phases, various apoptotic pathways converge. Enzymes such as the caspase proteases are produced, and so are by products such as ceramide (Hannun and Obeid, 2008). However, when the regulation of apoptosis is interrupted abnormally, the

process can become a contributor to the pathogenesis of diseases such as asthma, acute respiratory distress syndrome, and emphysema (Pierce *et al.*, 2007).

Recent evidence has emerged from studies in both human and animal models of emphysema that suggest the loss of alveolar tissue that characterises changes to the alveolar wall in emphysema may occur as the result of abnormal regulation of apoptosis (Demedts *et al.*, 2006).

1.4.1 The Regulation of apoptosis

Apoptosis is regulated by three pathways, each involving different caspases. During the first pathway, known as the receptor mediated extrinsic pathway, cells up-regulate death ligand receptors such as TNF-receptor, Fas-receptor, and TNF-related apoptosis inducing ligand (TRAIL) receptor. Activation of these receptors by extracellular signals (e.g. TNF-α and Fas ligand) drives the apoptotic events forward through the activation of different caspases such as caspase-8 and caspase-3 (Demedts *et al.*, 2006). These caspases eventually execute apoptosis by releasing caspase-activated DNAse (CAD) (Tang and Kidd, 1998).

The second pathway is termed the mitochondrial intrinsic pathway, which responds to physical and chemical stress signals by releasing cytochrome C from the mitochondria. Cytochrome C, apoptotic protease activating factor-1 (Apaf-1)

and caspase-9 then form the apoptosome, and in the process activates caspase-9. In turn, caspase-9 activates caspase-3 and drives the apoptotic process (Li *et al.*, 1997; Zou *et al.*, 1997; Slee *et al.*, 1999).

Finally, the third pathway is termed endoplasmic reticulum pathway. Here, caspase-12 is activated in response to stress signals (Rao *et al.*, 2001; Szegezdi *et al.*, 2003; Demedts *et al.*, 2006). This particular pathway can either target the nucleus directly to break down DNA (*via* an unknown process) or activate *via* the second pathway through the release of cytochome C.

Caspase-3 activation is an important indication of apoptotic processes. Indeed, a significant increase in caspase-3 activity was observed in a rat model of emphysema when VEGF-receptors were blocked, leading to the induction of apoptosis, and eventually the development of emphysematous-like lesions.

1.4.2 Ceramide and Apoptosis

Ceramide is a sphingolipid second messenger involved in co-ordination of the stress response, and, under certain conditions is a regulator of apoptosis. A simplified overview of ceramide synthesis is shown in Figure 1-1. Different sphingolipid families can be converted to or from ceramide by different enzymes such as dihydroceramide synthase (LASS), sphingomyelinase (SMase) and ceramidase. This suggests that a balance of the products at different stages may

drive the increase or decrease of ceramide levels which may lead to the advancement of apoptosis.

In a mouse model of emphysema, the direct administration of exogenous ceramide to the lungs induced alveolar epithelial cell apoptosis and increased the diameter of the alveoli indicating the presence of emphysematous-like lesions (Petrache *et al.*, 2005). Sphingosine-1-phosphate (S1-P) is another bioactive lipid synthesised in the ceramide pathway but has been shown to inhibit ceramide-induced emphysema suggesting that the balance of sphingolipid products may critically regulate cell activation and survival (Petrache *et al.*, 2005).

TNF-α, initially named due to its ability to induce cell death, has been demonstrated to increase intracellular ceramide concentrations in macrophages. Ceramide is a co-ordinator of stress responses as well as a regulator of cell death through apoptosis (Hannun and Obeid, 2008). Patients with emphysema have been shown to express higher levels of ceramide (Demedts *et al.*, 2006; Doggrell, 2006).

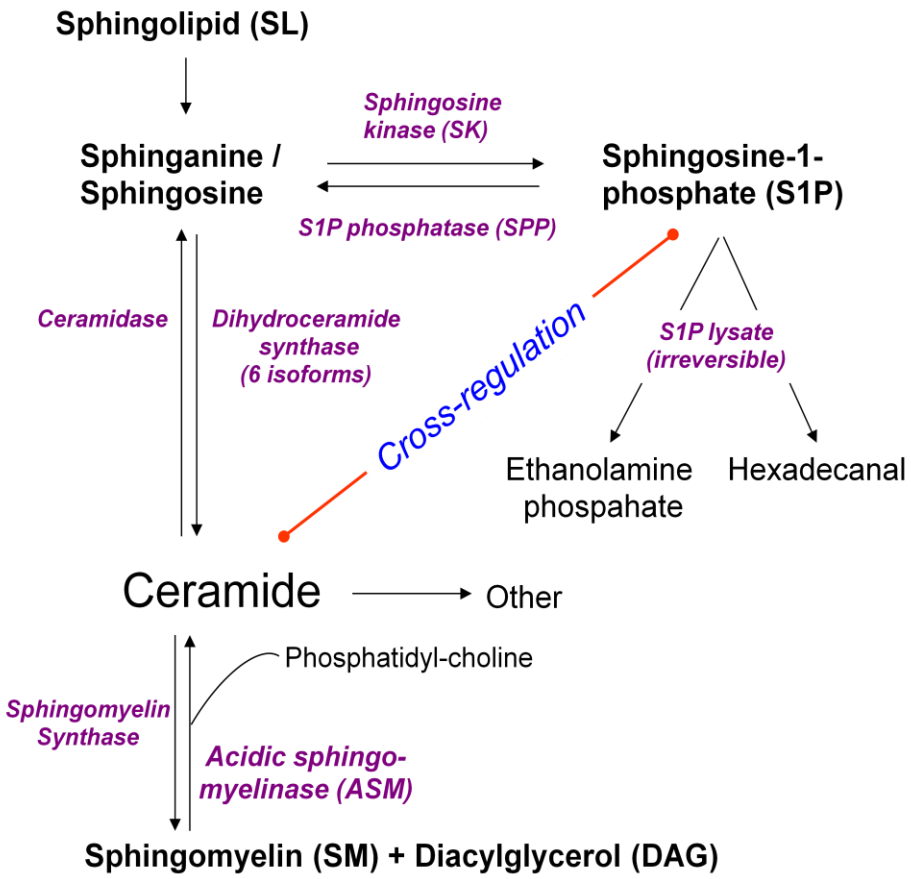

Figure 1-1: The Ceramide production pathway. An overview of the ceramide production pathway adapted from Hannun and Obeid (2008). Of interest are how sphingomyelin and sphinganine/ sphingosine can be converted by enzymes into ceramide, a core component of apoptosis.

1.4.3 Synthesis of ceramide

The synthesis of ceramide is a complex process, with a balance of each by-product tightly regulated by enzymes, which can break down or form the product through different steps (Figure 1-1). In essence, the three main groups of enzymes involved directly with ceramide synthesis are dihydro-ceramide synthase (LASS), sphingomyelinase, and ceramidase.

1.4.3.1 Dihydro-Ceramide Synthase (LASS)

Sphingolipds are first formed *de novo* from serine and palmitate, which goes through a series of alterations before finally being reduced to dihydro-sphingosine, followed by acylation by Dihydroceramide Synthase (LASS) (Pewzner-Jung *et al.*, 2006). LASS enzymes specifically introduce the acyl chain to sphingoid bases, altering them to form dihydro-ceramides with N-linked fatty acids (Hannun and Obeid, 2008). LASS enzymes have also been found to exist in up to six different isoforms but the specific functions are as yet unknown. Ceramide is finally formed through the desaturation of dihydro-ceramide by desaturase. LASS can also convert sphingosine to ceramide as shown in Figure 1-1.

1.4.3.2 Sphingomyelinase

During the biosynthesis of sphingomyelin, ceramide can also be converted by sphingomyelinase synthase (SMS) through acquiring a phosphocholine headgroup from phosphatidylcholine (PC). In reverse, sphingomyelin can be broken down by sphingomyelinase (SMase) to regenerate ceramide. Similar to the cermidases, SMases can be categorised to three distinct families, differentiated by their optimum pH levels (acid, neutral, and alkaline).

1.4.3.3 Ceramidase

Ceramide can also be broken down by different enzymes to form various by-products. Ceramide can be converted back to sphingosine by ceramidases,

which are hydrolases that remove the fatty acid acyl groups (Pewzner-Jung *et al.*, 2006; Sebastian *et al.*, 2006). Essentially, they reverse the roles played by the LASS enzymes. Three distinct families are differentiated by the different optimum pH levels (acid, neutral, and alkaline) needed for their function.

Sphingosine may be "salvaged" and reconverted back to ceramide, or it can be further converted to sphingosine-1-phosphate (S1-P) through phosphorylation by sphingosine kinases (SK). As mentioned earlier, S1-P has been shown to inhibit ceramide-induced emphysema (Petrache *et al.*, 2005).

1.5 Summary

LPS is a common endotoxin and a constituent of the cell wall of gram negative bacteria, as well as found ubiquitously in the environment. It has been shown that LPS is high in concentration in cigarette smoke and indeed investigations have demonstrated that LPS levels in the homes of smokers is increased by 4-63 times (Sebastian *et al.*, 2006).

NTHi is a common commensal gram negative (hence LPS-producing) bacteria residing in the upper airways of humans. However, emphysema exacerbations in patients are commonly associated with bacterial infections and NTHi is one of the commonly isolated bacteria in COPD patients. LPS and infections may induce disease by promoting apoptosis and this may occur through the production of ceramide.

Multiple mouse models using LPS or bacteria (such as NTHi) to induce disease have implicated inflammation at the site of infection as a cause of disease (Vernooy *et al.*, 2002; Brass *et al.*, 2008). These data, together with other smoking models suggests that blocking inflammation may be beneficial for the treatment of emphysema.

1.6 Hypothesis and Aims

Hypothesis: Inoculationion of the lower respiratory tract with NTHi or exposure to LPS induces emphysematous-like lesions in mice through apoptotic processes.

The aims of this study were:

- To investigate whether the development of emphysematous-like lesions induced by LPS administration was an apoptotic process and which pathways downstream of LPS-TLR4 signalling were activated.
- To investigate whether the development of emphysematous-like lesions induced by NHTi challenge was an apoptotic process and if the pathways involved were TLR4 dependent.
- To determine if the anti-inflammatory peptide, C15 (Cash *et al.*, 2008) would block LPS and NTHi-induced lung inflammation and hence the development of emphysema in a mouse model.
- To investigate the role of macrophages in LPS- and NTHi-induced emphysema

**Chemerin, chemerin-derived peptide (C15) and chemerin receptors will be discussed in Chapter 4.

Chapter 2

LPS and the Development of Emphysema "like" lesions in the Parenchyma of Mice

Chapter 2: LPS and the Development of Emphysema "like" lesions in the Airways of Mice

2.1 Introduction

Cigarette smoking has been shown to be a significant risk factor in the development of emphysema in approximately 85% of COPD cases (Taylor *et al.*, 2004). However, it is estimated the only 15% of smokers will develop emphysema, albeit much higher than non-smokers at 1.6% (Lindberg *et al.*, 2006). This suggests that other risk factors such as air pollutants (e.g. LPS, asbestos, factory smog) and/or infections (e.g. bacterial and viral) in the lungs can drive the development of emphysema (Murphy and S., 1992; Hasday et al., 1999; Sethi et al., 2006).

Bacterial lung infections may play a role in the development of emphysema (Moller *et al.*, 1998; Moghaddam *et al.*, 2008). LPS released from gram negative bacteria may contribute to the disease by inducing inflammation and apoptosis (Vernooy *et al.*, 2002; Brass *et al.*, 2008). While LPS is known to exist ubiquitously, it also found in unusually higher concentrations in cigarettes, as well as areas used by farming industries (Sebastian *et al.*, 2006). Thus LPS derived from infections and/or smoking may drive the pathogenesis of emphysema through activation of inflammatory pathways involving TLR4 and NF-kB.

Indeed, animal models of LPS-induced emphysema have shown increased inflammatory cells such as neutrophils and macrophages in the lung tissue that correlates with the onset of disease. LPS-induced inflammation is also associated with enhanced production of a range of proinflammatory chemokines (e.g. macrophage elastase (MMP-12) and matrix metallopeptidase (MMP)-9) and cytokines (e.g. TNF-α, IL-1β, and IL-6) which have a role the in recruitment and activation of inflammatory cells.

In 2001 and 2002 Vernooy and colleagues demonstrated in a mouse model of LPS-induced emphysema that 12 weeks of exposure to LPS administered *via* an intratracheal route can induce the significant development of emphysematous-like lesions. They observed LPS-induced inflammation, apoptosis to bronchial epithelial cells and alterations in the morphology in the lungs including: mucus cell metaplasia; airway wall thickening; and irreversible alveolar enlargement. These are all hallmark features of emphysema in humans.

In this study, we aimed to develop a mouse model of LPS-induced emphysema, and temporally characterise the development of 1) emphysematous-like lesions, 2) inflammation, 3) expression of chemokines and cytokines, and 4) determine if the ceramide pathway is activated and may be contributing to disease through apoptosis.

Firstly, we will employ an LPS-induced model of emphysema that will temporally and spatially reflect the inflammatory responses and lesions

associated with emphysema (Vernooy *et al.*, 2002). Initially we will determine whether this model can be established through inhalational aerosol exposure to LPS or whether it is dependent on intratracheal administration as employed previously (Vernooy *et al.*, 2002).

We will further characterise the molecular and cellular processes that underpin the development of LPS-induced emphysema by using multi-factorial techniques including gene deficient mice (Chapters 2 and 3), and pharmacological intervention (Chapter 4). Once we have established LPS–induced models of emphysema we will determine the requirement for MyD88 by employing MyD88-deficient ($MyD88^{-/-}$) mice. It has been well documented that LPS is the ligand that signals through TLR4, however TLR4 activates pathways downstream *via* either the MyD88 pathway or the TRIF-TRAM pathway. After LPS administration, the molecular and cellular pathology of the $MyD88^{-/-}$ mice will be compared to wild-type (WT) mice.

Together these studies will provide insight into the cellular and molecular pathways that contribute to LPS-induced emphysematous-like lesions.

2.2 Materials and Methods

2.2.1 Wild type and Genetically modified mice

BALB/c wild type (WT) mice were obtained from Central Animal House (Animal Services Unit, University of Newcastle) or purchased from Animal Resources Centre (Perth, WA, Australia) and delivered to the animal holding facility at 7 or 15 weeks of age. BALB/c MyD88$^{-/-}$ mice were kindly provided by Dr. Shizuo Akira (Osaka University, Japan). Mice were housed in the David Maddison Building animal holding facilities (Newcastle) in individually ventilated cages (IVC) under specific pathogen-free conditions with a 12 hour light/dark cycle. Mice had access to food and water *ad libitum*. Mice were housed in groups of 4 to 5 to prevent overcrowding. Mice were first treated when they reached 8 weeks or 16 weeks of age. All experiments were conducted according to Animal Welfare Guidelines set by the University of Newcastle, and under protocols approved by the Animal Care and Ethics Committee, University of Newcastle. To keep results consistent all mice were male.

Age matched (6 week) BALB/c WT, TLR2-deficient (TLR2$^{-/-}$), TLR4$^{-/-}$ and TLR2&TLR4-deficient (TLR2$^{-/-}$TLR4$^{-/-}$) mice were used in studies investigating function of TLR4 and age-dependent studies.

2.2.2 Mouse models of LPS-induced emphysema

2.2.2.1 An Intratracheal model of LPS-induced emphysema

BALB/c WT mice were anaesthetised (alfaxan diluted 1:4 in sterile hospital grade saline administered intravenously via tail vein), placed in a vertical position and the trachea exposed under a microscope. LPS from *Escherichia coli* (*E. coli*), serotype 0111:B4 (Sigma) (0.2µg/g body weight) diluted in 50µl hospital grade sterile saline was instilled *via* a sterile 20-gauge catheter. Control mice received 50µl of saline only. Mice were administered LPS or saline twice per week for 8 consecutive weeks **(Figure 2-1).** This dose of LPS (5 µg per exposure; or 0.2 µg/g body weight) corresponds to the amount of LPS inhaled by a person smoking approximately 25 cigarettes per day (Vernooy *et al.*, 2002). Mice were sacrificed 6 days after the last saline / LPS instillation (to allow for resolution of inflammation (Vernooy *et al.*, 2001)), and lungs collected for morphometric analysis.

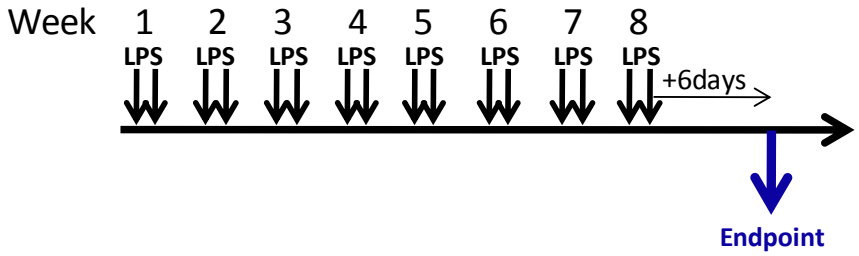

Figure 2-1: Study design of intratracheal (i.t.) model of LPS-induced emphysema. LPS was administered intratracheally twice per week (Tuesday and Fridays) for a period of 8 weeks. Mice were then sacrificed 6 days after the final LPS administration for tissue collection and analysis.

2.2.2.2 An Aerosol model of LPS-induced emphysema

Mice were placed in a perspex box (approximately 20L) divided into 4 quadrants, with each quadrant holding up to 8 mice to allow for whole body exposure to an aerosol. Mice were exposed to an aerosol consisting of 500µg LPS/10ml sterile saline generated by nebulisation at 20 PSI (Brass *et al.*, 2004; Brass *et al.*, 2008) for 30 mins until complete aerosolisation of the LPS solution. Control mice were exposed to aerosolised saline only in a separate set of equipment (to prevent LPS contamination). Control mice were always treated prior to mice exposed to LPS. Mice were exposed to aerosolised saline or LPS twice a week, for a period of 1, 2, 4, 6 or 8 weeks **(Figure 2.2).**

All mice were sacrificed 6 days after the last LPS administration. For each exposure regime outlined in **Figure 2.2** mice were allocated as follows for sample collection: one group was used for the collection of lung tissue with the large left lobe used for flow cytometry **(section 2.2.4),** half of the smaller lobes used for ELISA (**section 2.2.6**) and the other half for mRNA (**section 2.2.5**)**.** A second group of mice were used for all morphometric analysis.

2.2.2.3 Two week aerosol model of LPS-induced emphysema

Analysis of our models demonstrated that 2 weeks of exposure was sufficient to induce emphysematous-like disease. Thus, this model was utilised for all subsequent experiments.

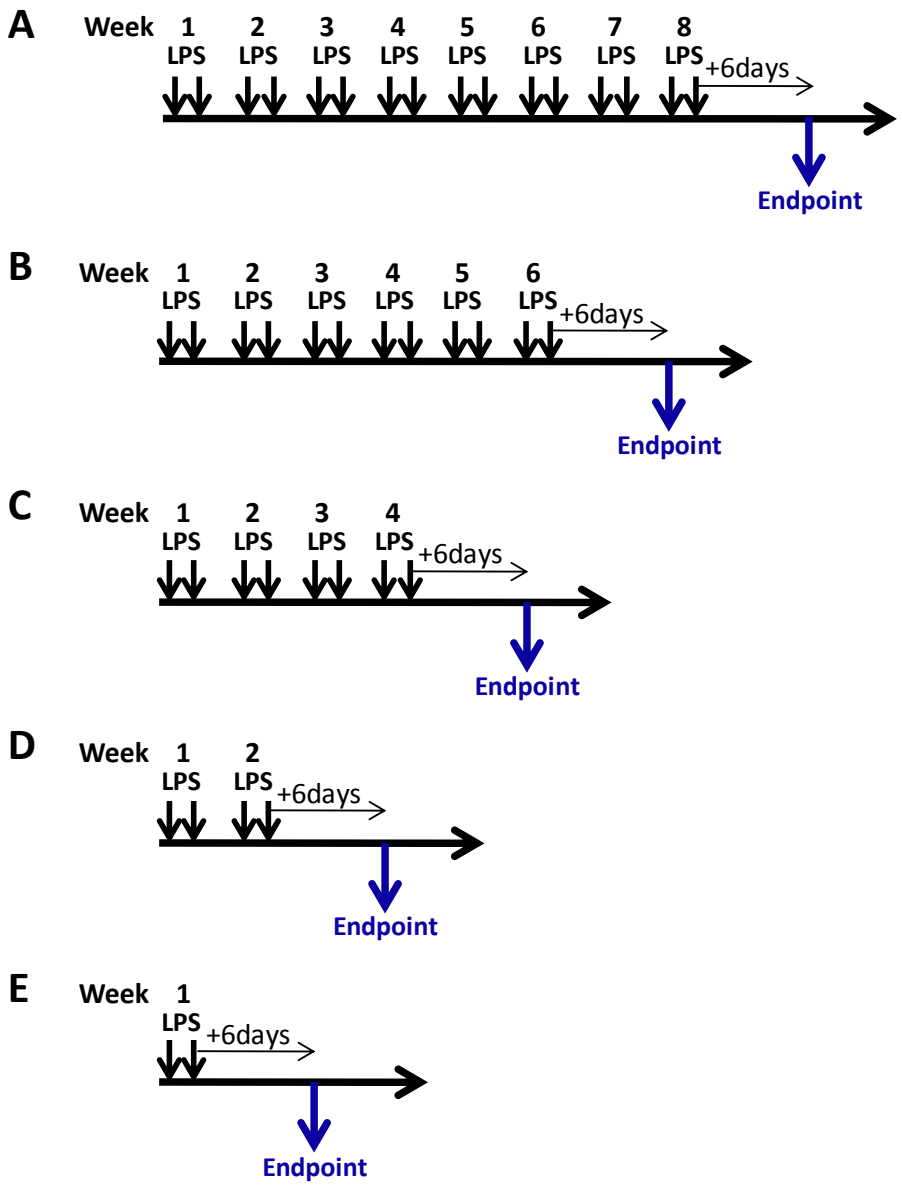

Figure 2.2: Study design for temporal analysis of disease induction and progression using an aerosol model of LPS-induced emphysema. Mice were exposed to 30mins of aerosolised LPS (500µg in 10ml Saline at 20 PSI), twice a week for up to 8 weeks **(A)**. Some mice were exposed for 6, 4, 2 and 1 week of aerosolised LPS **(B-E respectively).**

2.2.3 Morphometric analysis

Lungs collected for morphometric analysis were analysed for volume, mean linear intercepts (MLI), and percentage alveolar airspace (% alv airspace). Mice were euthanased *via* a lethal dose of Sodium pentobarbitone (diluted 1:5 v/v in saline). The entire thoracic region was excised (including trachea, lungs and heart) and the lungs perfused *via* the heart with distilled water at a pressure of 80cmH_2O to remove red blood cells from the capillary bed. Lungs were then inflated with 4% paraformaldehyde (PFA) (Sigma) at a pressure of 20cmH_2O and then submerged in 4% PFA for 24 hours. Fixed lungs were stored in 70% ethanol (EtOH) until required.

The volume of the lungs was determined by liquid displacement. The mass of liquid displaced was determined and the volume calculated as:

Volume (cm^3) = density of liquid (g/cm^3) / mass of liquid displaced (g)

Lungs were then cut into 3 sections. The middle section was placed into 70% EtOH, and sent for histological processing (Microscopy and Cytometry Resource Facility, John Curtin School of Medical Research (JCSMR), ANU). Sections (2µm thick) were prepared and orcein-stained to determine MLI and % alveolar airspace. Sections (4µm thick) were prepared for immunohistochemistry.

Orcein-stained sections were randomly imaged at 400x magnification using a motorised stage and microscope (Olympus BX-51 microscope, Olympus DP-760 Imaging unit), controlled by PRIOR Proscan II module and Image Pro Plus

Software (version 6.0). Random imaging positions were determined by software's algorithm within a boundary set by user that encompassed the lung section to be imaged. A total of 20 images per lung section were collected and blank images discarded. Each image was duplicated and overlayed with 11 equally spaced horizontal lines of known length (µm) or 63 equally spaced cross points. Images were then analysed using the software ImageJ (with cell counter plug-in) (Abramoff *et al.*, 2004) for mean linear intercept and percentage alveolar airspace, respectively.

For mean linear intercept analysis (**refer to Figure 2-MLI**), random lines on each image were chosen (by investigator; Red lines from edge to edge, each 492.05µm) and the number of parenchyma-line intercepts recorded. A minimum of 200 intercepts were counted per image. The total length of lines used was calculated to give value **A** (below) (Figure 2-MLI shows 5 red lines selected, thus A = 5x492.05 µm). The total length of sections of these selected lines that fall on non-parenchymal space (e.g. bronchial airways, blood vessels; Green lines in Figure 2-MLI) was calculated to give value **B** (below). MLI (µm) is expressed as:

[A-B] / number of intercepts

The average of the value obtained from 5 to 10 random slides per mouse was calculated to obtain a final average MLI value per mouse.

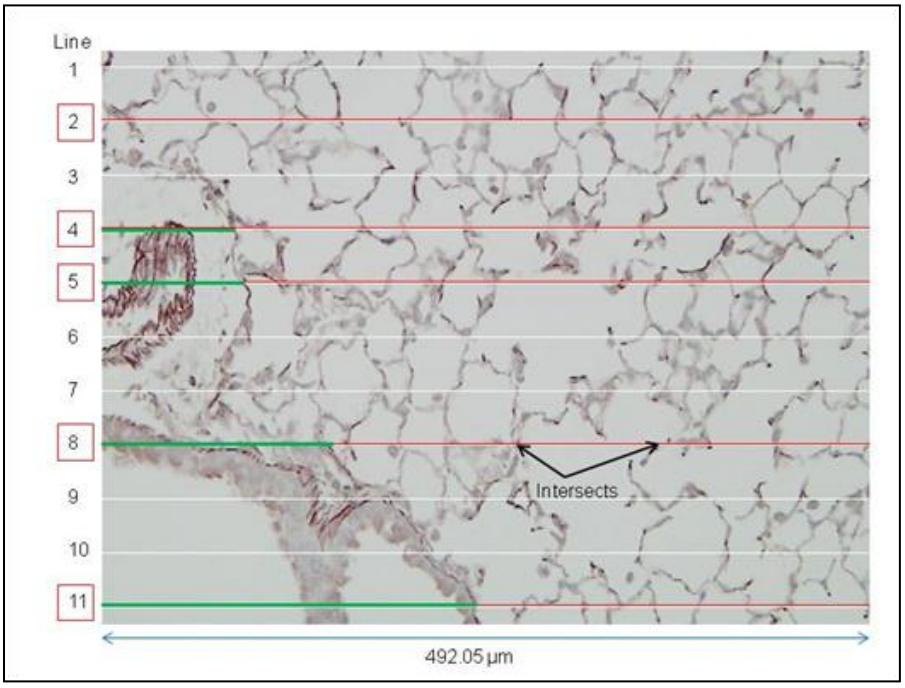

Figure 2-MLI: An example of determining mean linear intercept for 1 section of the lung

For percentage alveolar airspace, crosses falling on non-parenchymal spaces and tissue were disregarded (eg bronchial airways, blood vessels). Number of crosses falling on parenchymal tissue **(A)** and parenchymal airway **(B)** were calculated. Percentage alveolar airspace (%AA) was expressed as:

$$\%AA = [B / (A+B)] \times 100$$

A total of 200 crosses over parenchymal tissue (typically 10-18 of 20 collected images) were counted per section.

2.2.4 Flow Cytometry

The large left lung lobe was consistently used for flow cytometric analysis for all models. The lung tissue was first harvested into ice-cold PBS containing 2% HI-FCS. Lungs were then dissected into smaller pieces and gently pushed through 70µm nylon cell strainer (Falcon, BD Biosciences). The cell suspension was centrifuge and the remaining pellet resuspended in 500µl of into ice-cold PBS containing 2% HI-FCS. Red blood cells were removed with red blood cell lysis buffer and the remaining cells washed by centrifugation and removing the supernatant before a final resuspension in 1ml of ice-cold PBS containing 2% HI-FCS. The total number of cells collected was then enumerated using a standard haemocytometer. The number of viable cells was determined by trypan blue exclusion. The cells were then incubated with Fc Block (2.4G2 antibody) to block Fcγ III/II receptors in ice-cold PBS containing 1% HI-FCS for 10mins before being plated out at $1x10^6$ cells per well and stained for specific cell surface receptors. Cells were stained with PE-conjugated anti-CD11c (BD Biosciences, Pharmingen), PerCP-conjugated anti-CD11b (BD Biosciences, Pharmingen), Allophycocyanin-conjugated GR-1 (BD Biosciences, Pharmingen), PerCPCy7-conjugated anti-F4/80 (Biolegend) and PeCy7-conjugated anti-CD45 (Biolegend)

Cells were incubated in the dark at 4°C for 20mins before being washed 3 times with ice-cold PBS containing 1% HI-FCS to remove unbound antibodies. Cells were finally incubated in FACS-FIX solution overnight before analysis.

Cell data acquisition was carried out using the FACSCanto and analysed with FACSDiva v5.01 software (Becton and Dickinson). Alveolar macrophages were identified as $CD11c^{+}CD11b^{lo}GR1^{-}F4/80^{+}CD45^{hi}FSC^{hi}SSC^{med}$ and neutrophils were identified as $CD11c^{-}CD11b^{+}GR1^{hi}F4/80^{-}CD45^{+}FSC^{med}SSC^{med}$. Alveolar macrophages or neutrophils were enumerated by multiplying the percentage of identified cell population per $1x10^{6}$ cells to total cell numbers per lung sample.

For intracellular staining of Ceramide (MAb to Ceramide (Alexis Biochemicals, San Diego, CA) and Caspase-3 (anti-mouse cleaved caspase-3, (Cell Signalling, Beverly MA), cells were first permeabilised using 0.5% Saponin in PBS for 5 mins, then temporarily fixed with 4% PFA before being incubated with primary antibody. The cells were then washed in ice-cold PBS 3 times, including centrifuging as described above prior to incubation with a FITC-conjugated secondary antibody.

2.2.5 Messenger RNA analysis

2.2.5.1 Total RNA extraction

The upper right lung lobe from each mouse was excised, immersed in 500µl RNA-later (Ambion) and stored at -80°C until further analysis. For mRNA extraction, lungs were thawed and transferred to 500µl of TriReagent (Ambion). mRNA was extracted as per the following protocol. Briefly, lungs were mashed using a sterile plastic pestle and the cell free supernatant transferred into fresh eppendorf tubes. 200µl of chloroform (Sigma) was added to the supernatant and

shaken vigorously to separate the RNA from protein. The mixture was then centrifuged and the top aqueous phase transferred to a new tube. 200µl of isopropanol (Sigma) was then added and the tube vortexed to precipitate mRNA. Samples were then centrifuged and the supernatant discarded. The pellet was washed with 1ml of 75% ethanol and left to dry before being resuspended in 50µl of $T_{10}E_{0.1}$ buffer. The concentration of mRNA was measured using a NanoDrop Spectrophotometer (ND-1000) with associated software (ND-1000, v3.8.0) (BioLab).

2.2.5.2 Reverse Transcription

1000ng of mRNA was reverse transcribed to generate complementary DNA (cDNA). Briefly, mRNA was mixed with a 2µl dNTP (Promega, Madison, WI) and random primer mix (Invitrogen, Carlsbad, CA). The mixture was adjusted to 12µl with nuclease-free distilled water (Ambion) and heated to 65°C for 5mins and cooled on ice. 4µl of 5x 1st Strand Buffer (Invitrogen), 2µl of 0.1 mM DDT (Invitrogen) and 1µl of distilled water was added and the mixture heated at 37°C for 2mins. 1µl of M-MLV reverse transcriptase (Invitrogen) was added and the mixture incubated at room temperature for 10mins. Samples were then heated at 37°C for 50mins, then 70°C for 15mins to inactivate any enzymes and finally resuspended in 130µl of $T_{10}E_{0.1}$ buffer.

2.2.5.3 Primers

Primers for the genes of interest were designed to span large introns of more than 1000 base pairs so as not to amplify contaminating DNA sequences. Primers were synthesised by Sigma-Genosys, Australia. Genes of interest are shown in **Table 2-1.**

Table 2-1: Murine Primers used for qPCR.

Gene	Primer	Sequence (5' to 3')	Gene ID
HPRT	Forward	AGGCCAGACTTTGTTGGATTTGAA	15452
	Reverse	CAACTTGCGCTCATCTTAGGCTTT	
TNFa	Forward	TCTCAGCCTCTTCTCATTCCTGCT	21926
	Reverse	CTCCTCCACTTGGTGGTTTGCTAC	
IL-1B	Forward	GGATGAGGACATGAGCACCTTCTT	16176
	Reverse	TGTCGTTGCTTGGTTCTCCTTGTA	
IL-6	Forward	AGAAAACAATCTGAAACTTCCAGAGAT	16193
	Reverse	GAAGACCAGAGGAAATTTTCAATAGG	
MMP9	Forward	CCCTGGAACTCACACGACA	17395
	Reverse	GGAAACTCACACGCCAGAAG	
MMP12	Forward	CATTTCGCCTCTCTGCTGATG	17381
	Reverse	TTGATGGTGGACTGCTAGGTTTT	
CCL2 (MCP-1)	Forward	CCAACTCTCACTGAAGCCAGCTCT	20296
	Reverse	TCAGCACAGACCTCTCTCTTGAGC	
CCL3 (MiP-1α)	Forward	CCTCTGTCACCTGCTCAACA	20302
	Reverse	GATGAATTGGCGTGGAATC	

2.2.5.4 Analysis of gene expression by quantitative real-time PCR (qPCR)

Quantitative real-time polymerase chain reaction (qPCR) was performed on the Mastercycler EP Realplex system (Eppendorf, Australia) in 25 µl volume reactions. 5µl of cDNA was added to 12.5µl of Syber green mix (with ROX as a passive reference dye) (SYBR GreenER^{TM} reagent system, Invitrogen), 5.5µl of distilled H_2O, and 1µl of each of the sense and anti-sense primers (used at 5µM).

Cycling conditions were as follows:

Holding stages: 50°C for 20s, 95°C for 2mins,

Cycling stages: 95°C for 15s, 60°C for 30s (40 cycles)

Melt Curve/Dissociation stages: 95°C for 15s, 60°C for 1min, 95°C for 30s, 60°C for 15s.

The threshold values (Ct values) for each sample were determined as the number of cycles required for the fluorescent signal to cross the threshold which is set above the background levels of fluorescence (background noise). Ct values from each gene were normalised against a constant housekeeping gene (HPRT). The amount of gene of interest from treated mice was then expressed as a relative quantity to vehicle treated control group.

2.2.6 ELISA

The other lung lobes harvested from mice treated and sacrificed for characterising the inflammatory profile were collected and one portion was stored in RIPA buffer (Sigma) at -20°C until further processed. The time points samples were collected include 6, 48 and 72 hours after each LPS exposure, as well as 6 days after the final LPS exposure in the 2 week LPS model.

Samples were thawed and homogenised within the RIPA buffer using a Tissue-Tearor (Biospec Products, Bartlesville, OK). Samples were then centrifuged at 13200rpm for 10mins at 4°C in a 5415R centrifuge (Eppendorf). The

supernatant was then collected and stored for protein analysis. Total protein concentration for each sample was determined using BCA™ Protein Assay Kit (Thermo Scientific, Rockford, IL) according to manufacture's instructions. Levels of TNF-α and CCL3 from lung homogenates were determined using the DuoSet® ELISA Development System (R&D Systems, MN). IL-1β and IL-6 in lung homogenates were determined using the respective murine ELISA Ready-Set-GO! Reagent sets (eBioscience). Cytokine concentrations were normalised to total protein concentration of each sample.

2.2.7 Immunohistochemistry (IHC)

Paraffin-embedded lung sections were baked at 70°C for 60 mins and then sequentially passed through a series of solutions as follows: twice in xylene (10mins then 5mins), twice in absolute ethanol (5mins each), once in 70% ethanol, (5mins) and once in deionized water (5mins).

Immunohistochemistry was used to detect ceramide as well as Caspase-3 in lung sections. Antigen retrieval was performed on de-paraffinized slides by boiling in 10mM citrate buffer, pH 6 in a pressure cooker (Nordie Ware) for 10mins in a microwave. Slides were left to cool at room temperature for 30mins and washed 3 times with PBS-T buffer (3mins each wash). The slides were then blocked with rabbit serum (5% Rabbit Serum + 1% Fetal calf serum (FCS) in PBS) at room temperature in a humidity chamber for 60mins. The blocking buffer was removed by washing in deionized water, and the slides incubated with

monoclonal antibody to Ceramide (Alexis Biochemicals, San Diego, CA) overnight at 4°C in the humidity chamber.

Slides were then washed 3 times in PBS-T (5mins per wash) to remove the primary antibody and then incubated with rabbit anti-mouse IgG (1:30 dilution) for 30mins. Slides were washed twice with PBS-T (5mins each), and once in TBS for 5mins. Slides were then incubated with the tertiary antibody (mouse alkaline-phosphatase anti-alkaline-phosphatase (APAAP)) for 30mins (1:30 dilution) then washed three times in TBS, 5mins each.

Slides were developed using the Fast Red TR/Napthol As-MX substrate (Sigma, Saint Louis, Missouri) made up according to the manufacturer's instructions. The reaction was stopped by rinsing slides in tap water for 3mins. Slides were flash stained in Harris Hematoxylin (Fronine) and coverslipped with Glycergel mounting medium (DakoCytomation, Carpinteria, CA).

Slides were imaged as described in Section 2.2.3. Ceramide positive macrophages were identified by their large multi-lobed nuclei (stained purple) and granulated cytoplasm (stained pink from the developed alkaline phosphatases), and close to the alveolar parenchyma. 20 random images were taken and the number of ceramide or caspase-3 positive macrophages were enumerated and averaged by the number of images. This value is represented as the averaged number of ceramide or caspase-3 positive macrophage per 40x field per mouse.

2.2.8 Statistic analysis

Data are presented as mean ± SEM. Where stated in figure legends, two-way ANOVA with Bonferroni post-test was used to determine statistical significance between experimental groups in the time course analysis. Two-tailed Student's unpaired t test was used for all other data. P values of less than 0.05 were considered statistically significant. Data was analysed using PRISM 4 software (GraphPad Software, La Jolla, CA).

Table 2-2: Buffers and Solutions.

Buffer/Solution	Components
Dulbecco's PBS (1x)	0.137M NaCl 2.7mM KCl 1.1mM KH_2PO_4 0.5mM $MgCl_2.6H_2O$ 9.1mM $Na_2HPO_4.7H_2O$ 0.9mM anhydrous $CaCl_2$
PBS-T	0.05% Tween 20 in PBS
TBS	50mM Tris 150mM NaCl Adjust pH to 7.6
RBC lysis buffer	4.1g NH_4Cl 1.0g $NaHCO_3$ 0.185 EDTA Made up to 500ml in distilled water and filter sterilised
ELISA coating buffer	0.05M carbonated-bicarbonate buffer
ELISA wash buffer	0.05% Tween 20 in PBS
ELISA assay diluents	1% BSA in PBS
ELISA blocking buffer	3% BSA in PBS
FACS wash buffer	0.05M phosphate citrate buffer pH5.0
FACS permeabilization buffer	2% FCS in PBS
FACS fix	0.5% formaldehyde in PBS
Animal cell culture media	0.1mM sodium pyruvate 10% FCS 2mM L-glutamine 20mM HEPES 100U/ml Penicillin/Streptomycin 50µM 2-mercaptoethanol Made up with RPMI1640
TE buffer	10mM Tris-CL (pH 7.5) 0.1mM EDTA
0.01M citrate buffer pH6	10mM citric acid Made up in distilled water

2.3 Results

To determine if we can replicate the data of Vernooy and colleagues (2002), their study design was repeated as shown (**Figure 2-1**).

2.3.1 An intratracheal model of LPS-induced emphysema

There was a significant increase in the distance between the alveolar walls (increased MLI values) observed in the lungs of mice treated with LPS for 8 weeks compared to saline (vehicle) treated controls (**Figure 2-3A).** The representative images (400x magnification) show the alveolar tissue of vehicle treated mice (left panel) and LPS treated mice (right panel). The MLI in LPS treated mice (37.00µm ± 1.06µm; n = 4) was significantly higher ($p<0.001$) when compared to vehicle treated controls (28.13µm ± 1.02µm; n = 4) **(Figure 2-3B)**. The increase of approximately 32% in average distance between alveolar walls is comparable to the observations by Vernooy and colleagues (Vernooy *et al.*, 2002). There was also a significant increase ($P<0.0001$) in the percentage of alveolar airspace in the lungs of mice treated with LPS for 8 weeks (n = 6; 76.69% ± 0.33%) compared to vehicle treated control mice (n = 6; 69.43% ± 0.91%) **(Figure 2-3C)**.

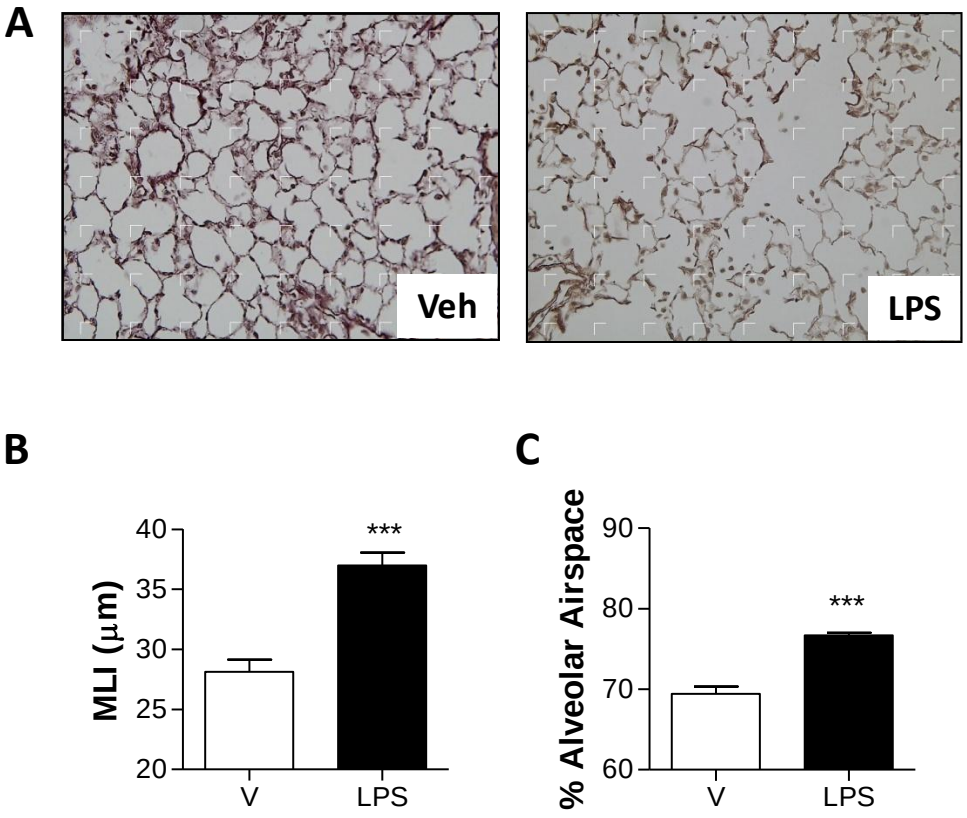

Figure 2-3: Intratracheal administration of LPS induced the development of emphysematous-like lesions. As per study design in **Figure 2-1**, vehicle (Veh / V) only (clear bars) or LPS (solid bars) was administered intratracheally to BALB/c WT mice twice a week for 8 weeks. Mice were sacrificed 6 days after the final LPS administration and lungs processed for morphometric analysis. Representative photos of sections of lungs from mice exposed to either vehicle only (left image) or LPS (right image) **(A)**. Measurements of mean linear intercepts (MLI) **(B)** and percentage alveolar airspace **(C)** were determined. Vehicle: n = 4 mice per group; LPS: n = 6 mice per group. ***P<0.001, Student's unpaired t-test.

2.3.2 An aerosol model of LPS-induced emphysema

In a parallel study mice were also exposed to aerosolised LPS or saline (vehicle; section 2.2.2.2) twice per week for 8 weeks to allow a direct comparison of results with the intratracheal model.

Surprisingly, there was a significant increase ($P<0.0005$) in the MLI of LPS treated mice (n = 4; 32.46µm ± 1.18µm) compared to vehicle treated mice (n = 6; 24.80µm ± 0.54µm) (**Figure 2-4A**) using the aerosol regime. Similarly, there was a significant increase ($P<0.0001$) in the percentage alveolar airspace of LPS treated mice (n = 4; 75.59% ± 0.90%) compared to vehicle treated controls (n = 6; 68.35% ± 0.52%) (**Figure 2-4B**).

While there was a slight difference ($P<0.05$) in the MLI of mice treated *via* the intratracheal route compared to aerosol exposure in both the vehicle and LPS groups (**Figure 2-4A**) these results overall indicate that the two different methods of LPS delivery to the lung does not affect the degree of changes in MLI or percentage alveolar airspace after 8 weeks of exposure.

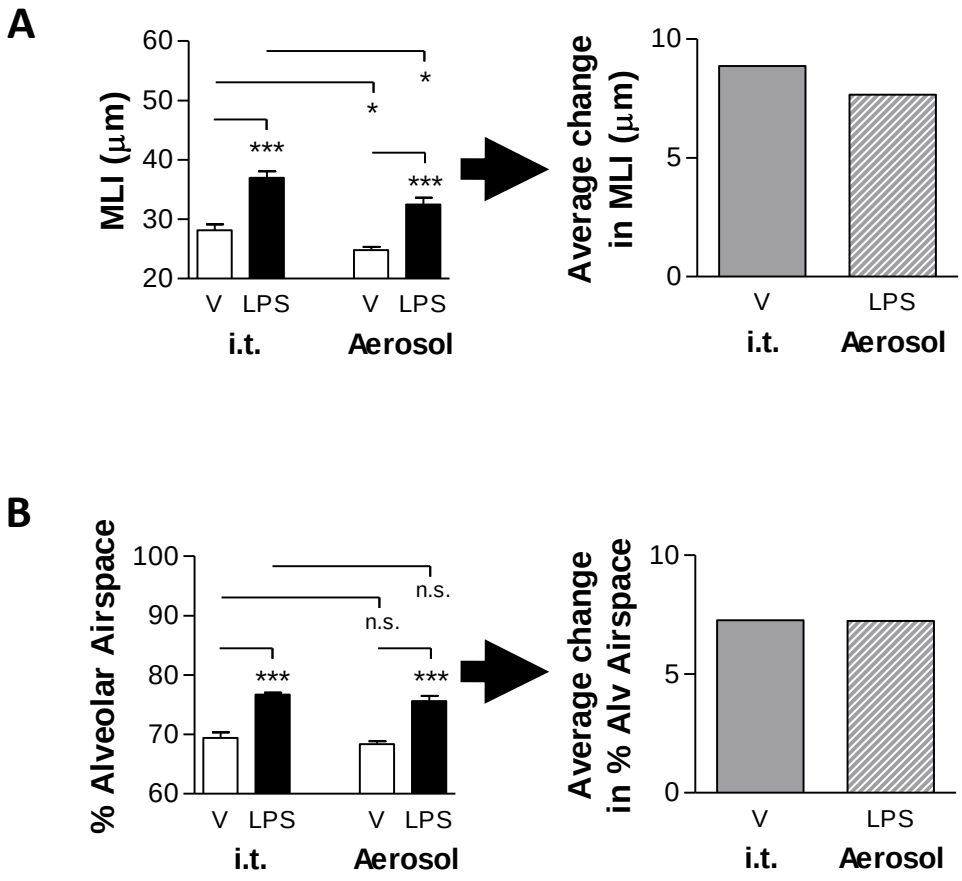

Figure 2-4: Intratracheal and aerosolised routes of LPS administration induced similar levels of change in both MLI and percentage alveolar airspace. Comparison of MLI between mice exposed to LPS or vehicle (V) delivered *via* the intratracheal route or aerosolised for 8 consecutive weeks **(A)**. Comparison of percentage alveolar airspace between mice exposed to LPS or vehicle delivered *via* the intratracheal route or aerosolised for 8 consecutive weeks **(B)**. The graph on the right represents the average change between LPS treated compared to control groups in the respective routes of LPS administration. Open bars represent mice exposed to vehicle only and closed bars represent mice exposed to LPS. n = 4-6 mice per group. *P<0.05, *** P<0.001, n.s. = not significant, Student's unpaired t-test.

2.3.3 Temporal analysis of LPS exposure on the development of emphysema

Mice were exposed to aerosolised LPS or saline (vehicle) for 1, 2, 4 or 6 weeks before being sacrificed 6 days after the final exposure (**Figure 2.2B-E**). A similar increase ($P<0.0005$) in both MLI (n = 4-6 mice per group; ~34µm) and percentage alveolar airspace (n = 4-6 mice per group; ~77%) was observed in mice treated for 2, 4 or 6 weeks when compared to those treated for 8 weeks (**Figure 2-5A and B**).

Interestingly, 1 week of exposure resulted in no significant changes to MLI and percentage alveolar airspace as compared to vehicle treated controls.

2.3.4 LPS and lung volume

To confirm that the LPS-induced increase in MLI and percentage alveolar airspace in is not due to expansion, we compared the lung volumes between LPS and saline (vehicle) treated mice (**Figure 2-6A**). We demonstrated that lung volumes after 2 or 8 weeks exposure to aerosolised LPS was not significantly different (n = 5; ~0.3 cm^3) from those in the vehicle exposed control group.

2.3.5 LPS and lung development

The lungs of BALB/c WT mice are often considered to have reached maturity by 8 weeks old, however we questioned whether this was the case. We exposed 16 week old mice to aerosolised LPS or saline (vehicle) for 2 weeks (**Figure 2-6B**). Following exposure to LPS, there was a significant increase in MLI (n = 6; 36.42µm ± 1.45µm) compared to vehicle exposed controls (n = 6; 26.53µm

± 0.63µm) (P<0.0002). These changes are directly comparable to the MLI observed in mice exposed to LPS or vehicle from the age of 8 weeks.

2.3.6 Resolution of LPS-induced emphysema

As 2 weeks of LPS exposure induced the same degree of structural changes to the lungs as 8 weeks of exposure, we used this as our model to further investigate pathogenesis. We investigated whether LPS-induced alveolar enlargement is a reversible process by resting the mice for an extended period of time after the final exposure to aerosolised LPS. Mice were exposed to LPS for 2 weeks and examined 4 or 8 weeks after the final exposure. Mice were then sacrificed and the lungs processed for morphometric analysis. The MLI remained elevated (n = 4-6 mice per group; ~35µm) compared to saline (vehicle) treated controls at 4 or 8 weeks (**Figure 2-7A**) following the last LPS exposure with no significant difference from mice rested for 0 weeks (6 days). Similarly, there was no significant increase in LPS-induced percentage alveolar airspace in mice that were rested for 0, 4 or 8 weeks (**Figure 2-7B**).

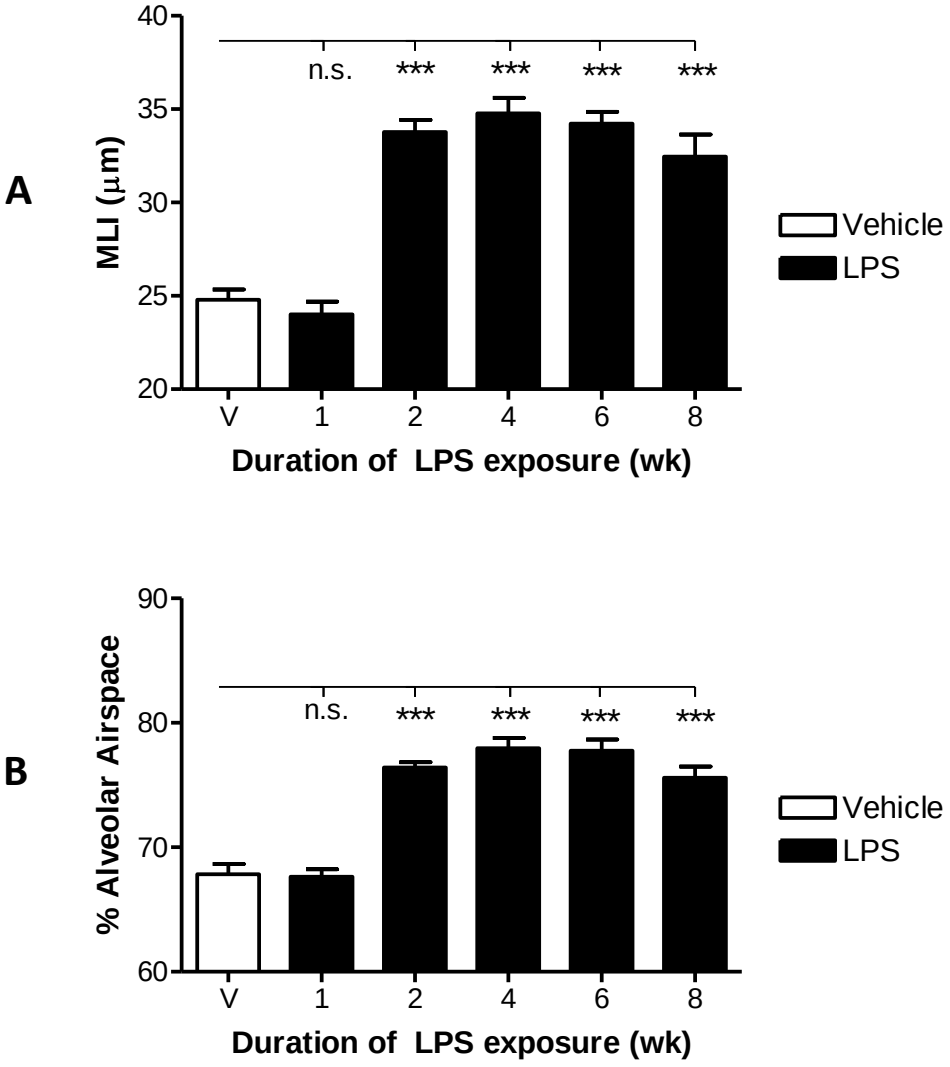

Figure 2-5: Aerosolised LPS induced an increase in mean linear intercepts (MLI) and percentage alveolar airspace in the lungs of BALB/c WT mice after 2 weeks exposure. Mice were exposed to either aerosolised saline (vehicle (V); open bars) for 8 weeks, or aerosolised LPS (30min, 500μg LPS/10ml V at 25Pa; closed bars) for 1, 2, 4, 6, or 8 weeks. Mice were sacrificed 6 days after the final LPS exposure. The mean linear intercept (MLI) **(A)** and percentage alveolar airspace **(B)** were determined and compared to the vehicle only treated group. n = 4-6 mice per group. ***P<0.0005, n.s. = not significant, Student's unpaired t-test.

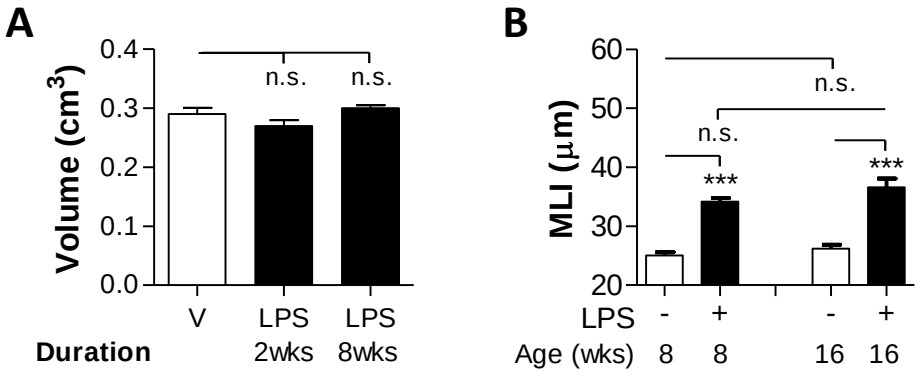

Figure 2-6: LPS exposure does not alter lung volume and changes in phenotype are still evident in older mice. Lung volume was compared between mice exposed to aerosolised saline (vehicle (V)) for 8 weeks (open bar), to mice exposed to aerosolised LPS (solid bars) for 2 or 8 weeks **(A).** The MLI of mice exposed to aerosolised vehicle (open bars) or LPS (solid bars) is similar regardless of whether they were 8 or 16 weeks old at the time of first exposure **(B).** n = 5-6 mice per group. ***P<0.0002, n.s. = not significant, Student's unpaired t-test.

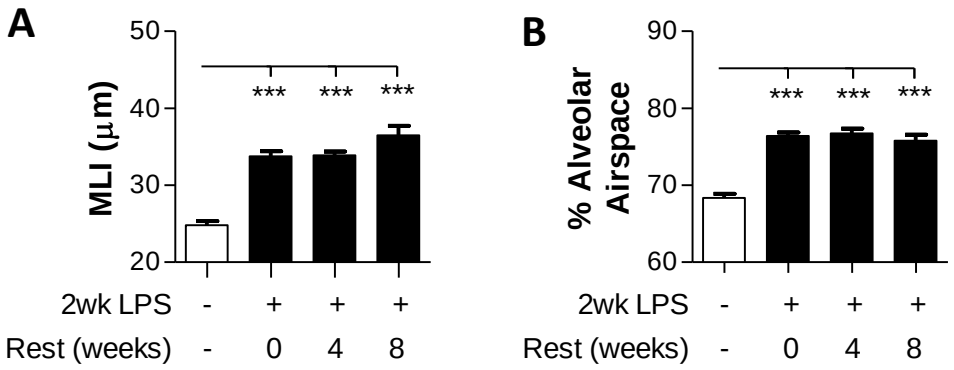

Figure 2-7: LPS-induced alveolar enlargement was not resolved after an 8 week resolution phase. BALB/c WT mice were exposed to aerosolised LPS (solid bars) for 2 weeks and allowed to rest for 4 or 8 weeks. Mice were then sacrificed and the lungs processed to determine MLI **(A)** and percentage alveolar tissue **(B)**. n = 4-6 mice per group. There was no significant differences between LPS treated groups. ***P<0.0001, Student's unpaired t-test.

2.3.7 Role of MyD88 in LPS-induced emphysema

BALB/c MyD88$^{-/-}$ mice were exposed to aerosolised LPS or saline (vehicle) for 2 weeks. Mice were sacrificed 6 days after the last LPS exposure and lungs were processed for morphometric analysis (**Figure 2-8**). There was no significant difference in MLI or percentage alveolar airspace between vehicle or LPS treated MyD88$^{-/-}$ mice (n = 5). These results suggest that the development of LPS-induced emphysematous-like lesions in the lung is dependent on the adaptor protein MyD88.

In contrast, there was a significant difference in MLI and percentage alveolar airspace between BALB/c WT and BALB/c MyD88$^{-/-}$mice in the vehicle treated groups (**Figures 2-8A and B**).

2.3.8 Role of MyD88 in LPS-induced inflammation

To investigate the characteristics of the LPS-induced inflammatory response BALB/c WT mice and BALB/c MyD88$^{-/-}$ mice were exposed to aerosolised LPS for 2 weeks and sacrificed at 6 hours, 2, 3 and 6 days after the final exposure to LPS. The lungs were collected and single cell suspensions generated for flow cytometric analysis to determine the number of neutrophils ($CD11c^{-}CD11b^{+}GR1^{hi}F4/80^{-}CD45^{+}FSC^{med}SSC^{med}$) and macrophages ($CD11c^{+}CD11b^{lo}GR1^{-}F4/80^{+}CD45^{hi}FSC^{hi}SSC^{med}$).

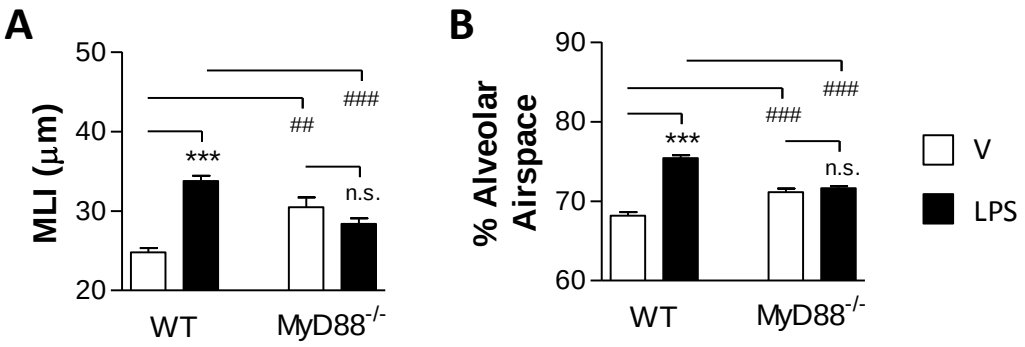

Figure 2-8: Aerosolised LPS-induced increase in MLI and percentage alveolar airspace is MyD88-dependent. BALB/c WT (WT) mice and BALB/c MyD88-deficient mice (MyD88$^{-/-}$) were exposed to aerosolised LPS for 2 weeks. The lungs were analysed for MLI **(A)** and percentage alveolar airspace **(B).** Open bars represent mice exposed to saline only (vehicle), while solid bars represent mice exposed to aerosolised LPS. n= 5-6 mice per group. ***P<0.0001, $^{\#\#}$P<0.002, $^{\#\#\#}$P<0.001, n.s. = not significant, Student's unpaired t-test.

There was a rapid and significant peak in neutrophils in the lungs of WT mice 6 hours (~0.6 x10^6 cells; n = 5; P<0.0001) after the last LPS treatment compared to saline (vehicle) treated controls (**Figure 2-9A**). This neutrophilia had resolved back to baseline (~0.15 x 10^6 cells; n = 5) 3 days after the final LPS exposure. In contrast, LPS-induced neutrophilia in MyD88$^{-/-}$ mice was significantly (n = 5 mice per group; P<0.0001) abrogated compared to their WT counterparts during the peak of inflammation.

Interestingly, macrophage numbers in WT mice were also observed to increase significantly 6 hours after the final LPS exposure (~0.75x10^6 cells; P<0.005), however their peak was not observed until day 2 (~1.6x10^6 cells; P<0.0001) (**Figure 2-9B**). The number of macrophages gradually declines over the next 96 hours to return to baseline (~0.6x10^6 cells; n = 4-5 mice per group).

Similarly to the neutrophils, the influx of macrophages induced through LPS exposure was completely abrogated in MyD88$^{-/-}$ mice compared to their WT counterparts (**Figure 2-9B**).

We next temporally characterised inflammation after each LPS exposure in the 2 week induction model of LPS induced emphysema. BALB/c WT mice were exposed to aerosolised vehicle or LPS and sacrificed at 6, 48 and 72 hours after each exposure (1x, 2x, and 3x) (**Figure 2-10**). Single cell suspensions were generated from lung tissue for flow cytometric analysis to enumerate neutrophils and macrophages. The profile after the 4th exposure to vehicle or LPS was from

the results observed in **Figure 2-9**. Lung tissue was also collected to determine whether there were any changes to proinflammatory genes and/or proteins, active caspase-3 activity, messenger RNA (mRNA) and/or protein levels of specific apoptosis related genes.

The number of neutrophils in the lungs rapidly increased 6 hours after each LPS exposure and consistently resolved back to baseline by 72 hours. This demonstrates that this 2 week exposure model does not induce endotoxic tolerance, nor does it induce the persistent accumulation of neutrophils in the lungs.

In contrast to neutrophils, macrophages were found to peak consistently 3 days after each LPS exposure (**Figure 2-10B**). We expected constant accumulation of macrophages over the duration of the 2 week model as prior to each LPS exposure inflammatory macrophages peaked in numbers. However, immediately (6 hours) following each LPS exposure the number of macrophages dropped rapidly followed by a continual increase until the next LPS exposure.

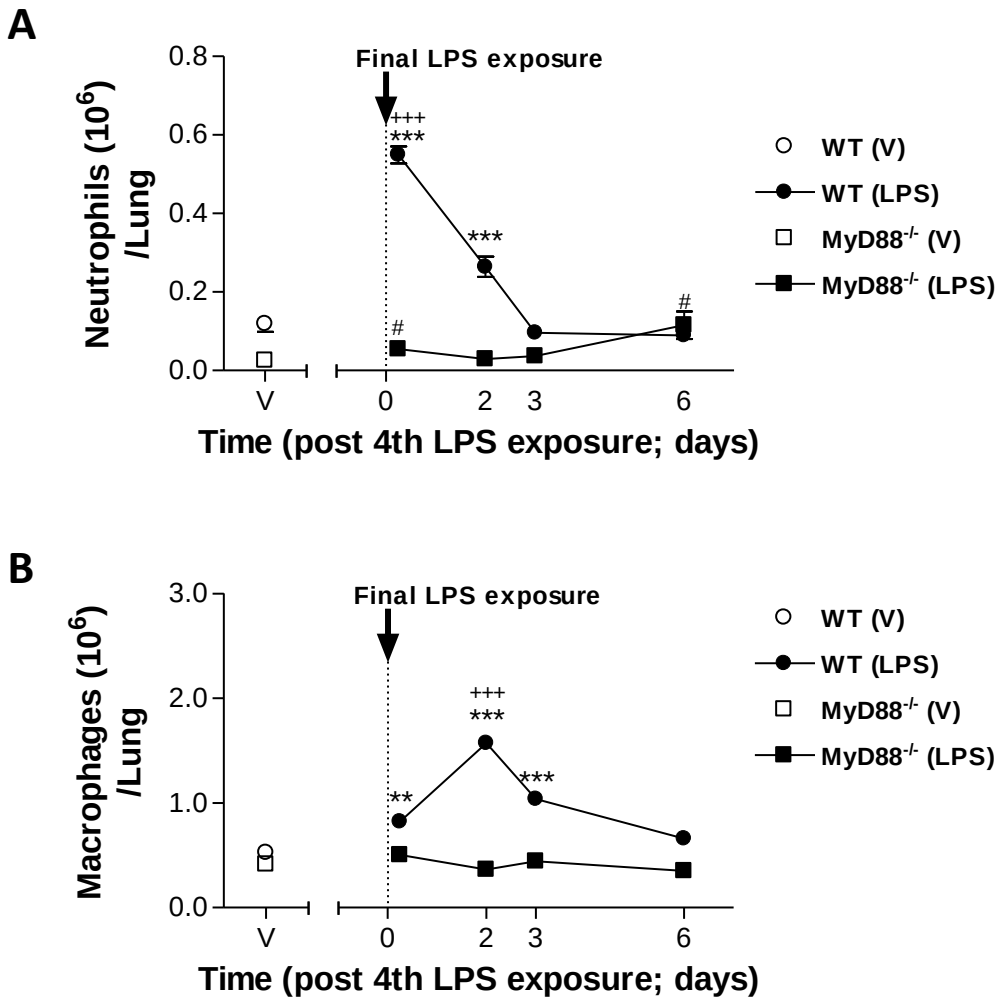

Figure 2-9: Inflammatory cell profile of neutrophils and macrophages in the lungs of BALB/c WT vs BALB/c MyD88$^{-/-}$ mice after the final exposure to aerosolised LPS. WT (circles) and MyD88$^{-/-}$ (squares) mice were exposed to aerosolised saline only (vehicle (V); open circle or square) or LPS (solid circles or squares) for 2 weeks. Mice were sacrificed at 6 hours, 2, 3 and 6 days after the final LPS exposure. Single cell suspensions were generated from the lungs and flow cytometry was used to enumerate **(A)** neutrophils and **(B)** macrophages. n = 4-5 mice per group. **P<0.005, ***P<0.001 (WT+LPS vs WT+Sal); #P<0.05 (MyD88$^{-/-}$ +LPS vs MyD88$^{-/-}$ +Sal); +++P<0.0001 (WT+LPS vs MyD88$^{-/-}$ +LPS), Student's unpaired t-test.

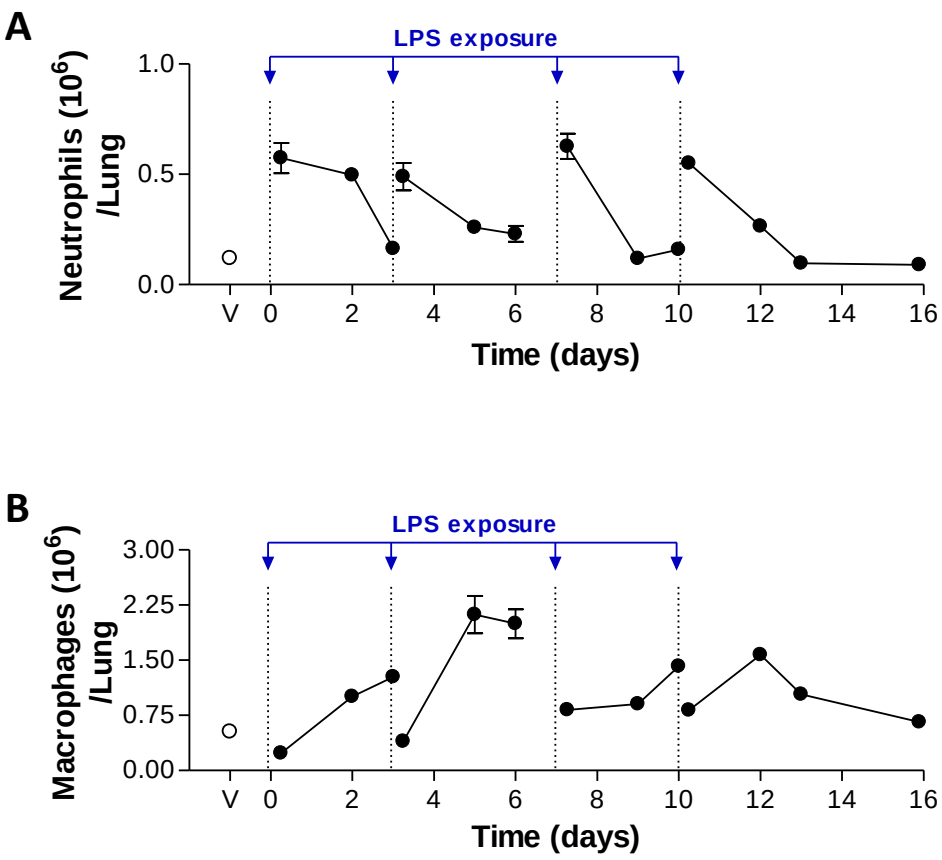

Figure 2-10: Recruitment of neutrophils and macrophages in the lungs of BALB/c WT mice after each exposure in the 2 week LPS model. WT mice were exposed to aerosolised vehicle only (open circles; V) or LPS in a 2 week model. Separate groups of mice were sacrificed at 6 hours, 2 and 3 days after each LPS exposure. Single cell suspensions were generated from lungs and neutrophils **(A)** and macrophages **(B)** enumerated *via* flow cytometry. Here we have included the profile from **Figure 2-9** to complete the inflammatory profile.

2.3.9 LPS and CD11c expression on alveolar macrophages

From the inflammatory studies, we observed total cell numbers obtained from excised lungs between 72hrs after LPS exposure versus 6 hours after subsequent LPS exposure to be similar and these numbers were significantly higher than control mice treated with saline (vehicle). However, the inflammatory profile of macrophages shown in **Figure 2-10** showed that at these specific times, there was a marked drop in alveolar macrophages. To elucidate these differences, we investigated the expression of CD11c on infiltrating cells. Three new groups of mice were set up as follows: group 1: vehicle treated controls, group 2: 2xLPS + 3 days rest, and group 3: 3xLPS + 6 hours rest. The mice were sacrificed together, single cell suspensions generated from lung tissue and total cell counts performed. Mice treated with LPS (groups 2 and 3) had significantly higher total cell counts (n = 5; $P<0.005$ and $P<0.0001$) than vehicle treated animals (**Figure 2-11A**). This confirms our first observation of similar increased total cell count between the 2 groups.

Next, we investigated CD11c expression on the surface of broncho-alveolar lavaged (BAL) cells isolated from the lungs of naïve BALB/c WT mice followed by stimulation with LPS *in vitro*. There was a significant decrease (n = 4 samples; $P<0.02$) in the number of $CD11c^+$ expressing cells detected following pretreatment with LPS compared to culture media only treated cells (**Figure 2-11 B**).

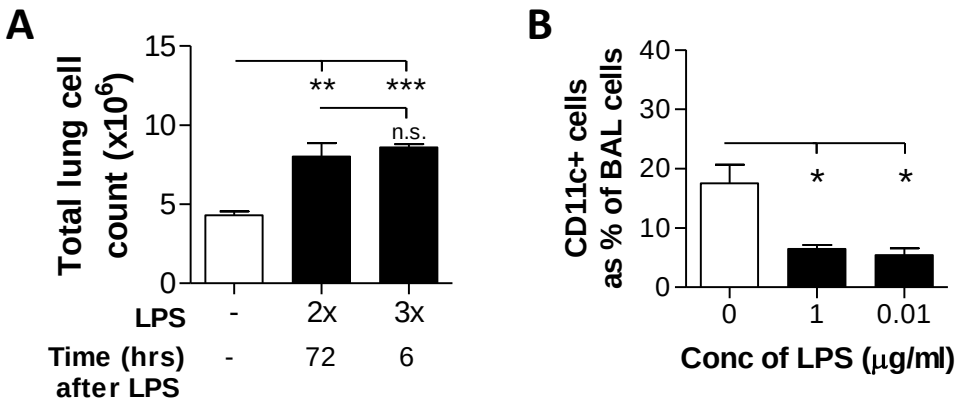

Figure 2-11: LPS increases total cell count in lungs but down-regulates CD11c expression on alveolar macrophages *in vitro*. (A) Total cell counts from lung tissue of saline (vehicle) treated mice (open bar), compared to LPS treated mice (2xLPS+72hrs rest, 3xLPS+6hr rest) (both solid bars). (B) Lavaged alveolar cells were incubated with culture media only (control; open bar) or LPS (solid bars) at different concentrations *in vitro* for 3 hours. After treatment, alveolar macrophages were identified and enumerated using flow cytometry. n = 4-5 mice or sample wells. *P<0.02, **P<0.005, ***P<0.0001, n.s.= not significant, Student's unpaired t-test.

2.3.10 LPS and proinflammatory cytokines in the lung

The concentrations of the proinflammatory cytokines TNF-α, IL-1β and IL-6 in the lungs of mice during a 2 week exposure to aerosolised LPS was determined by ELISA. There was a significant and rapid increase in the concentration of all three cytokines in the lungs after just 6 hours from exposure to LPS (**Figure 2-12A - C**)**.** The concentration of all cytokines returned to baseline by 48 hours. Interestingly, there was approximately a 3 fold higher concentration of TNF-α produced at 6 hours after the first LPS exposure, as compared to the same time point after the 2^{nd}, 3^{rd} and 4^{th} LPS exposure. However this was not observed with IL-1β and IL-6 protein levels.

Our data demonstrated that protein expression of TNF-α, IL-1β, and IL-6 is rapidly enhanced as early as 6 hours after LPS exposure. As messenger RNA precedes protein production, investigating messenger RNA levels at a time point prior to 6 hours after LPS exposure may provide us with additional insights into the kinetics of mRNA versus protein production. To investigate this, 4 groups of BALB/c WT mice were exposed to 1x, 2x, 3x, or 4x aerosolised LPS and sacrificed immediately after exposure. Lungs were excised and stored in RNA-later until further analysis. The level of mRNA expression was expressed as a fold change over the control group (vehicle treated) (**Figure 2-13**). Exposure to LPS induced a significant and rapid increase in expression of mRNA in the lungs of each of the three proinflammatory cytokines compared to control mice (TNF-α: >80 fold, IL-1β: >10 fold, and IL-6: > 50 fold) (n = 4-5 mice per group; $P<0.05$). Interestingly,

the relatively constant mRNA expression across all LPS treatment groups suggests there was no acute endotoxic tolerance induced as a result of the repeated exposures.

2.3.11 LPS and proinflammatory chemokines in the lung

Changes in the level of mRNA of the genes associated with the inflammatory response during the second week of LPS exposure were quantified in lung tissue. mRNA levels for MMP-9, MMP-12, CCL-2 (MCP-1), CCL3 (MiP-1α) were determined 48hours after the last LPS exposure. mRNA was expressed as a fold change over saline (vehicle) treated mice (mice exposed to 4x vehicle and sacrificed 48 hours after the last exposure). Levels of MMP-9 remain relatively unchanged throughout the treatment (**Figure 2-14A**), however mRNA levels for MMP-12, CCL-2, and CCL3 were significantly enhanced (n = 4-5 mice per group; $P<0.05$) in the second week of LPS exposure (**Figure 2-14B-D**), especially after the last exposure on day 12, as compared to the first week.

We also compared protein levels for CCL3 by ELISA between mice exposed to 4x vehicle or LPS, 48 hours after the last exposure (**Figure 2-14E**). LPS treatment was found to induce a significant increase (n = 4-5 mice per group; $P<0.05$) in the level of CCL3 protein compared to control mice. In contrast, by 72 hours after the last LPS exposure, mRNA for MMP-12 and CCL3 (the two most prominent changes in mRNA levels at 48hours) were no longer significantly different from control groups (**Figure 2-14F and G**).

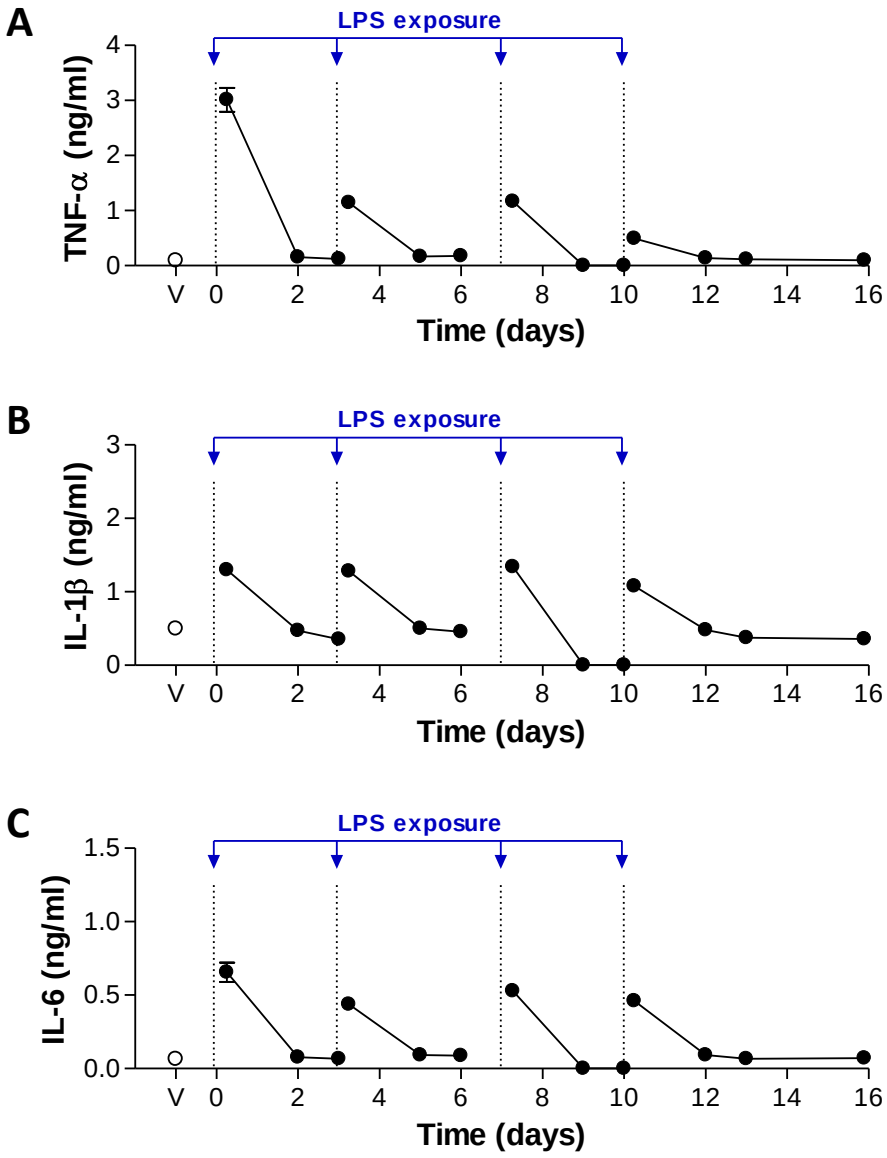

Figure 2-12: Proinflammatory cytokines profile in the 2 week LPS exposure model. BALB/c WT mice were exposed to aerosolised saline only (vehicle (V); open circles) or LPS (solid circles) for 2 weeks. Mice were sacrificed at 6 hours, 2 and 3 days after each LPS exposure, as well as 6 days after the final LPS exposure (day 16). Lungs homogenates were obtained and protein levels of **(A)** TNF-α, **(B)** IL-1β, and **(C)** IL-6 were determined by ELISA.

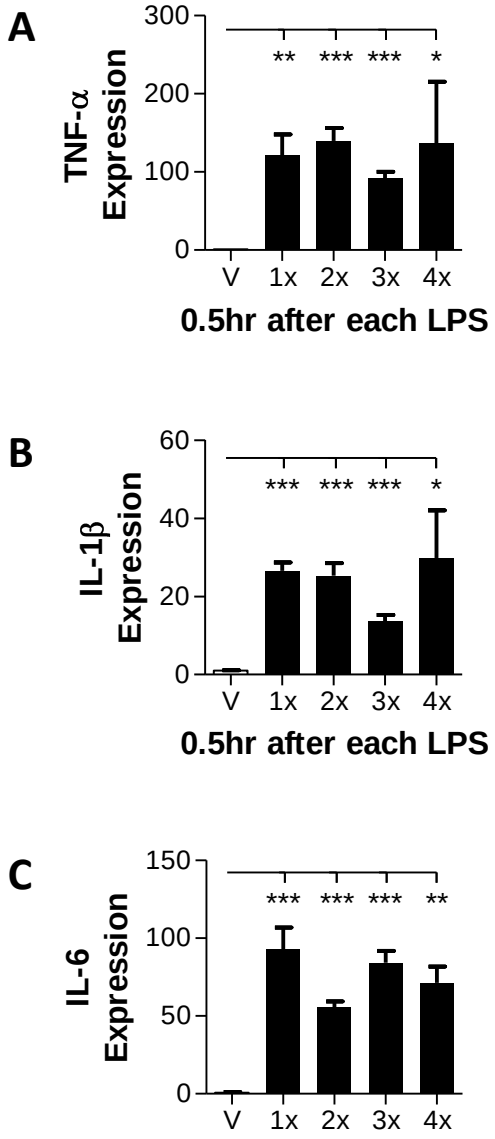

Figure 2-13: Messenger RNA expression of inflammatory cytokines 30mins after each LPS exposure during a 2 week LPS model. Mice were exposed to aerosolised saline only (vehicle (V); open circles) or aerosolised LPS (solid circles) in a 2 week model. Mice were sacrificed immediately after exposure to LPS (30mins from start of exposure) and mRNA expression levels of proinflammatory cytokines **(A)** TNF-α, **(B)** IL-1β, and **(C)** IL-6 in lung tissue were determined by real time quantitative-PCR (RT qPCR). n = 4-5 mice per group. *P<0.05, **P<0.002, ***P<0.0004, Student's unpaired t-test.

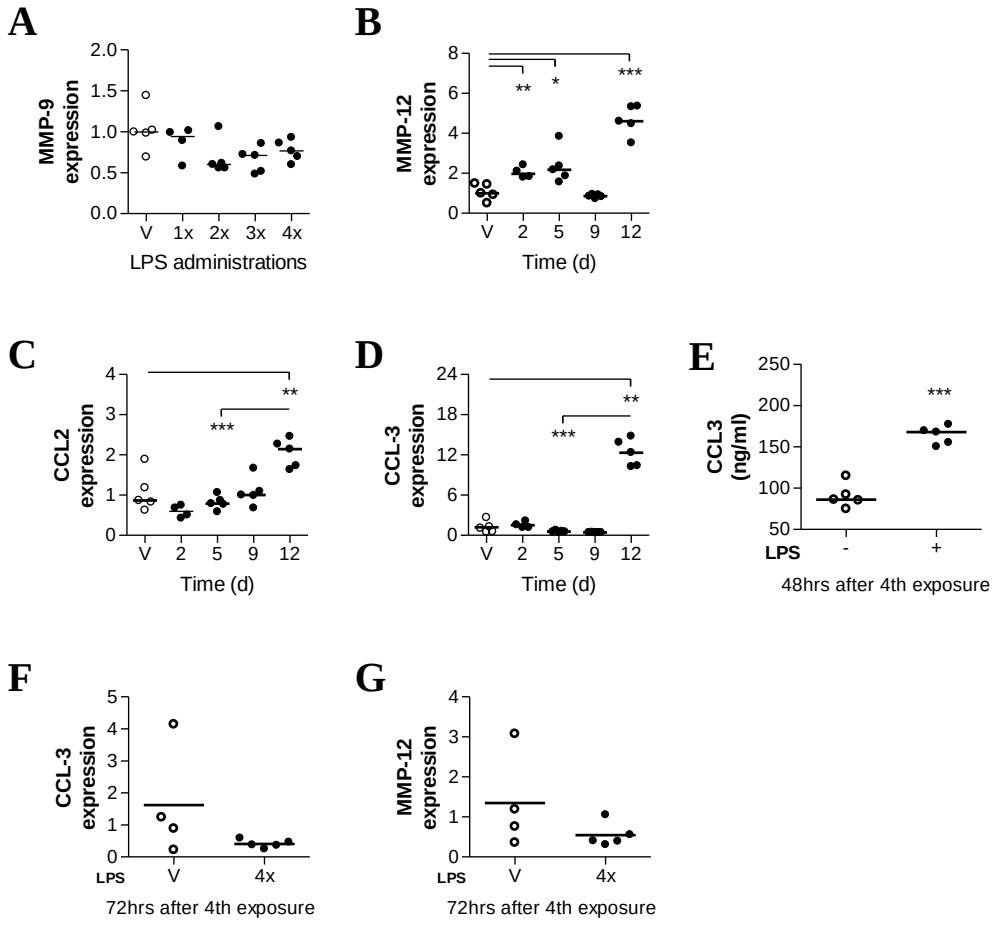

Figure 2-14: mRNA levels of LPS-induced inflammatory-associated proteins are enhanced in the 2nd week of LPS exposure. BALB/c WT mice were exposed to aerosolised LPS (closed circles) for 2, 5, 9, or 12 days and were sacrificed 48 hours after the last exposure for each timepoint (A, B, C, D). Control mice were exposed to saline (vehicle (V); open circles) and sacrificed 48 hours after the last exposure. mRNA for MMP-9, MMP-12, CCL-2 (MCP-1), and CCL3 (MiP-1α) was determined by qPCR and expressed as fold change over controls group. Mice were also exposed to 4x vehicle or LPS and sacrificed 48 hours after the last exposure and the concentration of CCL3 protein in lung tissue determined by ELISA (E). Mice were exposed to 4x Vehicle or LPS and sacrificed 72 hours after the last exposure and the fold change in mRNA for CCL3 and MMP-12 was determined (F, G). n = 4-5 mice per group. *P<0.05, **P<0.002, ***P<0.0004, Student's unpaired t-test.

2.3.12 LPS and Apoptosis

Next, we determined the effects of LPS exposure on the production of ceramide and active caspase-3 in the lungs. BALB/c WT mice were exposed to aerosolised saline (vehicle (V); control group) or LPS in the 2 week LPS model, and sacrificed 3 or 6 days after the final exposure. The lungs were excised from mice sacrificed on day 3, and single cell suspensions generated. Cells were stained for macrophages ($CD11c^{+}CD11b^{-}$), ceramide and active caspase-3. Mice sacrificed 3 days after the last LPS exposure had a significantly increased (n = 4-6 mice per group) percentage of ceramide positive (~30%; P<0.0002) and active caspase-3 positive (~7%) macrophages found in the lungs compared to vehicle treated mice (18% ceramide positive, and 1.7% active caspase-3 positive macrophages) (**Figure 2-15A**). The mice sacrificed 6 days after the final LPS exposure were used for immunohistochemistry staining for ceramide (representative images **Figure 2-15C**) or active caspase-3 in the lungs. Lung sections were imaged at random positions at 400x magnification and the number of ceramide positive and active caspase-3 alveolar macrophages per field enumerated. Exposure to LPS resulted in a significant increase (n = 5-7 mice per group; P<0.02) in the average number of ceramide positive macrophages per field (~5/field) compared to vehicle treated controls (~2/field), as well as an increase (n = 5-7 mice per group; P<0.0002) in the number of active caspase-3 positive macrophages (~3/field) compared to vehicle treated animals (~1/field) (**Figure 2-15B**).

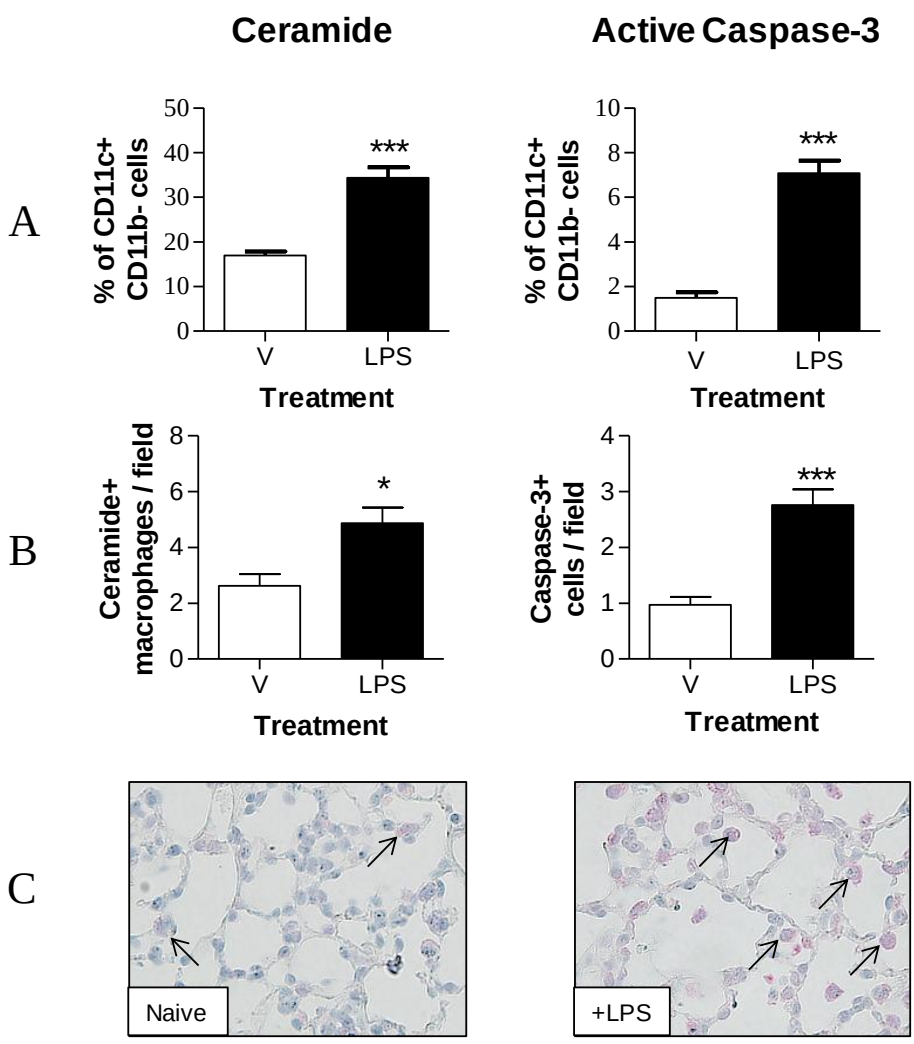

Figure 2-15: LPS-induced increase in ceramide and active caspase-3 in the lungs of mice. BALB/c WT mice were exposed to saline (vehicle (V); open bars) or aerosolised LPS (solid bars) in a 2 week LPS model. **(A)** Single cell suspensions of lung from mice were obtained 3 days after the last LPS exposure to determine the percentage of macrophages (CD11c+CD11b-) that were Ceramide or active caspase-3 positive by flow cytometry. **(B)** Similarly, lung sections were processed from mice sacrificed 6 days after the last LPS exposure and immunohistochemistry (IHC) used to detect the number of cells positive for Ceramide or active caspase-3. **(C)** Representative images of histology sections stained for Ceramide (pink; black arrows). n = 4-7 mice per group. *P<0.02, ***P≤0.0002, Student's unpaired t-test.

2.3.13 Age-dependent development of emphysema in TLR-deficient mice

Intrigued by the findings of Patty and colleagues (2006), that TLR-deficient mice (e.g. TLR4$^{-/-}$) on a C57BL/6 background develop spontaneous emphysematous-like lesions as they age (past 8 weeks of age), we investigated whether TLR-deficient BALB/c mice exhibit a similar phenotype. Briefly, BALB/c WT, BALB/c TLR2$^{-/-}$, BALB/c TLR4$^{-/-}$, BALB/c TLR2$^{-/-}$TLR4$^{-/-}$, and BALB/c MyD88$^{-/-}$ were sacrificed when the mice reached ages 8, 12 and 16 weeks. All mice were naive. Percentage alveolar airspace was measured and the results confirmed the findings of Patty Lee and colleagues. All TLR-deficient mice exhibited significantly higher percentage alveolar airspace compared their age-matched WT counter parts. The loss of parenchymal tissue was the most severe in TLR2$^{-/-}$TLR4$^{-/-}$ mice.

As shown in **Figure 2-16D**, we compared the percentage alveolar airspace from the aging naïve MyD88$^{-/-}$ mice to the data we previously obtained in **Figure 2-8B** (WT or MyD88$^{-/-}$ mice treated with vehicle or LPS). The results demonstrate that firstly mice (WT or My88$^{-/-}$) exposed to aerosolised vehicle do not exhibit increased percentage alveolar airspace (comparable values to naïve mice). Secondly, the comparisons further confirmed that LPS induced emphysema is MyD88-dependent.

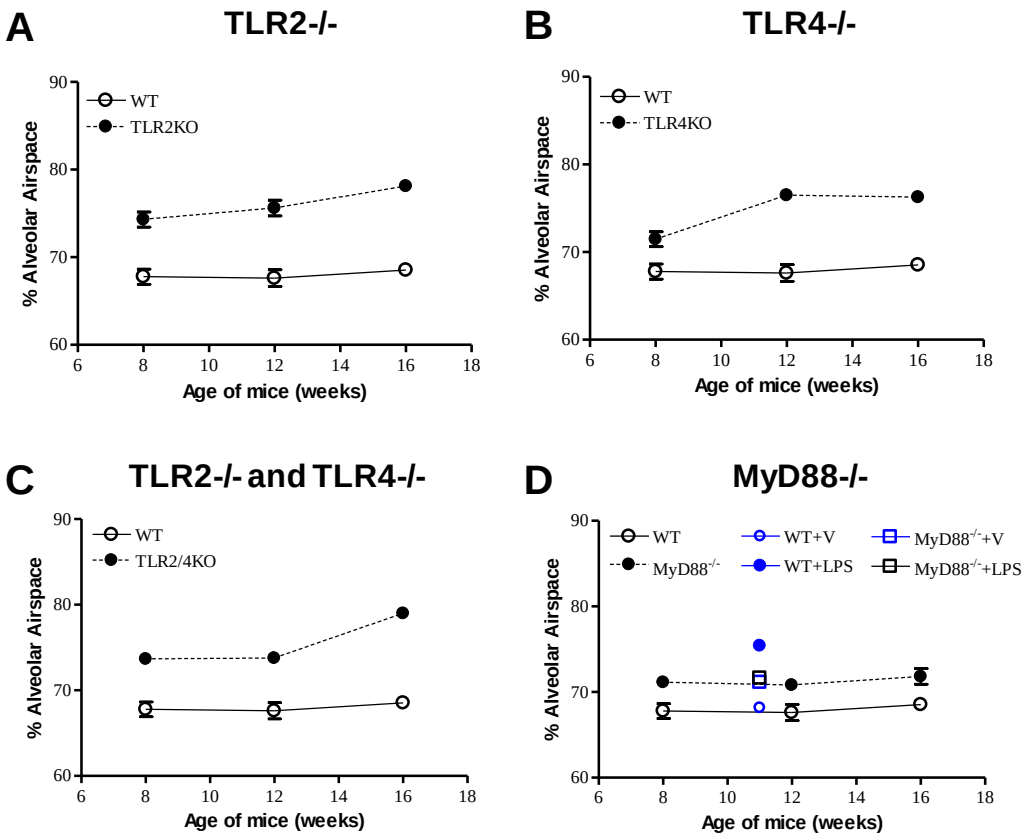

Figure 2-16: Age-dependent emphysema onset in TLR-deficient mice. (A) TLR2$^{-/-}$, **(B)** TLR4$^{-/-}$, **(C)** TLR2$^{-/-}$TLR4$^{-/-}$, and **(D)** My88$^{-/-}$ mice were allowed to age without treatment (naïve) and sacrificed at 8, 12, or 16 weeks old. Percentage alveolar airspace was determined. Data from Figure 2-8 was compared [WT+Vehicle (V) (open blue circle); WT+LPS (solid blue circle); My88$^{-/-}$+V (open blue square); My88$^{-/-}$+LPS (open black square)]. n= 5-6 mice per group. All points between solid circle and open circles in the same age group are significant (P<0.0001). Difference between open blue square and open black square is not significant (P>0.05), Student's unpaired t-test.

2.4 Discussion

Although cigarette smoke has been recognised as a significant risk factor in the development of COPD, only 15-25% of smokers go on to develop emphysema (Lindberg *et al.*, 2006; Warburton *et al.*, 2006; Roth, 2008). Importantly, cessation of smoking does not inhibit the progression of the disease. Emphysema patients also suffer from periodic exacerbations commonly associated with bacterial infections. One of leading causes is the gram negative bacteria non-typeable *Haemophilus influenzae* (NTHi).

LPS is a common endotoxin produced by gram negative bacteria such as NTHi. While LPS is detected ubiquitously in the environment, it is also found in unusually high levels in cigarettes (presumably arising from the tobacco leaves). Thus, we hypothesised that LPS plays a significant role in the development of emphysema. Previous animal models of emphysema have demonstrated that long term exposure to LPS can induce the hallmark features of emphysema such as the loss of parenchymal airway tissue through apoptosis in the lungs of mice (Vernooy *et al.*, 2002). We can also demonstrate that LPS exposure induces emphysematous-like lesions in a mouse model.

The initial stage of the investigation was to determine whether we could replicate the findings of Vernooy and colleagues. The model employed by Vernooy involved exposing 8 week old mice to 5µg of LPS twice per week, for a period of 12 weeks *via* intratracheal instillation and calculating the mean linear intercepts of the lung airway. Mice subjected to LPS treatment showed higher

MLI compared to control mice. Indeed, as shown in Figure 2-3, we were able to replicate their findings. Using morphometric analysis, we characterised the alveolar enlargement using two different methods; measurement of MLI and determining the percentage of alveolar airspace. MLI is a measurement of the average diameter between alveolar walls in the lungs of the particular section, while and an increase in MLI indicates the development of emphysematous-like lesions. Similarly, the percentage alveolar airspace is a semi-quantitative measurement of the percent of alveolar airspace in the lung excluding airway branches (bronchus and bronchioles) and blood vessels. We observed that while the MLI is a more tedious process, it provides a more accurate representative measurement of lung structure (or alveolar airspace) compared to the percentage alveolar airspace.

By using two different methods, we also discovered that the conventional method of MLI measurement yielded results which may be flawed in determining the true condition of the airways. In conventional methods, lines that fall on non-parenchyma (eg bronchial airways or blood vessels) are discounted (D'hulst *et al.*, 2006) or only images that are devoid of non-parenchymal structures were chosen (Robbesom *et al.*, 2003). We found that by using this traditional method, some of our initial measurements did not tally with our percentage alveolar airspace measurements (which takes into account all structures in the image as described in section 2.2.3). By revising the method, when we took into account all lines

(whether they crossed non-parenchymal structures or not), the resulting MLI values corresponded with the percentage alveolar airspace.

The levels of LPS found inside the homes of smokers is several fold higher than inside the homes of non smokers (Sebastian *et al.*, 2006). The intratracheal (i.t.) method of substance administration is invasive and therefore may not be an ideal model to investigate the exposure of humans to LPS in the environment. Indeed, we found a small but significant difference in MLI between mice exposed to saline *via* the i.t. route compared to aerosol exposure (Figure 2-4A and B), suggesting that the i.t. method may contribute to changes in lung structure.

Therefore, we developed a model whereby mice were exposed to aerosolised LPS in a whole body environment. We found that delivery of LPS or saline *via* an aerosol did not affect results obtained with MLI or percentage alveolar airspace compared to the traditional i.t. methods (Figure 2-4). Indeed, our results were similar to those obtained by Vernooy and colleagues (2002). Thus we had generated a mouse model of LPS-induced emphysema using a delivery method (aerosol) which was more akin to the everyday exposure of humans to ubiquitous LPS in the environment.

Next we wanted to determine if we could develop an aerosol model with a shorter exposure that would still elicit the desired response. We found that just 2 weeks of aerosol exposure to LPS (Figure 2-5) was enough to induce the development of emphysematous-like lesions similar that that observed in mice

exposed for up to 8 weeks. Intriguingly, mice showed no significant changes to MLI or percentage alveolar airspace if exposed to only 1 week of aerosolised LPS. This suggested that there may be a requirement for certain factors to build up post LPS exposure before emphysematous-like lesions begin to develop. It also suggests that the persistent bacterial or viral lung infections in emphysema patients may continue to drive disease development even after the cessation of smoking.

Emphysema in humans not only causes the enlargement of airspaces due to the deterioration of lung structure, but also an increase in overall lung size. This occurs due to hyper-expansion as a result of easy filling of the lung with air but poor emptying during breathing meaning that some patients have to undergo lung volume reduction surgery (Hillier J, 2004; Schipper *et al.*, 2004). To determine that the LPS-induced increase in MLI and percentage alveolar airspace in our model was not due to expansion of the lungs, lung volumes were compared. We demonstrated that lung volumes between mice exposed to saline for 2 weeks, or LPS for 8 weeks were not significantly different (Figure 2-6A) suggesting that the changes observed in MLI is due to a loss of parenchymal structure.

It has been demonstrated that there is minimal growth in the murine lung past young adulthood (Mund *et al.*, 2008). We therefore investigated whether the lungs of mice were fully developed by 8 weeks of age. We exposed 16 week

old mice to aerosolised saline or LPS for 2 weeks. There was a significant increase in MLI in LPS treated mice compared to controls and these results were also comparable (not significantly different from) to those observed in 8 week old mice (Figure 2-6B). The constant lung volume in vehicle and LPS treated mice, together with the similar phenotype observed in 16 week old mice suggests that the increase in MLI is likely due to the destruction or loss of alveolar lung tissue and not from an increase in lung volume or under-development of the alveolar walls.

As our data indicated that emphysematous-like lesions induced by LPS were maximal after 2 weeks of exposure and sustained for at least 4 weeks, this model was used for more detailed characterisation of inflammation.

To further test if the characteristics of LPS induced emphysematous-like lesions in mice resembled those in humans, we investigated whether the process was reversible if the mice were rested for an extended period of time after the final LPS exposure. The MLI (approximately 34µm) was not significantly different between mice rested for 0 weeks (mice sacrificed 6 days after final LPS exposure), 4 or 8 weeks (Figure 2-7). This trend was also reflected in the percentage alveolar airspace data, demonstrating that aerosolised LPS-induced alveolar enlargement is an irreversible process similar to that observed in the human condition.

BALB/c MyD88$^{-/-}$ mice were used to investigate whether the development of LPS-induced emphysematous-like lesions is MyD88-dependent. The

development of LPS-induced emphysematous-like lesions was significantly attenuated in MyD88$^{-/-}$ mice (Figure 2-9), suggesting that LPS-induced emphysema is a MyD88-dependent process. BALB/c MyD88$^{-/-}$ mice exposed to aerosolised saline exhibited a small but significant increase in both MLI and percentage alveolar airspace. TLR4 has also been implicated in maintaining the integrity of airway structures during lung injury by interactions with hyaluronans and associated fragments (Noble and Jiang, 2006; Jiang *et al.*, 2007; Jiang *et al.*, 2011). The loss of the MyD88 signalling pathway could have affected the development of the lung during or after alveolarisation. Interestingly, it has now been demonstrated that TLR$^{-/-}$ mice (C57BL/6 background) can exhibit age-dependent emphysema (Patty J. L. *et al.*, 2006). Similarly, TLR2$^{-/-}$, TLR4$^{-/-}$, and TLR2$^{-/-}$TLR4$^{-/-}$ mice showed significantly greater alveolar enlargement compared to WT naive counterparts from 8 weeks of age, and this further increases as the mice continue to age beyond 12 weeks. The spontaneous emphysema development in the TLR$^{-/-}$ mice was attributed to an increase in oxidative stress in the lungs (Patty J. L. *et al.*, 2006). However, unlike other TLR$^{-/-}$ mice, the small increase in percentage alveolar airspace observed in MyD88$^{-/-}$ mice compared to age-matched counterparts remained constant as the mice aged. The data in Chapter 2 Figure 2-16D, together with Figure 2-8B confirms LPS-induced emphysema-like lesions is MyD88-dependent. These findings strongly suggest that 1) TLRs may play essential roles other than specific pathogen sensing; and 2)

we may need to use younger TLR4$^{-/-}$ mice and age matched WT controls should we wish to determine the role of TLR4 in LPS-induced emphysema.

Next, we characterised the inflammatory response to LPS exposure. The number of neutrophils in the lungs peaked within 6 hours following LPS exposure (Figure 2-10) and this preceeded the peak in macrophage numbers. The level of the inflammatory response was consistent between LPS exposures. Neutrophil numbers had resolved back to baseline prior to each LPS exposure (within 48 hours), however, the number of macrophages did not resolve until much later (over 72 hours). This suggested that localised alveolar macrophages and infiltrating inflammatory monocytes/macrophages may play important roles associated with emphysema development (Taylor *et al.*, 2004). In contrast, LPS-induced neutrophilia and macrophage influx was abrogated in MyD88$^{-/-}$ mice. These results once again demonstrate that LPS-induced inflammation (neutrophils and macrophages) is in part involved with TLR4 signalling and is MyD88-dependent.

The different response between macrophages and neutrophils suggests that endotoxic tolerance did not occur. Interestingly, repeated stimulation with LPS in the 2 week model does not induce an accumulation of neutrophils. In contrast, macrophages accumulate in the lung over time. Since macrophages are long living cells, their extended presence at the site of inflammation (the lung) may play a more central role to LPS-induced emphysema.

Intriguingly, the profile of macrophages gave rise to some unusual observations. We expected to see a constant accumulation of macrophages over the duration of the 2 week model, however the number of macrophages showed a rapid drop immediately following (6 hours) LPS exposure, followed by an increase peaking 3 days later (Figure 2-10). This rapid change in macrophage numbers warranted further investigation. The total cell numbers between saline, 2xLPS + 72hrs rest, and 3xLPS + 6hrs rest were compared and found to be significantly increased (compared to vehicle) in both LPS treatment groups. This suggested that there was no outward movement of cells from the lung. Therefore, we hypothesised that LPS stimulation may have led to the down-regulation of cell surface markers used in our flow cytometric analysis rather than a major out-flux of cells from the lung or apoptosis.

We therefore cultured alveolar macrophages obtained from the BAL fluid of naïve BALB/c WT mice in the absence or presence of LPS and analysed them by flow cytometry to evaluate the number of cells expressing CD11c, the primary cell surface marker on macrophages. To our surprise, LPS treatment resulted in the down-regulation of CD11c on the surface of macrophages. While this is a new and novel observation, it requires much further investigation, such as whether this down regulation is transient or permanent, whether the same effect is observed in interstitial macrophages, is the effect TLR4 dependent, and the possible reasons the two LPS doses elicited the same effect.

Next, we also characterised the expression profiles of three proinflammatory cytokines TNF-α, IL-1β, and IL-6 in the 2 week aerosol model of LPS-induced emphysema.

In general, the production of all three cytokines was found to be significantly and rapidly increased in the lungs of LPS treated mice as early as 6 hours following the last exposure (Figure 2-12). The levels of these cytokines then resolved to baseline by 48 hours. Interestingly, there was approximately a 3 fold higher increase in the amount of TNF-α produced at 6 hours after the first LPS exposure compared to the same time point after the 2^{nd}, 3^{rd} and 4^{th} exposures. We do not believe that this is due to the effects of endotoxin tolerance as the effect was not apparent with regard to IL-6 or IL-1β levels.

Given that messenger RNA (mRNA) precedes protein production, investigating mRNA levels at a time point prior to 6 hours after LPS exposure may be informative. Moreover, TNF-α appears to play a key role as a mediator responsible for neutrophil motility and entry into the lung (Bhalla *et al.*, 2009). This suggests that TNF-α may be expressed at a much earlier time point since our inflammatory profiles show a peak in neutrophilia within 6 hours after each LPS exposure. A separate group of mice were exposed to 1x, 2x, 3x, or 4x aerosolised LPS and sacrificed immediately after. mRNA levels for TNF-α, IL-1β, and IL-6 in the lung was determined. LPS induced a much more significant, and rapid increase in mRNA expression (especially TNF-α) of the three proinflammatory cytokines

(Figure 2-13) compared to vehicle treated controls. Interestingly, the high mRNA expression observed was relatively consistent across all LPS treated groups/time points compared to protein levels determined at a later time after LPS exposure (6 hours post).

The data observed between mRNA levels at 30 minutes after each LPS exposure and that of protein levels at 6hours after each LPS exposure suggests strongly that the resolution of protein level may have started earlier than the 6 hour time point. This may also suggest that peak recruitment of inflammatory cells such as neutrophils may have occurred earlier than 6 hours post LPS exposure. However, further studies will be needed to verify this hypothesis.

We also investigate mRNA levels of proinflammatory chemokines associated with neutrophils and macrophages. Based on previous observations that mRNA levels peak at an earlier time point, we determined mRNA levels for MMP-9, MMP-12, MCP-1 (CCL-2), and CCL3, 48 hours after each LPS exposure in the 2 week aerosol model. Our data demonstrates that MMP-9 is not significantly different between LPS or saline treated mice suggesting neutrophils may not be a major component involved with apoptosis although they may be important in the inflammatory process. However MMP-12, CCL-2, and CCL3 are significantly up-regulated during the second week of LPS exposure, compared to the control mice. These data together with the MLI data (Figure 2-5) suggests that the release of chemokines needs to be significantly increased prior to disease onset. As MMP-

12, CCL-2 and CCL3 are associated with macrophages, our results suggest that macrophages play a major role in the development of LPS-induced emphysema.

While the increase in mRNA expression may be due to an increase in total cell numbers, the data collected at 72 hours suggests this is not the case as the level of mRNA expression here (after 4x LPS exposures) when the number of inflammatory cells (in particular macrophages) in the lungs is the highest are not significantly higher than controls.

Several mechanisms contribute to the pathogenesis of emphysema, such as noxious particles that induce severe inflammatory responses, disruption of the balance between proteolytic and anti-proteolytic molecules that maintain the integrity of the lung structure, oxidative stress resulting from increased oxidants in the lungs, and the disruption between apoptosis and replenishment of structural cells (Demedts *et al.*, 2006). Animal models of emphysema have also been shown to be largely associated with apoptosis (Vernooy *et al.*, 2001; Petrache *et al.*, 2005; Brass *et al.*, 2008). Apoptosis is a tightly regulated event aimed to clear out naturally dying cells. However, if it is unregulated or its activation increased, then an imbalance occurs which may tip towards tissue destruction as evident in emphysema. The two most prominent factors associated with the apoptotic process are caspase-3 and ceramide.

Petrache and colleagues (Petrache *et al.*, 2005) demonstrated that by instilling ceramide directly into the lungs of mice (intratracheally), they could

induce pulmonary apoptosis and the hallmark features of emphysema. Both Vernooy (Vernooy *et al.*, 2001) and Brass (Brass *et al.*, 2008) demonstrated that LPS administeration can also induce emphysema which is associated with increased apoptosis. Therefore, we also investigated whether our mouse model of acute LPS-induced emphysema was associated with apoptosis and caspase-3 activation.

Using flow cytometry and IHC, we demonstrated that LPS-induced emphysema is associated with an increase in both ceramide production and active caspase-3, especially in macrophages (Figure 2-15). This does not necessarily mean that the macrophages are apoptotic as they are highly phagocytic cells. They may have phagocytosed parenchymal cells that had undergone apoptosis. This theory is supported by the fact that the ratio of macrophages (LPS treated vs control) positive for ceramide detected by flow cytometry (Figure 2-15A) 72 hours after the last LPS exposure is the same as the ratio of macrophages positive for ceramide detected by IHC 6 days after the last LPS exposure (Figure 2-15B). A similar trend is observed in the level of active caspase-3 detected. This data also suggests to an extent that there is continued apoptosis (although at a lower degree) even up to 6 days after last LPS exposure. Perhaps ideally, we should have investigated ceramide and caspase-3 activity levels after the mice had been subjected to cessation to LPS exposure (eg in Figure 2-7)

The age-dependent onset of emphysema in TLR-deficient mice demonstrated by Patty Lee *et al* (2006) was intriguing and since we were using MyD88-/- mice, we sought to determine if these mice used at age 8 weeks were suitable for comparison for our data. Our results demonstrated that the observations by Lee and colleagues were reproducible and suggested that we have to be careful on what age group of TLR4-/- mice we use. However the results as shown in Figure 2-16D, also demonstrates that the use of the MyD88-/- mice and the results obtained can be comparable to the age-matched wild type in our studies. The results also strongly suggests that the maintenance of lung integrity may be dependent on more than one TLR as shown in the higher MLI observed in TLR2 and TLR4 double knockout mice as compared to the single TLR-/- or TLR4-/- mice. Further studies will be required to determine why we observed a plateau in the TLR4-/- mice.

Overall, our results demonstrate that acute exposure to LPS results in the induction of emphysematous-like lesions in the lung that are irreversible for at least 4 weeks. Onset of disease is characterised by infiltration of neutrophils, a sustained increase in macrophage numbers in the lung, increased levels of proinflammatory cytokines and factors that induce apoptosis (ceramide and active caspase-3).

Chapter 3

Haemophilus influenzae and the Development of Emphysema "like" lesions in the Parenchyma of Mice

Chapter 3: *Haemophilus influenzae* and the Development of Emphysema

3.1 Introduction

Patients with COPD and emphysema commonly suffer exacerbations from recurring or persistent bacterial infections (Murphy and S., 1992; Moller *et al.*, 1998). Non-typeable (unencapsulated) *Haemophilus influenzae* (NTHi) is a gram-negative bacteria commonly isolated from the lower respiratory tract of these patients (Chin *et al.*, 2005). Furthermore, NTHi also expresses lipooligosaccharides (LOS), which is a major virulence factor (DeMaria *et al.*, 1997). LOS is analogous to LPS of enteric gram-negative bacteria (e.g. *E. coli*) in that it contains lipid A, however differs in that it does not contain repeating O-antigen units (Mandrell *et al.*, 1992; Schweda *et al.*, 1995). Lipid A has been demonstrated to activate cells *via* TLR4, MD-2 (a TLR4 helper molecule) and CD14 on the cell surface (Poltorak *et al.*, 1998; Beutler and Poltorak, 2000; Park *et al.*, 2009). Increased bacterial load of NTHi is commonly associated with the development and progression of emphysematous-like lesions. However, the exact role that infection plays is largely unknown. Our observations (Chapter 2) strongly suggest that LPS potentially secreted from NTHi may be a primary driver of inflammation and the onset and progression of emphysematous-like lesions.

In this chapter, we developed a mouse model of NTHi challenge to determine the role of LPS activated pathways in its pathogenesis. We inoculated mice with NTHi and measured changes in lung volume, MLI and percentage alveolar airspace using the morphological techniques described in Chapter 2. We

also investigated the inflammatory response (numbers of neutrophils and macrophages) to the bacterial challenge using flow cytometry, and determined the requirement for TLR4 in activation of the immune response by employing $TLR4^{-/-}$ mice. We then characterised the expression of inflammatory chemokines and cytokines, and whether ceramide and caspase-3 pathways were activated.

3.2 Materials and Methods

3.2.1 Wild type and genetically modified mice

Refer to Section 2.2.1 for overall guidelines and ethics approvals.

8 week old BALB/c WT mice were used in the NTHi model. Age matched (6 week) BALB/c WT and TLR4$^{-/-}$ mice were used in studies investigating the function of TLR4.

3.2.2 Mouse models of NTHi-induced emphysema

3.2.2.1 A single challenge model of NTHi-induced disease

NTHi (Strain: NTHi-289, kindly supplied by our collaborator), was stored in glycerol at -80°C at a stock concentration of 1x10^{9} CFU. Prior to use, the stock bacteria is streaked out onto choc agar plates (oxoid) and incubated overnight. NTHi was then resuspended in sterile PBS to working concentrations.

Male BALB/c WT mice were inoculated intratracheally with a single dose (1x10^{5} CFU per mouse) of NTHi (**Figure 3-1A**), resuspend in 50µl of hospital grade sterile saline. Control mice were administered 50µl of hospital grade sterile saline only. Mice were anaesthetised with alfaxan (1:4 dilution in sterile hospital grade saline) *via* the tail vein. The trachea was then exposed (as described in Chapter 2), visualised under a microscope and the NTHi suspension instilled *via* a sterile 20-guage catheter. Mice were allowed to recover and sacrificed 16 days later. The duration of this challenge corresponds to the duration of the 2 week LPS aerosol model described in Chapter 2.

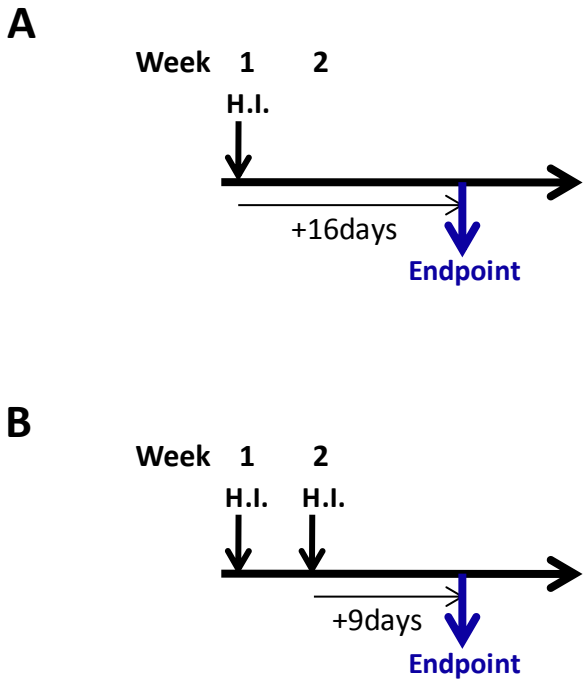

Figure 3-1: Study design for Non-typeable *Haemophilus influenzae* (NTHi) model of emphysema. Saline (vehicle) only or Non-typeable *Haemophilus influenzae* (NTHi) ($1x10^5$ CFU/50µl saline) was administered intratracheally once per week for 1 week **(A)** or once per week for 2 consecutive weeks **(B)** prior to sacrifice on day 16.

3.2.2.2 A double challenge model of NTHi-induced disease

Mice were inoculated with NTHi as described in 3.2.2.1, once per week for 2 weeks (**Figure 3-1 B**) (control mice received sterile saline only) and sacrificed 9 days after the final inoculation. Similarly, the duration of the model corresponds to the 2 week LPS aerosol model in Chapter 2.

3.2.3 Morphometric analysis

See Section 2.2.3

3.2.4 Flow Cytometry analysis

See Section 2.2.4

3.2.5 Messenger RNA analysis

3.2.5.1 Total RNA extraction

See Section 2.2.5.1

3.2.5.2 Reverse Transcription

See Section 2.2.5.2

3.2.5.3 Primers

Additional primers for genes of interest were designed as per section 2.2.5.3 and are shown in **Table 3-1.**

Table 3-1: Additional Murine Primers for qPCR.

Gene	Primer	Sequence (5' to 3')	Gene ID
Nox3	Forward	**CTCGTTGCCTACGGGATAGC**	224480
	Reverse	**CCTTCAGCATCCTTGGCCT**	
HMGB1	Forward	**CCAAAGGGGAGACCAAAAAGAAGT**	15289
	Reverse	**TCGCTGCATCAGGTTTTCCTTTAG**	
LASS2	Forward	**CGCTAGAAGTGGGAAACGGAGTAG**	76893
	Reverse	**CCAGGGGGAGTGTGATGTAGAGAT**	
LASS6	Forward	**ACAAGGGTTGAACTGCTTCTGGTC**	241447
	Reverse	**TTGGTGGTTGTTGAAGAGTGTGGT**	
Neutral Ceremidase	Forward	**AGCAGAGAACCAGACCCATCAAAC**	54447
	Reverse	**GCATTGCTCAGACCCAGTATTCCT**	
Acid Sphingomyelinase	Forward	**GTTACCAGCTGATGCCCTTCACAC**	20597
	Reverse	**AGCTTCCGGGGTAGTTTCCATCTA**	

3.2.5.4 Analysis of gene expression by quantitative real-time PCR (qPCR)

See Section 2.2.5.4

3.2.6 Fluorometric Assay

A fluorometric assay was used to determine the level of caspase-3 activity in the lungs of mice 72 hours after the last NTHi inoculation. Refer to Section 2.2.6 for methods on isolating the lung homogenates for protein analysis. Active caspase-3 can also be detected from these samples using the CaspACE^{TM} Assay System (Fluorometric) (Promega) according to manufacturer's protocol. Fluorometric activity was measured using a FluoStar Optima machine with associated software (version 1.30) (BMG Labtech).

3.2.7 Immunohistochemistry (IHC)

IHC was performed on samples obtained 9 days after the last NTHi inoculation in the double challenge model. For preparation of paraffin embedded sections see Section 2.2.7.

Slides were incubated with peroxidase inhibitor for 10mins prior to blocking blocking with goat serum (5% goat serum + 1% fetal calf serum (FCS) in PBS) in a humidity chamber for 60mins at room temperature. Slides were then washed in deionized water, and incubated with primary monoclonal antibody to ceramide (Alexis Biochemicals) diluted 1:100 overnight at room temperature in a humidity chamber.

Excess primary antibody was removed by washing with PBS-T (3x 5mins) and slides were incubated with HRP-conjugated goat anti-mouse IgG/IgM (diluted 1:100) for 60mins. Slides were washed with PBS-T (3x 5mins) and incubated with DAB for 5-15mins. Slides were then washed in deionized H_2O, and flash stained in Harris Hematoxylin (Fronine) for 15seconds before rinsing in tap water. Slides were then coverslipped with glycergel mounting medium (DakoCytomation, Carpinteria, CA).

3.2.8 Statistic analysis

See Section 2.2.8.

Refer to **Table 2-2 in Chapter 2** for components of buffers and solutions.

3.3 Results

3.3.1 A mouse model of NTHi infection using a single challenge

We investigated whether a single inoculation with NTHi can induce alveolar enlargement in the mouse lung, and if so, whether the resultant changes in MLI and percentage alveolar airspace were comparable to those observed following exposure to LPS (Chapter 2, **Figure 2-5**)**.** There was a significant increase in both MLI (31.73µm ± 0.78µm; n = 7; P=0.0002) and percentage alveolar airspace (75.96% ± 0.33%; n = 6; P<0.0001) following a single inoculation with NTHi compared to vehicle treated controls (**Figure 3-2**)**.** Further, there was no significant difference between the level of alveolar enlargement (MLI and percentage alveolar airspace) in mice exposed to LPS compared to those inoculated with NTHi (**Figure 3-2**)**.**

3.3.2 A mouse model of double NTHi inoculation

We also investigated the effect that a second NTHi challenge might have on alveolar enlargement by inoculating the mice once per week for two consecutive weeks (**Figure 3-1B**). Following a second inoculation with NTHi there was a significant increase in both MLI (38.24µm ± 0.32µm; n = 5-7 mice; P<0.0001) and percentage alveolar airspace (74.16% ± 1.41%; P=0.0031) (**Figure 3-3A-B**) compared to vehicle treated control mice. MLI from mice exposed to a second NTHi inoculation showed a significant increase (P<0.0001) when compared to mice exposed to a single inoculation. However this difference was not reflected

in the percentage alveolar airspace measurements. We therefore decided to employ the double inoculation model for the remainder of the experiments as this is more representative of recurring infections experienced by emphysema patients.

3.3.3 NTHi challenge and lung volume

To determine whether NTHi-induced alveolar enlargement was due to changes in the size of the lungs or due to loss of parenchyma we measured the volumes of the lungs by liquid displacement. The volume of the lungs in NTHi challenged groups compared to vehicle treated control groups was not significantly different (**Figure 3-4**) indicating that this model was indeed comparable to that established using exposure to LPS.

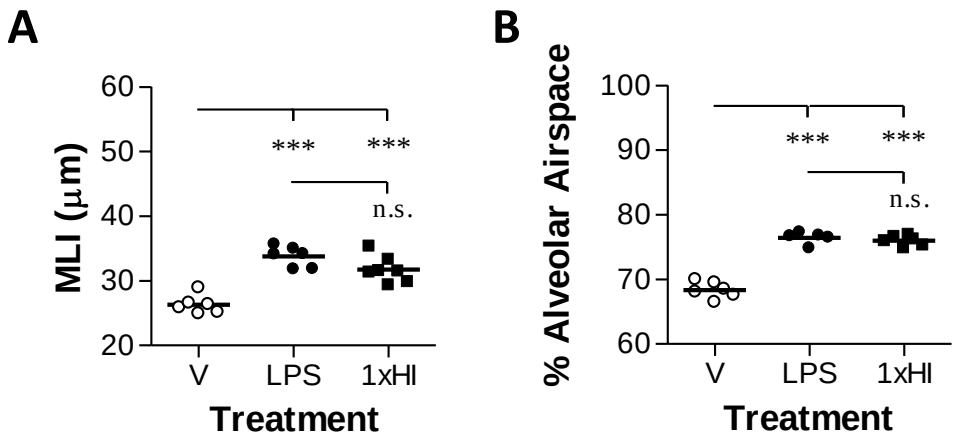

Figure 3-2: Emphysema induced by a single challenge with NTHi is comparable to the 2 week LPS aerosol model. BALB/c WT mice were exposed to a single dose of NTHi (solid squares; $1x10^5$ CFU/50µl saline) *via* the tracheal route, and sacrificed 16 days after final administration. Lungs were prepared to determine the mean linear intercept (MLI) **(A)** and percentage alveolar airspace **(B)**. Results were compared to those observed in the 2 week LPS aerosol model (solid circles) and vehicle treated controls (open circles). n = 5-7 mice per group. ***P≤0.0002, n.s. = not significant, Student's unpaired t-test.

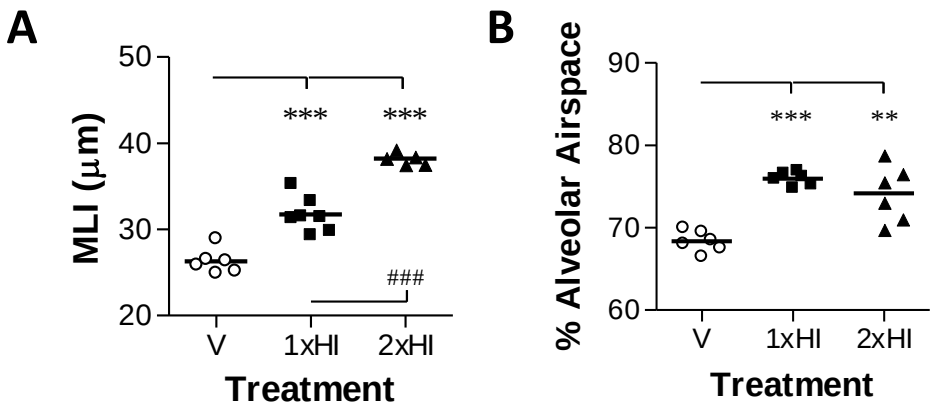

Figure 3-3: Double exposure to NTHi induced more damage to the lungs compared to a single exposure. BALB/c WT mice were inoculated with NTHi (solid triangles) once per week for 2 consecutive weeks *via* an intratracheal route and sacrificed 9 days after the last inoculation. Lungs were collected and the mean linear intercept (MLI) **(A)** and percent alveolar airspace **(B)** determined. Results were compared to those from the single NTHi inoculation model and vehicle (V) treated control mice. n = 5-7 mice per group. HI = NTHi. **P<0.005, ***P≤0.0002, ###P<0.0001, Student's unpaired t-test.

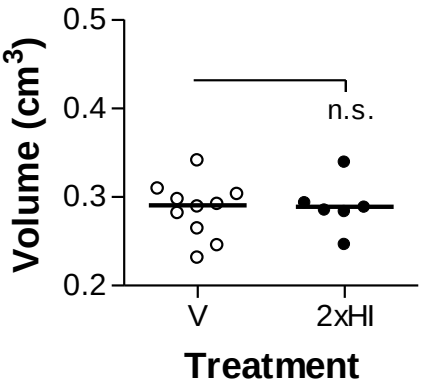

Figure 3-4: NTHi challenge does not alter lung volume in BALB/c WT mice. Lung volumes were compared between mice which had been exposed to saline only (vehicle (V)) (open circles) and mice which had been inoculated twice with NTHi (closed circles). HI = NTHi. n.s. = not significant, Student's unpaired t-test.

3.3.4 NTHi-induced emphysema and TLR4 signalling

To determine whether the loss in lung parenchyma following NTHi infection was TLR4 dependent, BALB/c WT and BALB/c TLR4$^{-/-}$ mice were inoculated intratracheally with NTHi following the double challenge model. Controls received vehicle only. All mice were sacrificed 9 days after the final treatment and MLI from the lungs determined. The MLI was significantly increased (~+11µm; P<0.0001) following NTHi challenge in BALB/c WT mice compared to their vehicle treated controls (**Figure 3-5**)**.** There was also a small but significant increase in the MLI (~+2µm; P=0.0073) between TLR4$^{-/-}$ mice inoculated with NTHi compared to their vehicle controls. In contrast, MLI from NTHi inoculated BALB/c TLR4$^{-/-}$ mice was significantly lower (~ -7µm; P<0.0001) than that recorded for NTHi inoculated BALB/c WT mice. Interestingly, TLR4$^{-/-}$ control mice had a slightly significant higher (P=0.45) MLI than WT control mice. These results suggested that NTHi-induced emphysema is partly dependent on TLR4 as there is incomplete inhibition of NTHi-induced increases in MLI.

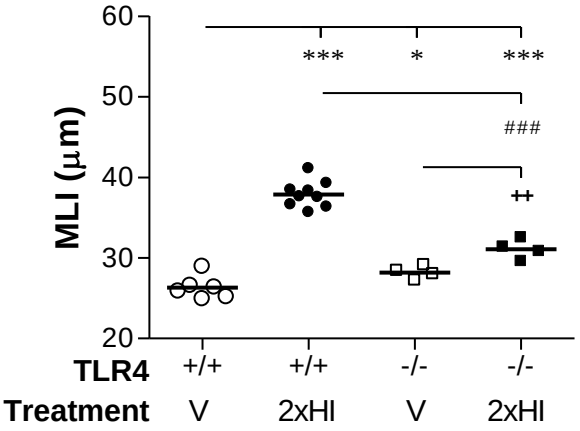

Figure 3-5: NTHi induced emphysematous-like lesions are partially dependent on Toll-like Receptor 4 (TLR4) signalling. BALB/c $TLR4^{-/-}$ mice were administered saline only (vehicle (V); open squares) or inoculated twice with NTHi (closed squares) *via* an intratracheal route. The lungs were processed and the mean linear intercepts (MLI) determined. Results were compared to the MLI from BALB/c WT mice exposed to vehicle only (open circles), or inoculated twice with NTHi. (closed circles). n = 4-9 mice per group. HI = NTHi. *P<0.05, ***P<0.0008, $^{###}$P<0.0001, $^{++}$P<0.008, Student's unpaired t-test.

3.3.5 NTHi challenge and the inflammatory response

The inflammatory response (neutrophils and macrophages) in the lungs of mice inoculated with NTHi was characterised. There was a significant increase in the number of macrophages ($1.58x10 \pm 0.10x10^6$; n = 6; P<0.0001) in the lungs of mice following NTHi inoculation compared to vehicle treated controls ($0.83\ x10^6 \pm 0.06x10^6$; n = 6) (**Figure 3-6**). Similarly, there was also a significant increase in the number of neutrophils ($0.21x10^6 \pm 0.02x10^6$; n = 6; P=0.0021) from NTHi treated mice compared to controls ($0.12\ x10^6 \pm 0.01x10^6$; n = 6).

3.3.6 NTHi challenge and the expression of proinflammatory cytokines

We investigated the mRNA expression levels of the proinflammatory cytokines TNF-α, IL-1β and IL-6 in the lung tissue following NTHi inoculation. Challenge with NTHi induced a significant increase (~2 fold; P<0.05; Student's T-Test) in mRNA expression levels of TNF-α compared to control mice 72 hours after the last NTHi inoculation (**Figure 3-7A**). However, there were no significant differences in the mRNA expression levels of both IL-1β and IL-6 (**Figure 3-7B and C**) in NTHi treated groups or vehicle treated controls.

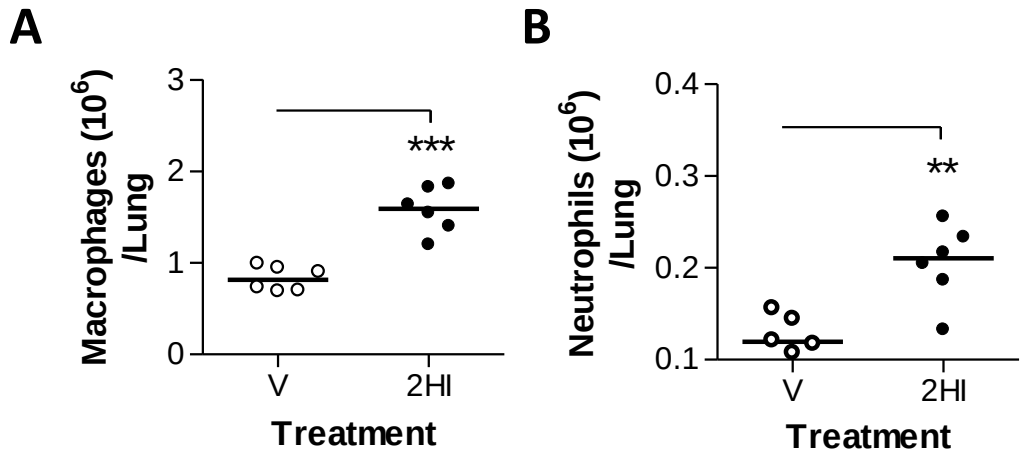

Figure 3-6: NTHi challenge induces inflammation (increased macrophages and neutrophils) in the lungs. Saline only (Vehicle (V); open circles) or NTHi (closed circles) was administered to BALB/c WT mice *via* an intratracheal route in the NTHi double challenge model. Mice were sacrificed 3 days after challenge and a single cell suspension generated from lung tissue. Macrophages **(A)** and neutrophils **(B)** were enumerated by flow cytometry. n = 6 mice per group. HI = NTHi. **P<0.005, ***P≤0.0001, Student's unpaired t-test.

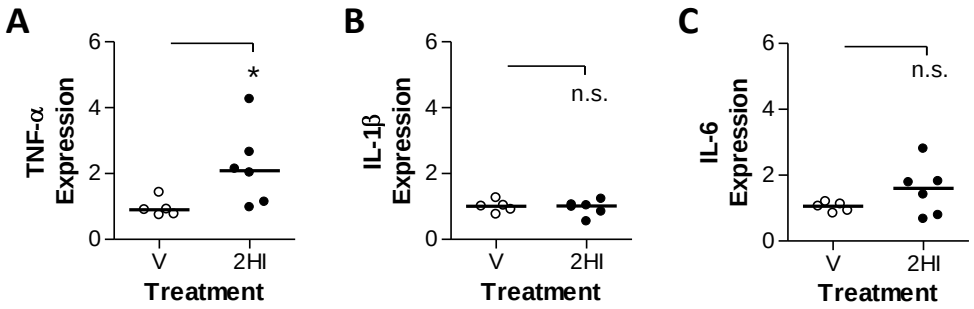

Figure 3-7: NTHi challenge induces the expression of proinflammatory cytokines. Mice were treated intratracheally with saline only (vehicle (V); open circles) or twice with NTHi (solid circles) and sacrificed 3 days after the last exposure. Lung were collected, mRNA extracted and expression levels for TNF-α **(A)**, IL-1β **(B)** and IL-6 **(C)** determined by RTqPCR. mRNA levels in NTHi treated mice are expressed as a fold change over the control group. n = 5-6 mice per group. HI = NTHi. *P<0.05, Student's unpaired t-test.

3.3.7 NTHi challenge and the expression of proinflammatory chemokines

We investigated the effect of NTHi challenge on the subsequent expression levels of the proinflammatory chemokines MMP-9, MMP-12, the oxidative stress marker NADPH-oxidase 3 (Nox-3), and high-mobility group protein B1 (HMGB1). The mRNA expression levels of MMP-12 were significantly up-regulated (n = 5; P=0.0338) in the lungs of mice following NTHi challenge compared to vehicle treated controls **(Figure 3-8).** In contrast, there was no change in the mRNA expression of MMP-9, Nox-3 or HMGB-1 in NTHi challenged mice compared to vehicle treated controls.

3.3.8 NTHi challenge and activation of the apoptotic pathway

To investigate whether NTHi challenge induced a loss of parenchymal tissue through apoptosis we measured the levels of active caspase-3 and the average number of ceramide positive macrophages in the lung. NTHi challenge induced a significant increase (P=0.0002) in caspase-3 activity ($1.82x10^4$ ± $0.29x10^4$FU; n = 5) compared to vehicle treated control mice ($0.16x10^4$ ± $0.05x10^4$FU; n = 6) (**Figure 3-9A and B**).

We also found that NTHi challenge increased the average number of ceramide positive macrophages compared to vehicle treated controls. Representative images of ceramide stained lung sections from each treatment group are shown in **Figure 3-9C**. The image on the left is from vehicle treated mice with macrophages expressing no ceramide, indicated by the full headed

arrows, while the image on the right shows ceramide positive macrophages (stained brown), indicated by open arrows.

3.3.9 NTHi challenge and the synthesis of ceramide

We investigated whether NTHi challenge resulted in an imbalance in the levels of enzymes involved in ceramide synthesis by determining mRNA expression (as shown in **Figure 2-10**) of acid sphingomyelinase (ASMase) **(A)**, neutral ceramidase (NCdase) **(B)**, and dihydroceramide synthase (isoforms 2 (LASS-2) and 6 (LASS-6)) **(C-D)**. There were no significant changes in mRNA levels detected in any of these four enzymes between NTHi infected mice and control mice. This suggests that potentially the time points chosen for sample collection were not optimal and it was likely that changes in mRNA expression occurred prior to 72 hours after the last NTHi challenge and thus had already returned to baseline.

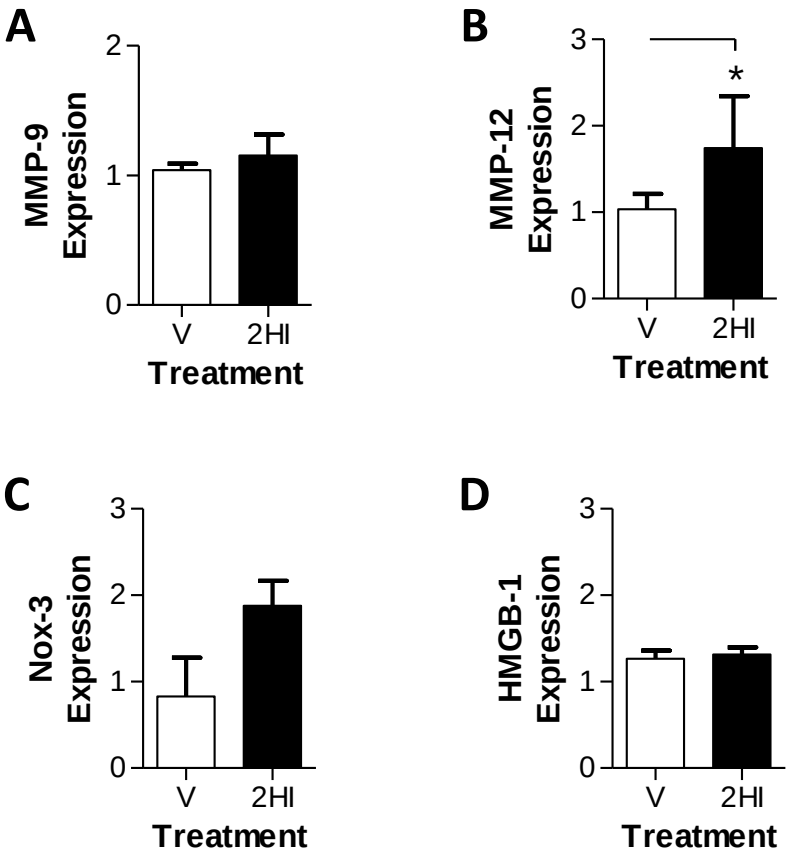

Figure 3-8: NTHi-induced changes in the mRNA expression levels of MMP-9 and MMP-12, Nox-3 and HMGB-1. Mice were treated intratracheally with saline only (vehicle (V); open circles) or infected twice with NTHi (solid circles) and sacrificed 3 days after the last treatment. Lungs were collected, mRNA extracted and the expression levels of MMP9 **(A),** MMP-12 **(B),** Nox-3 **(C)** and HMGB-1 **(D)** determined by RTqPCR. mRNA levels in NTHi infected mice are expressed as a fold change over the control group. n = 4-6 mice per group. HI = NTHi. *P<0.05, Student's unpaired t-test.

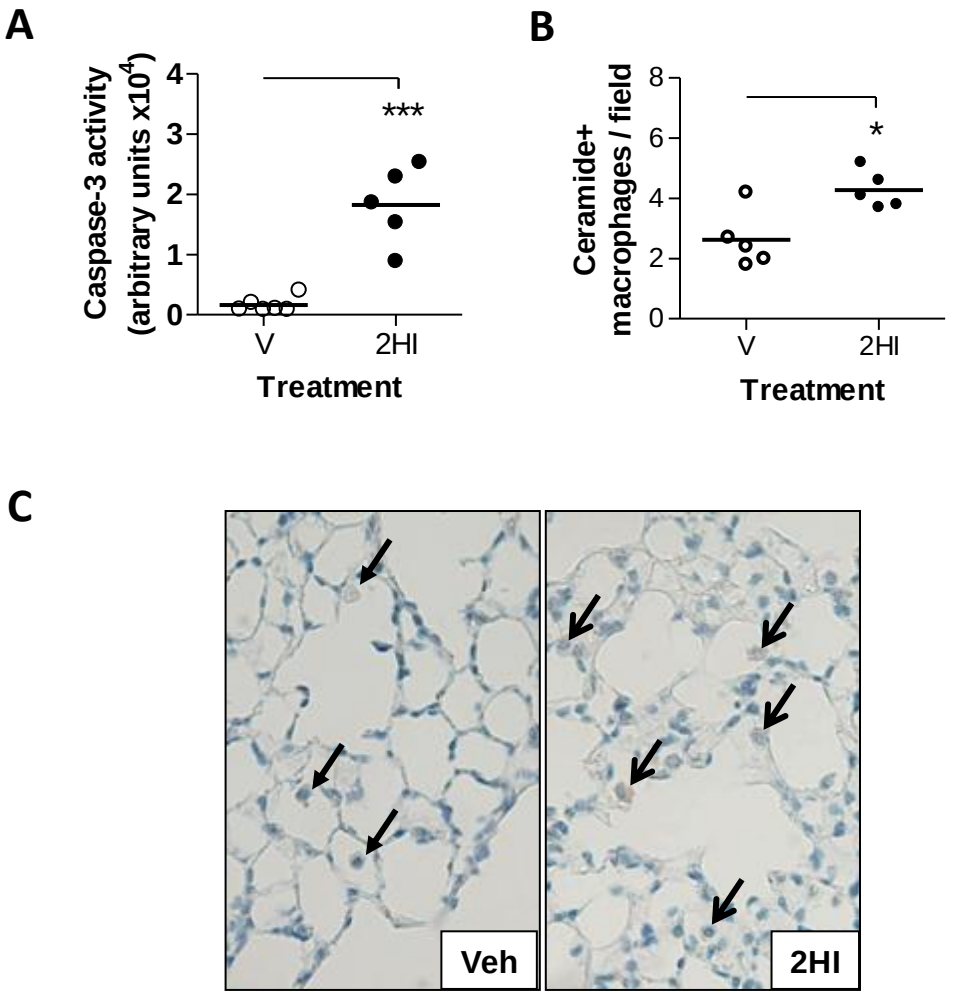

Figure 3-9: NTHi-induced expression of apoptotic markers in the lungs of mice. BALB/c WT mice were treated with saline only (vehicle (V); open circles/bar) or infected twice with NTHi (black circles/bar) and sacrificed 3 days after the final treatment. Lungs were collected, homogenised and the supernatants used to determine the levels of active caspase-3 activity *via* a fluorometric assay **(A).** Mice were also sacrificed 9 days after the final NTHi challenge and the lungs prepared for IHC to enumerate macrophages positive for ceramide **(B).** Representative images show ceramide positive macrophages (stained brown) in mice infected with NTHi compared to vehicle only treated controls **(C)**. n = 5-6 mice per group. HI = NTHi. ***P≤0.0002, *P<0.02, Student's unpaired t-test.

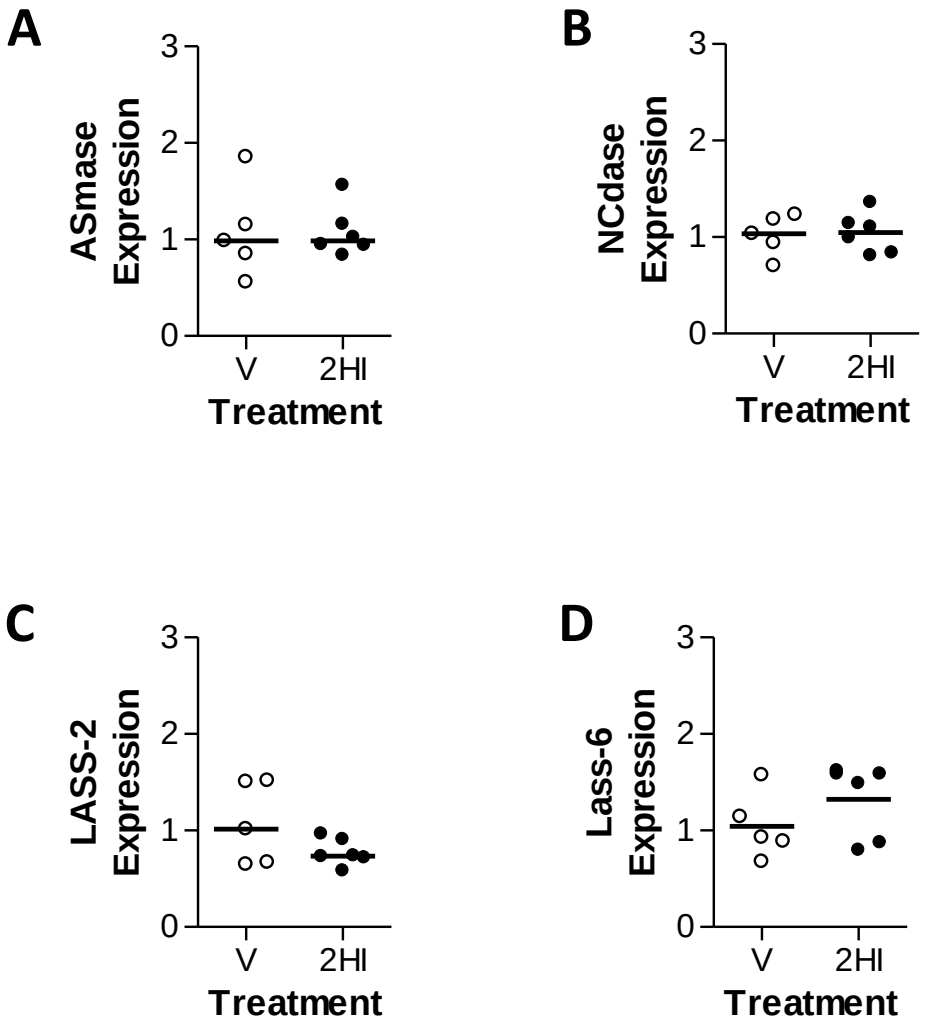

Figure 3-10: NTHi-induced changes in the expression of enzymes related to ceramide synthesis. BALB/c WT mice were administered saline only (vehicle (V); open circles) or infected twice with NTHi (solid circles) intratracheally. Mice were sacrificed 72 hours after the last NTHi challenge and mRNA extracted from the lungs. mRNA levels for enzymes involved in ceramide synthesis: ASmase **(A),** (NCdase) **(B),** LASS-2 **(C),** and LASS-6 **(D)** are expressed as fold change over vehicle treated controls. n = 5-6 mice per group. HI = NTHi, Student's unpaired t-test.

3.4 Discussion

Persistent and recurring bacterial infections are commonly associated with exacerbations in patients diagnosed with COPD and emphysema (Murphy and S., 1992; Moller *et al.*, 1998; Chin *et al.*, 2005; Sethi *et al.*, 2006). The gram-negative bacteria, NTHi is commonly found to colonise the lower respiratory tract of COPD and emphysema patients. We hypothesised that the continuous exposure of epithelial cells in the lung to endotoxic content (Lipid A-containing lipooligosaccharide (Pang *et al.*, 2008)) produced by NTHi can activate the inflammatory response through TLR4 signalling. This persisting inflammatory response then perpetuates the progressive development of irreversible emphysematous-like lesions through increased apoptosis.

To test our hypothesis, we needed to develop a mouse model of emphysema using a bacterial lung infection as the catalyst. There are currently little, or no animal models of emphysema using NTHi to induce disease. The only research thus far was by Moghaddam and colleagues (Moghaddam *et al.*, 2008), where they utilised aerosolised NTHi lysate to establish a mouse model of COPD. For the purposes of direct comparison, we established our model of NTHi-induced emphysema (Figure 3-1) based around the 2 week LPS aerosol model that we had established previously (Chapter 2). The aim of the NTHi model was to use live bacteria to induce emphysematous-like lesions and other hallmark features of emphysema.

Initially mice were treated with a single dose of NTHi intratracheally and the degree of alveolar enlargement was determined using morphometric analysis. A single challenge with NTHi was able to induce a significant loss in parenchyma as indicated by increased MLI and percentage alveolar airspace compared to vehicle treated controls (Figure 3-2). Lung volume in these mice remained constant. The constant lung volume between NTHi infected and control treated mice (Figure 3-4) confirms that the changes in MLI and percentage alveolar airspace are independent of lung development, similar to the studies in Chapter 2. The difference between NTHi infected mice and vehicle treated controls was surprisingly comparable to the results obtained following 2 weeks exposure to aerosolised LPS (Chapter 2). An intratracheal administration route was employed as we believe that this resembles the development and presence of an inoculation as per in human, as compared to administrating via an aerosol method. Moreover, utilizing an aerosol method requires an extremely high dose/concentration of bacteria which we may not have the necessary level of containment required.

We then established a model of NTHi infection which employed a second challenge as this is more relevant to recurring infections experienced during colonization and exacerbation in patients with emphysema. Mice were infected with NTHi once a week for 2 consecutive weeks and sacrificed at a time point similar to the 2 week LPS aerosol model (Chapter 2).

We found that there was a further enhancement to the loss in parenchymal tissue after a second challenge compared to results seen after a single challenge (Figure 3-3 A). Interestingly, percentage alveolar airspace was comparable between mice exposed to a single or double NTHi challenge. We attribute this difference observed to the level of sensitivity of measuring percentage alveolar airspace. In the methods, 63 points were used in each acquired image. We think that should this number be increased at the expense of time investing in counting, we would see a much more accurate representation of the data and that it would be similar to the MLI measured. However, due to time constraints (as it would mean we would have to re-analyze all our previous airspace measurements) and already having the MLI measurements (industrial standard), we kept the same format of measurements.

Subsequent experiments therefore utilised the double challenge model. This data strongly demonstrates that repetitive lung infections by bacteria can cause incremental damage to the lung.

It has been previously demonstrated that clearance of bacteria such as NTHi from the lungs is dependent on the TLR4 and MyD88 pathway (Wieland *et al.*, 2005). NTHi has also been demonstrated to activate cells through various receptors such as TLR2 (Wieland *et al.*, 2005), as well as through NOD-like receptors (NLRs) (Månsson *et al.*, 2010; Moghaddam S.J. *et al.*, 2011). To determine whether LOS (LPS) from NTHi plays a central role in emphysema

development, BALB/c WT and BALB/c TLR4$^{-/-}$ mice were infected with NTHi. Mice deficient in TLR4 signalling exhibited a significant decrease in alveolar enlargement compared to WT counterparts (Figure 3-5). However, these TLR4$^{-/-}$ mice also exhibited a small yet significant increase in MLI when compared to the control group, suggesting that alternate pathways activated *via* other PAMPs may also contribute to emphysema development (Pang *et al.*, 2008).

Of note however, in this particular set of experiments, we employed younger mice (6 weeks old) than what was used in previous studies (Chapter 2, Figure 2-16 and (Patty J. L. *et al.*, 2006)) looking at age-dependent development of emphysema in naïve toll-like receptor deficient mice. It had previously been demonstrated that TLR4$^{-/-}$ mice (on a C57BL/6 background) exhibited emphysema development as they aged, mediated through oxidative stress. Age-dependent spontaneous development of emphysema-like lesions in mice seems to occur after 8 weeks of age. Indeed, our results in Figure 3-5 demonstrated minimal differences between control groups (WT vs TLR4$^{-/-}$) and thus any differences observed in NTHi treated mice should be due to the NTHi challenge.

The NTHi inoculation induced an inflammatory response (Figure 3-6), which is similar to that seen after 2 weeks exposure to aerosolised LPS (Chapter 2). Mice infected with NTHi had significantly higher numbers of infiltrating macrophages. Interestingly, neutrophils seem to persist at a significantly higher level than observed in control mice, which seems to correspond to the results

observed by Moghaddam and colleagues in 2008 where they established a mouse model of NTHi lysate-induced COPD (Moghaddam *et al.*, 2008).

Interestingly, the numbers of macrophages and neutrophils in bacterially infected mice were slightly lower than the numbers observed in LPS treated mice during this time period. This is did not correspond to the degree of damage observed in the increased MLI and percentage alveolar airspace. Perhaps this can be explained by a few factors. Firstly, LPS introduced to the lungs may only be either a transient process (J. T. Rosenbaum and Mandell, 1983), which serves to attract or induce inflammatory cell influx. During this process, certain apoptotic pathways were activated and the resulting levels of caspase-3 activity and ceramide production are low. These levels require at least a second week of continuous exposure before there is enough accumulation to cause the development of emphysematous-like lesions.

The results from TLR4$^{-/-}$ mice, suggest that NTHi may induce inflammation *via* other signalling pathways (such as TLR2 or NLRs) and the effects arising from these additional pathways may be additive or synergistic in nature. Indeed, TLR2 and TLR4 have been demonstrated to work synergistically (Shinohara *et al.*, 2007; Ferwerda *et al.*, 2008; Wikén *et al.*, 2009). Bacterial clearance from the lungs of WT mice took at least 3-5 days. During this period, there is potentially a continual recruitment and activation of inflammatory cells, leading to increasing detrimental effects arising from the various signalling pathways. The kinetics of

inflammation during the period between challenges requires further investigation.

We observed a trend in increased production of mRNA of proinflammatory cytokines (TNF-α, IL-1β, and IL-6) similar to the LPS model. However, the results were not as significant at the particular time point chosen (Figure 3-7). mRNA expression could have occurred at an earlier time point after the last NTHi challenge similar to our findings in Chapter 2 where LPS exposure induced rapid up-regulation of TNF-α within 30mins. The particular time point (72hours after the last NTHi challenge) was chosen because the number of inflammatory cells is lower (i.e. after neutrophils have resolved) so as not to dilute the levels of tissue specific mRNA we were interested in. However, the caveat is that increased mRNA expression for certain genes may have resolved by this time. Future studies would involve a time course for the expression of these factors.

Similarly, when we looked at the mRNA expression of proinflammatory chemokines (Figure 3-8), only MMP-12 was significantly up-regulated compared to control mice. However there were no significant differences detected for MMP-9, Nox-3, and HMGB1. The data however may also mean that NTHi-induced emphysema is not associated with MMP-9, and oxidative stress (Nox-3 and HMGB1 are markers of oxidative stress), implicated in emphysema development.

We then determined if NTHi-induced emphysema in the mouse model is associated with apoptosis by determining the level of caspase-3 activity using a colorimetric assay; and number of ceramide positive macrophages *via* IHC. Here we got access to caspase-3 activity kit and think that it gives a better representation of our findings as compared to using flow cytometry (which only determines the presence of the protein/enzyme). Our results (**Figure 3-10**) demonstrate that NTHi challenge induced up-regulation of ceramide production, and increased caspase-3 activity.

Enzymes involved with ceramide synthesis or breakdown were not significantly altered at the particular time point (72 hours after the last NTHi challenge). However, we did observe a positive trend for LASS-6 to be increased in NTHi treated mice, compared to control mice. LASS enzymes convert sphingosine to ceramide, though the specific functions of the 6 different isoforms of LASS remains relatively unknown. Once again, investigation at earlier time points are required in future studies.

In this chapter, we demonstrate that NTHi challenge induces emphysema-like lesions in the airways and this is TLR4 dependent. The development of emphysematous-like lesions was associated with the recruitment of macrophages and neutrophils to the lung; upregulation of TNF-α and increased production of ceramide suggesting apoptosis may play a role in pathogenesis.

Chapter 4

New approaches to inhibit the development of LPS- or *Haemophilus influenzae*-induced emphysema.

Chapter 4: New approaches to inhibit the development of LPS or *Haemophilus influenzae*-induced emphysema

4.1 Introduction

We have successfully established mouse models of LPS- or NTHi-induced emphysema (Chapters 2 and 3), which mimic the hallmark features of disease such as irreversible alveolar enlargement, increased inflammation, and induction of the apoptotic pathway. Progression of the diseased state can be inhibited in the absence of TLR4 signalling and is largely dependent on the MyD88 pathway downstream of TLR4. Activation of TLR4 by its natural ligand LPS, induces inflammation to prevent the spread of infection and is a primary host defense response (Maes *et al.*, 2006; Ferwerda *et al.*, 2008; Sarir *et al.*, 2009). However, when inflammation becomes dysregulated, disease states such as emphysema arise. Emphysema is an irreversible and progressive disease involving the loss of parenchyma. The onset of disease is strongly correlated with smoking, as well as other factors triggering an initial irregularity in homeostasis of the lung structure. Subsequent infections from opportunistic micro-organisms leads to persistent and recurring exacerbations, and this helps drive the relentless progression of disease. Current available treatments aimed at reducing exacerbations include smoking cessation, pulmonary rehabilitation, oxygen therapy, inhaler therapy, alpha-1 anti-trypsin treatments, antibiotics, and lung volume reduction surgery (LVRS). However, these are of limited therapeutic efficacy and new specific treatments are urgently required.

In this chapter, we investigated alternative ways to inhibit emphysema by suppressing downstream factors that are linked to the recruitment of neutrophils and macrophages into the airways in response LPS or NTHi exposure.

Our findings in Chapters 2 and 3, as well as other animal models of emphysema such as cigarette smoke models (Hautamaki *et al.*, 1997; Bhalla *et al.*, 2009), vascular endothelial growth factor (VEGF) receptor blocking models (Kasahara *et al.*, 2000; Petrache *et al.*, 2005) and other LPS models of COPD (Vernooy *et al.*, 2002; Brass *et al.*, 2008) indicate that inflammation has a profound effect in driving disease development. These data strongly suggests that blocking inflammation may be beneficial for the treatment of emphysema.

Chemerin is a proinflammatory protein that can be broken down to smaller peptides, one of which has been shown to exhibit anti-inflammatory effects. Cash and colleagues demonstrated that tail vein injection of a highly potent 15 amino acid long peptide (C15) could effectively attenuate inflammation in a mouse model of zymogen-induced peritonitis (Cash *et al.*, 2008). Specifically, their study demonstrated a significant but not total suppression of neutrophils (63%) and monocytes (62%) at the site of inflammation. In their study, they hypothesised that the proinflammatory protein chemerin can be further broken down by enzymes to shorter chains of amino acids, which then exert anti-inflammatory effects, thus providing a novel way to suppress inflammation. Chemerin and C15 both activate an

orphan G protein-coupled receptor, ChemR23. Since this investigation, alternative chemerin receptors have been discovered and characterised (Yoshimura and Oppenheim, 2008; Zabel *et al.*, 2008; Yoshimura and Oppenheim, 2011).

4.1.1 Chemerin

Chemerin was first identified as the natural ligand to its orphaned G protein-coupled receptor (GPCR) ChemR23 by Wittamer and colleagues in 2003 (Wittamer *et al.*, 2003). Chemerin is also known as tazzarotene induced gene 2 (TIG2) or retinoic acid receptor responder 2 (RARRES2) (Roh *et al.*, 2007). Chemerin is first secreted as an inactive, 143 amino acid (aa) long precursor (pro-chemerin) (Wittamer *et al.*, 2003; Yoshimura and Oppenheim, 2008). It is then activated when a 6-aa peptide is cleaved from its C-terminus by serine proteases associated with the coagulation, fibrinolytic and inflammatory cascades (Zabel *et al.*, 2005). Chemerin is a potent chemoattractant of immature DCs and macrophages. Bioactive chemerin has been found along with proinflammatory cytokines in samples taken from patients with severe inflammatory disorders, such as psoriasis, suggesting a pathological role for chemerin (Sozzani *et al.*, 1998).

Interestingly, since chemerin was first identified as the ligand to ChemR23 and linked to inflammatory diseases, further investigations on its role in inflammation have been limited. Chemerin was initially identified as a free floating plasma protein that was ubiquitous in an inactive form (Wittamer *et al.*, 2003). Years later, chemerin was identified as an adipokine,

secreted by adipose tissue (Bozaoglu *et al.*, 2007; Roh *et al.*, 2007). Since then studies have focused primarily on chemerin in adipogenesis, as well as on obesity and metabolic regulation.

However, the publication by Cash and colleagues in 2008 demonstrated the potential of chemerin to exert potent proinflammatory and anti-inflammatory properties refocused investigations into the role of chemerin in inflammatory diseases.

4.1.2 Chemerin receptors

4.1.2.1 Orphan chemerin receptor - ChemR23

The most well characterised receptor for chemerin is ChemR23. It was first known as chemokine-like receptor 1 (CMKLR1), a 7-transmembrane receptor, and first cloned in the late 1990s based on its similarity to GPCR. At the time of discovery, they were without known biological roles and thus are termed orphaned GPCRs (Samson *et al.*, 1998). The murine equivalent is known as GPCR-DEZ (Roh *et al.*, 2007). When the natural ligand chemerin was discovered, the receptor was re-named chemerinR (Wittamer *et al.*, 2003). In the present thesis, ChemR23 is the term used for chemerin receptor.

By using ChemR23-deficient mice in animal models of diseases, it has been demonstrated that chemerin signals through ChemR23 to activate proinflammatory responses (Cash *et al.*, 2008; Yoshimura and Oppenheim, 2008; Yoshimura and Oppenheim, 2011). Interestingly, the anti-inflammatory lipid mediator, resolvin E1, also activates ChemR23 (Campbell *et al.*, 2007; Yoshimura and Oppenheim, 2011), suggesting that this receptor is a

multifunctional receptor. Indeed, results from Cash and colleagues further confirm this observation when they demonstrated that the Chemerin-derived C15 peptide also exhibited anti-inflammatory effects through ChemR23.

ChemR23 is expressed by many cell types, including antigen presenting cells (APCs) such as macrophages and immature DCs.

4.1.2.2 Orphan chemerin receptor - CCRL2

The serpentine receptor chemokine (CC motif) receptor-like 2 (CCRL2) is another G-protein-coupled receptor that recognises chemerin. It is also known as LPS-inducible C-C chemokine receptor related gene (L-CCR), or Eo1 in mice; and human chemokine receptor (HKR), CRAM-A, CRAM-B, or chemokine receptor X (CKRX) in humans (Zabel *et al.*, 2008).

However unlike ChemR23, CCRL-2 has not been shown to contribute any significant activated responses (such as release of cytokines or chemokines) and thus thought to be a silent or non-signalling receptor. Studies suggest that CCRL-2 acts like a sink, which allows binding of signalling molecules such as the chemoattractant protein chemerin, controlling its concentration at inflammatory sites. This can then enhance or promote chemotaxis of cells to specific inflammation sites (Yoshimura and Oppenheim, 2008; Zabel *et al.*, 2008).

4.1.3 Chemerin-derived 15-amino acid (C15)

As described above, chemerin exists in the plasma as pro-chemerin and has low bioactivity. However, upon cleaving by serine proteases at the C-

terminal, active chemerin is formed which can bind to its appropriate receptors and exhibit potent chemotactic activities (Wittamer *et al.*, 2005; Zabel *et al.*, 2005).

In a study by Cash and colleagues (2008), they investigated whether active chemerin can be further cleaved by proteolytic processing by enzymes released from macrophages after activation. Their data showed that chemerin can exert inhibitory effects on macrophage activation in a cysteine protease-dependent manner, which is also dependent on calpains and cathepsin S.

They then designed multiple short length peptides with sequences derived from the full active chemerin sequence. They observed that in particular, the C15 sequence (A^{140}-A^{154}; AGEDPHGYELPGQFA) exerts no chemotactic effect, but is highly potent [1pM] in inhibiting LPS/IFN-γ-induced RANTES and TNF-α expression from peritoneal macrophages (Cash *et al.*, 2008). They used a scrambled sequence of the C15 as a control peptide. They also demonstrated that C15 is dependent on ChemR23 signalling to activate its anti-inflammatory effects.

4.1.4 Inhibiting inflammation

Multiple techniques have been employed to inhibit the detrimental effects of uncontrolled inflammation in diseases. Some of these involve broad spectrum suppression of inflammatory cells such as the use of corticosteroids in COPD. However, the problem with using such broad spectrum suppression is that it results in multiple undesired effects.

In mouse models of inflammation, different techniques can be employed to inhibit or deplete cell types. These include the use of clodronate or 2-Chloroadenosine (2CA) to deplete macrophages (Kubota *et al.*, 1999; Kumar *et al.*, 2010; Bang BR *et al.*, 2011). Neutrophils can be inhibited using specific monoclonal antibodies (Ismail *et al.*, 2003; Daley *et al.*, 2008), or chemical compounds (such as anti-KC + anti-MIP-2) to prevent infiltration during an infection (Horvat *et al.*, 2010). Other compounds such as the novel C15 peptide can inhibit the infiltration of more than one cell type (Cash *et al.*, 2008).

Administration of some of these compounds can be complicated. For example, using clodronate to deplete macrophages requires the time consuming process of enveloping the clodronate within liposomes prior to administration or else the depletion is ineffective. A new purine analog compound, 2CA, had been demonstrated to be selectively cytotoxic to cultured macrophages (Kubota *et al.*, 1999). Administration of 2CA is simple as it is easily dissolved in saline, and be directly administered through aerosol or intravenous injection (Kumar *et al.*, 2010).

In this chapter, we aimed to determine if inhibiting inflammatory cells (specifically neutrophils and macrophages) through the use of synthetic C15 peptide can protect mice from LPS- or NTHi-induced emphysema. We also aimed to deplete alveolar macrophages *via* the use of 2CA to further identify the role of alveolar macrophages in LPS- or NTHi-induced emphysema.

4.2 Materials and Methods

4.2.1 WT mice

For overall guidelines and ethics approvals see Section 2.2.1.

BALB/c WT mice were delivered to the animal holding facility at 7 or 15 weeks of age and allowed to acclimatise for 7 days.

4.2.2 Peptide synthesis

C15 and the scrambled peptide (SP; control peptide to C15) were synthesised at the Biomolecular Resource Facility (BRF) at the John Curtin School of Medical Research (JCSMR), Australian National University (ANU). The peptide was synthesised using a CEM Liberty Microwave Peptide Synthesizer, performed using Fmoc chemistry and solid phase peptide synthesis (SPPS) techniques (BRF-JCSMR-ANU, 2008).

Base on the publication by Cash and colleagues (2008), the scrambled peptide is a scrambling of the amino acid sequence of the functional C15 peptide. Initial results using SP indicated that there was a non-specific effect occurring (**Figure 4-1**). Re-analysis of the initial sequence (Cash *et al.*, 2008) suggested that the results may have been compromised due to the repeat of a 3 amino acid sequence Thus, the peptide was re-scrambled so that there were no more than 2 amino acids repeated between peptides (**Table 4-1**). Subsequent tests indicate that results from mice treated with the new SP sequence are comparable to saline only treated controls (**Figure 4-5 and 4-6**).

Table 4-1: Peptide sequence of SP (old), C15 and SP (new).

Peptide	Sequence
SP (old)	GLFHDQAGPPA**GYE**F
C15	AGEDPH**GYE**LPGQFA
SP (new)	GPAQEYAPLDFGHFG

**Note bold repeated sequence between old SP and C15*

4.2.3 Mouse models and treatment

4.2.3.1 Determining chemerin levels

Mice were treated to a single exposure of aerosolised LPS as described in Chapter 2, Section 2.2.2. Lungs were collected at 6, 24, 48 and 72 hours after the final LPS exposure, and lung homogenates assayed for Chemerin protein by ELISA. Lungs were also collected 24 and 48 hours after final LPS exposure in a 2 week model as described in Chapter 2 Section 2.2.2.3. Lungs were also collected 72 hours after a single challenge with NTHi ($1x10^5$ CFU per mouse; Chapter 3, Section 3.2.2.1).

4.2.3.2 Optimizing dose of old SP and C15

To determine the optimal concentration of C15, mice were injected with 0.5ng or 2.0ng of old SP or C15 dissolved in 100ul of sterile hospital grade saline *via* the tail vein 1 hour prior to LPS exposure (as described in Chapter 2, Section 2.2.2.3). Control mice received saline only followed by aerosolised saline. Mice were sacrificed 18 hours later and the number of neutrophils in the lungs enumerated by flow cytometry (**Figure 4-1**). Initial results found that old SP generated a response at both doses (**Figure 4-1**),

when compared to levels of neutrophils observed in Chapter 2 (**Figure 2-10A**) therefore a new sequence was generated (See Section 4.2.2). Treatment with C15 resulted in the attenuation of LPS-induced neutrophilia. The higher concentration of C15 (2.0ng/100ul) was more effective at reducing the number of neutrophils and was therefore used in subsequent experiments.

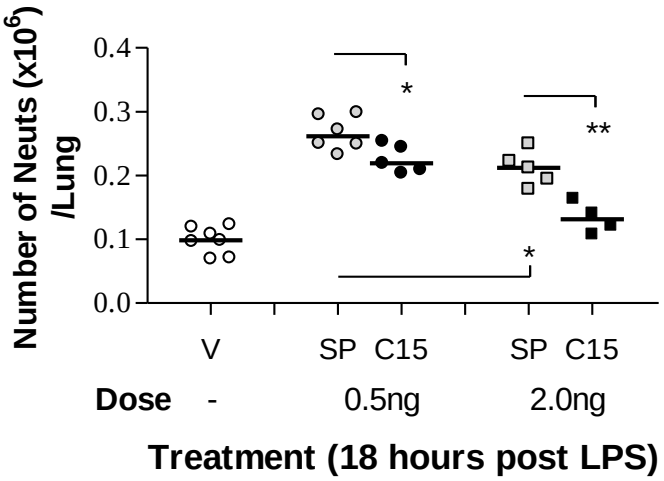

Figure 4-1: Effect of old SP or C15 on the number of lung neutrophils after a single exposure to aerosolised LPS. Mice were injected (i.v.) with saline only (vehicle (V)), old SP or C15 (0.5ng or 2.0ng/100µl) 1 hour prior to LPS exposure. Lungs were collected 18 hours later and the number of neutrophils in the lungs determined by flow cytometry. Both C15 concentrations significantly reduced LPS induced neutrophilia, however there was also a significant effect from old SP at 2.0ng. n = 4-7 mice per group, *P<0.03, **P<0.003, Student's unpaired t-test.

4.2.3.3 Determination of the optimal route of administration of SP and C15

Briefly, BALB/c WT mice were either 1) injected with SP or C15 at 2.0ng/100µl intraperitoneally, 2) instilled with SP or C15 at 2.0ng/50µl intratracheally, or 3) injected with SP or C15 at 2.0ng/100µl intravenously *via* the tail vein. Mice were then rested for 1 hour prior to exposure to a single dose of aerosolised LPS. Lungs were collected 6 hours after LPS exposure and neutrophils enumerated by flow cytometry.

4.2.3.4 Prophylactic administration of SP and C15

SP or C15 (2.0ng/100µl) was administered intravenously to mice during the first 2 weeks of the LPS aerosol model or the NTHi double challenge model (**Figure 4-2A and B**). SP or C15 was given 1 hour prior to each LPS exposure or each NTHi administration. Lungs were collected 24, 48, and 72 hours after final the final LPS exposure or NTHi challenge to determine inflammation (number of neutrophils and macrophages), mRNA expression and protein concentration of cytokines and chemokines (such as TNF-α, MMP-12, CCL3, active caspase-3). Lungs were also collected 6 days after the final LPS exposure or 9 days after NTHi challenge for morphometric analysis (volume, MLI and percentage alveolar airspace).

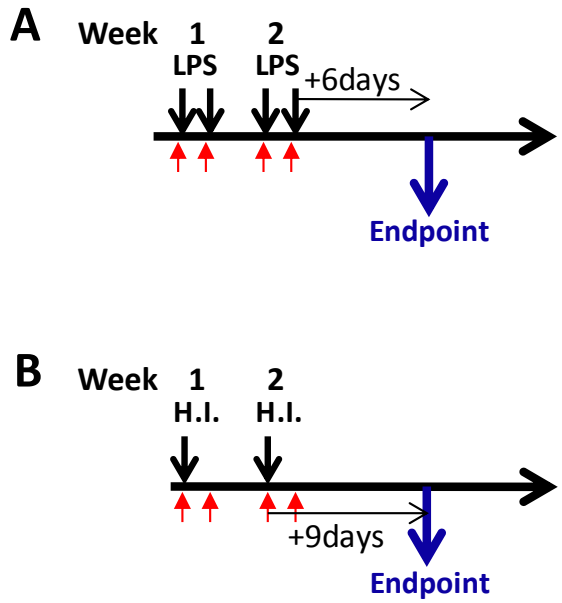

Figure 4-2: SP or C15 was administered during the 2 week LPS aerosol model or the double NTHi challenge model of emphysema. BALB/c WT mice were administered 2ng/100µl SP or C15 intravenously 1 hour prior to each aerosolised LPS exposure in a 2 week mouse model of LPS-induced emphysema **(A)**, or 1hr prior and 72 hours after each NTHi challenge **(B)**. Mice were then sacrificed 72 hours and 6 days after the last LPS exposure or 9 days after the last NTHi challenge to determine inflammatory responses and lung morphology, respectively.

4.2.3.5 Therapeutic administration of SP and C15

SP or C15 was also administered therapeutically by treating mice during the second week of the 2 week LPS aerosol model or the double NTHi challenge model (**Figure 4-2**)**.** Briefly, 2.0ng of SP or C15 was dissolved in 100µl of sterile hospital grade saline and injected *via* the tail vein, 1 hour prior to each LPS exposure or NTHi challenge. Lungs were collected and processed as described in Section 4.2.3.4

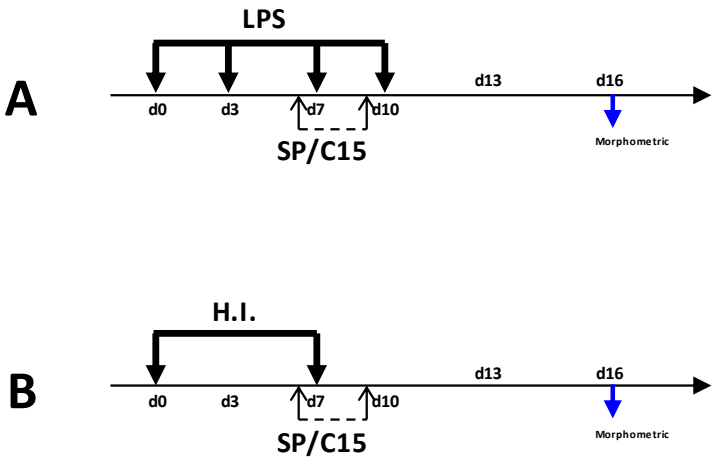

Figure 4-3: Models of therapeutic administration of SP or C15. Mice were treated with SP or C15 during the second week of the 2 week LPS aerosol model **(A)** or NTHi double challenge model **(B)**. SP or C15 was administered 1 hour prior to each LPS exposure or NTHi challenge.

4.2.4 Morphometric analysis

Refer to Section 2.2.3.

4.2.5 Flow Cytometry analysis

Refer to Section 2.2.4

4.2.6 Messenger RNA analysis

Refer to Section 2.2.5

4.2.6.1 Total RNA extraction

Refer to Section 2.2.5.1

4.2.6.2 Reverse Transcription

Refer to Section 2.2.5.2

4.2.6.3 Primers

Refer to Section 2.2.5.3, Section 3.2.5.3, Table 2-1, and Table 3-1

4.2.6.4 Analysis of gene expression by quantitative real-time PCR (qPCR)

Refer to Section 2.2.5.4

4.2.7 Fluorometric Assay

Refer to Section 3.2.6.

4.2.8 Immunohistochemistry

Refer to Section 3.2.7. The HRP-DAB system is used here.

4.2.9 Protein detection via ELISA

Refer to Section 2.2.6

4.2.9.1 Murine Chemerin

Murine chemerin was detected using the Quantikine Mouse Chemerin Immunoassay kit from R&D Systems (Minneapolis, MN) as per the manufacturer's instructions.

4.2.9.2 Human Chemerin

The concentration of chemerin in human sputum samples was determined using the DuoSet ELISA Development kit from RnD Systems (Minneapolis, MN) as per the manufacturer's instructions.

4.2.10 Statistic analysis

Refer to Section 2.2.8

All statistics done in human studies were handled by researchers over at the Hunter Medical Research Institute.

Refer to **Table 2-2 in Chapter 2** for components of buffers and solutions.

.

4.3 Results

4.3.1 Chemerin levels in LPS- or NTHi- treated mice

We first determined if chemerin was present in our mouse models of LPS- or NTHi-induced emphysema. Active chemerin protein levels in lung homogenates were detected by ELISA at 6, 24, 48, and 72 hours after a single exposure to aerosolised LPS. Active chemerin protein levels were significantly ($n = 5$; $P<0.0001$) elevated in mice exposed to LPS when compared to control mice. Chemerin levels peaked at 1 day (140.60ng/ml ± 5.90ng/ml; about 2 fold increase) after LPS exposure as compared to control mice (82.32ng/ml ± 5.03ng/ml) (**Figure 4-4A**).

We next determined chemerin protein levels in a 2 week aerosol model of LPS-induced emphysema. The concentration of chemerin protein in the lung tissue was significantly increased 1 day (139.80ng/ml ± 0.76ng/ml) and 2 days (120.50ng/ml ± 3.97ng/ml) after the final LPS exposure ($n = 5$; $P\leq0.0003$) compared to controls **(Figure 4-4B**).

We also observed significantly elevated ($n = 5$; $P<0.0001$) levels of chemerin protein in the lungs of mice 72 hours after a single exposure to NTHi (122.50ng/ml ± 2.02ng/ml) as compared to vehicle treated controls (**Figure 4-4C**).

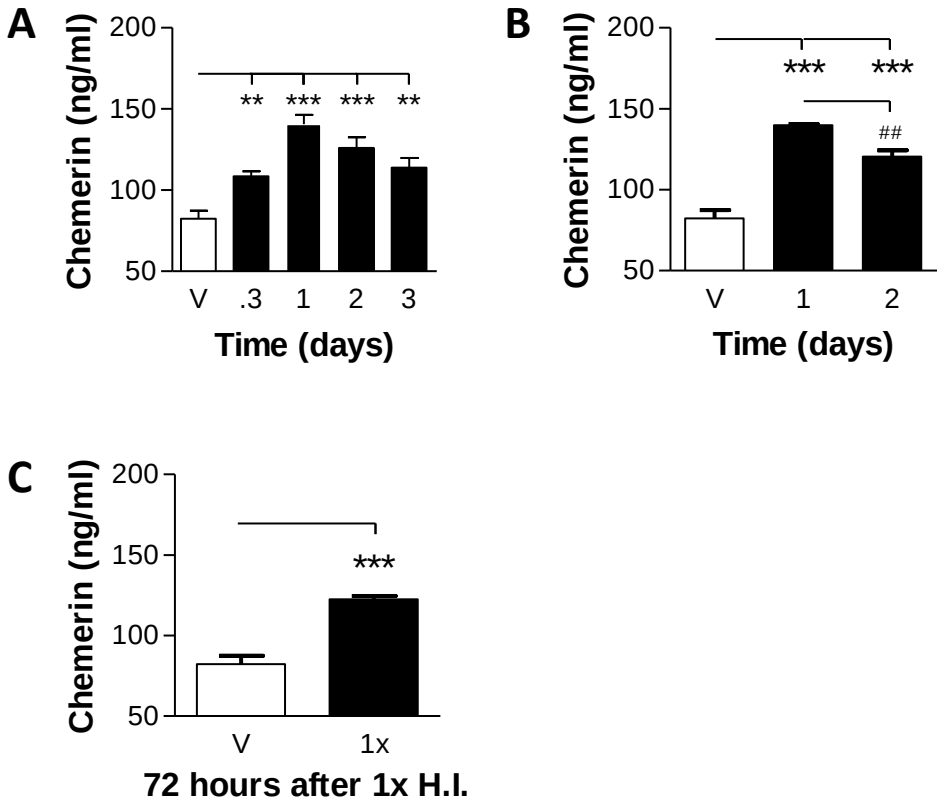

Figure 4-4: LPS- and NTHi -induced chemerin expression in the lungs of mice. Mice were exposed to LPS or NTHi and lung homogenates tested for chemerin protein by ELISA. Chemerin levels were significantly higher 6hrs (0.3 days), 1, 2 and 3 days following a single exposure to aerosolised LPS compared to controls **(A).** Chemerin levels were significantly higher 1 and 2 days after the last exposure to aerosolised LPS in the 2 week model **(B)**. Chemerin levels were significantly higher 72 hours after a single challenge with NTHi **(C).** n = 5 mice per group. **P<0.005, ***P<0.001, $^{\#\#}$P<0.002**,** Student's unpaired t-test.

4.3.2 New scrambled peptide (SP) exerts no effects on LPS or NTHi treatment

Using the new SP, we compared the number of neutrophils in mice lung induced by LPS within 24 hours to mice pretreated with C15. C15 pretreatment significantly reduced LPS-induced influx of neutrophils (**Figure 4-6C**). The number of neutrophils induced by LPS is comparable to observations in Chapter 2, **Figure 2-10**.

To test that the new sequence of the scrambled peptide does not alter inflammation induced by LPS, we next sought to confirm this in our models of emphysema. Mice were exposed to vehicle, LPS or NTHi only, or SP prior to LPS or NTHi administration (see study design **Figure 4-2**). Pre-treatment with new SP had no effect on the changes in lung structure (MLI and percentage alveolar airspace) in either the LPS-induced (**Figure 4-5A and B**) or NTHi-induced (**Figure 4-5C and D**) models of emphysema, confirming its suitability as a control peptide.

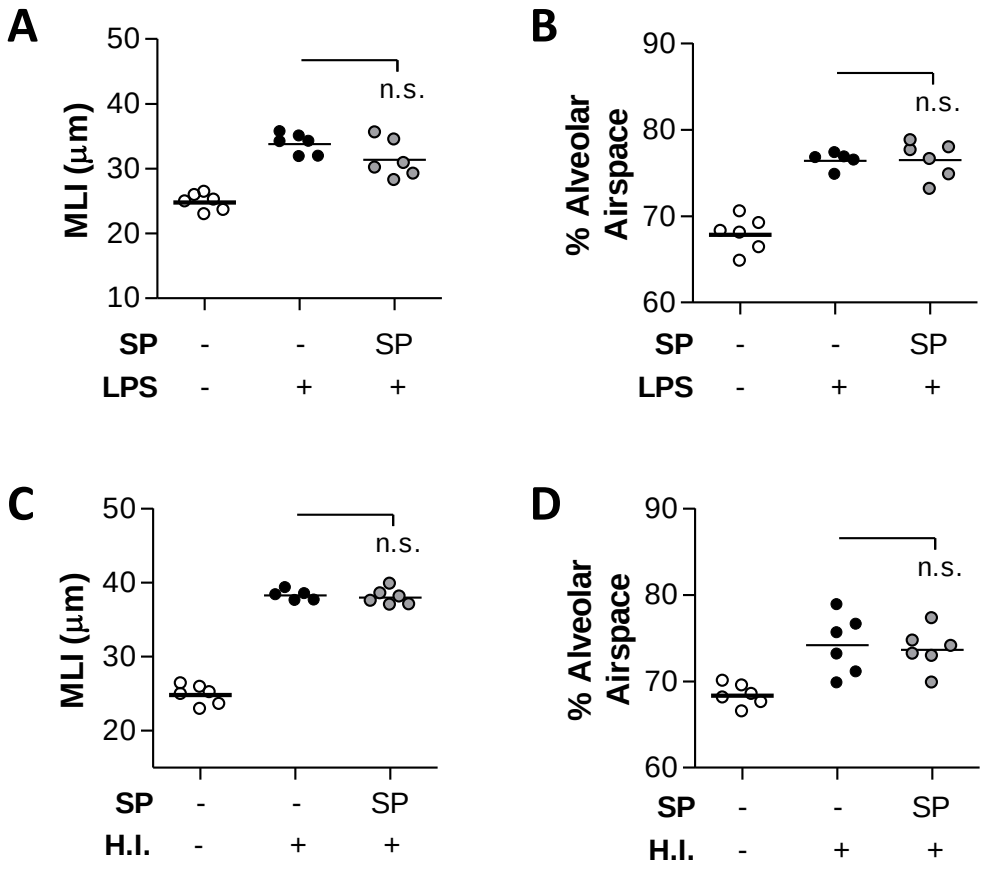

Figure 4-5: Pre-treatment with new scrambled peptide (SP) had no effect on morphology in the lungs of mice exposed to LPS or NTHi. Mice were exposed to vehicle only (open circles), LPS only, (solid circles) or intraveneous SP 1 hour prior to the beginning of the 2 week LPS model **(A and B)** or the 2 week NTHi model **(C and D)**. Lungs were collected 6 days after the last LPS exposure or 9 days after the last NTHi challenge for morphometric analysis. n = 5-6 mice. n.s. = not significant (P>0.05), Student's unpaired t-test.

4.3.3 Routes of administration of peptides (SP or C15) affect its efficacy

Next, we determined the efficacy of C15 for attenuating LPS-induced neutrophilia in the lungs. Intraperitoneal, intratracheal, and intravenous routes of administration of the peptide were tested as per material and methods section. Briefly, peptides (SP / C15) were administered 1 hour prior to LPS exposure. Flow cytometry techniques were used to detect neutrophils from the single cell suspensions generated. Both intraperitoneal and intravenous administration of C15 peptide significantly reduced (n = 3-4 mice per group; $P<0.01$ and $P<0.04$ respectively), but does not fully abrogate, the effects of LPS-induced neutrophilia in the lungs (**Figure 4-6: (A)** ~$1.2x10^6$ neutrophils; **(B)** ~$0.7x10^6$ neutrophils) compared to mice treated with the control scrambled peptide (**Figure 4-6: (A)** ~$2x10^6$ neutrophils; **(B)** ~$1x10^6$ neutrophils)**.** In contrast, there was no change in the number of neutrophils in the lung following intratracheal administration of C15 (**Figure 4-6C**)**.**

For the rest of these studies, we chose to administer SP or C15 *via* the intravenous route. The reason for this is that based on results from the SP treated mice, we felt that I.P. administration (higher neutrophilia) may have an effect. If it is route in-dependent and SP dependent, then similar levels of neutrophilia should be observed in all 3 routes in SP pre-treated mice.

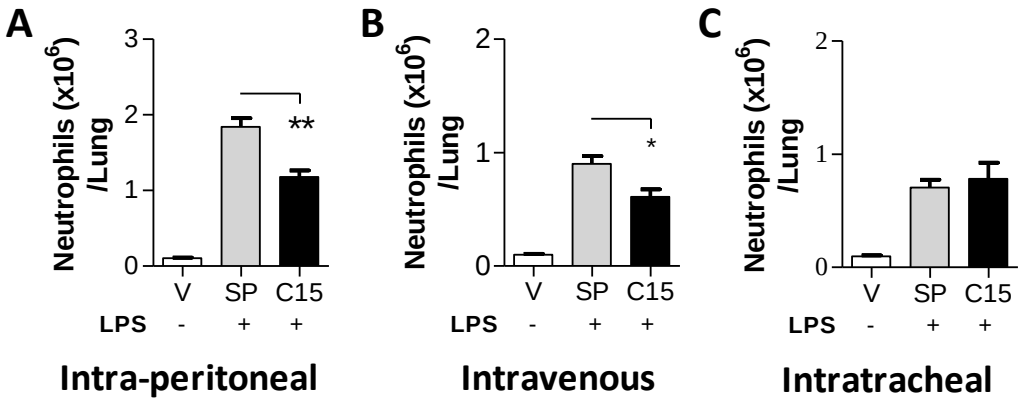

Figure 4-6: Number of lung neutrophils following administration of SP or C15 in a 2 week model of LPS-induced emphysema. Different routes of administration of 2.0ng of SP or C15 per mouse (intraperitoneal **(A),** intravenous **(B),** and intratracheal **(C)**) were used 1 hour prior to exposure to aerosolised LPS. The number of neutrophils in the lungs was determined 6 hours after LPS exposure by flow cytometry. n = 3-4 mice per group. *P<0.04, **P<0.01, Student's unpaired t-test.

4.3.4 Effect of C15 on LPS-induced emphysema in older mice

We also investigated whether pre-treatment with C15 would also attenuate the development of LPS-induced emphysema in older mice. LPS-induced increases in MLI in 16 week old mice were significantly attenuated following pre-treatment with C15 when compared to LPS only treated age matched mice (MLI: 30.29 ± 0.59 vs 36.42 ± 1.4µm; n = 6; P=0.0034) (**Figure 4-7**).

4.3.5 Effects of C15 on LPS and NTHi-induced emphysema

Having previously shown that exposure to LPS or challenge with NTHi induced an increase in both MLI and percentage alveolar airspace in the lungs of mice (Chapters 2 and 3), we investigated the effect that treatment with C15 peptide would have on the development of emphysema-like lesions induced by LPS or NTHi.

As shown in **Figure 4-8A and B**, LPS exposure induced a significant elevation of both MLI (31.38 ± 1.2µm vs 23.13 ± 0.79µm; n = 5-6; P<0.0001) and percentage alveolar airspace (76.46 ± 0.86% vs 69.23 ± 0.65%; n = 5-6; P<0.0001) in mice pre-treated with SP as compared to SP only treated controls. LPS-induced changes to both MLI and percentage alveolar airspace were significantly reduced in C15 pre-treated mice compared SP pre-treated mice (**MLI:** 25.58 ± 0.39µm vs 31.38 ± 1.2µm; n = 5-6; P=0.001; **% alveolar airspace:** 71.00 ± 0.42**%** vs 76.46 ± 0.86**%**; n = 5-6; P<0.0001).

Similarly, in **Figure 4-8C and D** SP+NTHi treated mice had significantly higher MLI and percentage alveolar airspace compared to SP only control group (**MLI:** 37.97 ± 0.43µm vs 23.13 ± 0.79µm; P<0.0001; **% alveolar airspace**: 73.64 ± 0.99% vs 69.23 ± 0.65%; P<0.0042). Pre-treatment with C15 significantly attenuated NTHi-induced increases in MLI and percentage alveolar airspace when compared to SP+NTHi mice (**MLI:** 30.21 ± 0.47µm vs 37.97 ± 0.43µm; P<0.0001; **% alveolar airspace**: 68.63 ± 0.80% vs v73.64 ± 0.99%; P<0.0042).

Notably, there was still a slight, but significant increase in MLI measurements in mice pre-treated with C15 prior to LPS or NTHi exposure when compared to control mice (C15+Vehicle treated) (**Figure 4-8A and C**), indicating that the effect is attenuated, but not totally abolished.

Mice administered SP or C15 alone showed a very slight but significant decrease in MLI following C15 treatment compared to vehicle only treated mice (**Figures 4-8A and C**). However this was not reflected in the percentage alveolar airspace compared with vehicle treated controls) (**Figure 4-8B and D**). From here, we will be using SP treated mice as a direct and more relevant control to C15 treated mice; and omit vehicle only treated groups as controls.

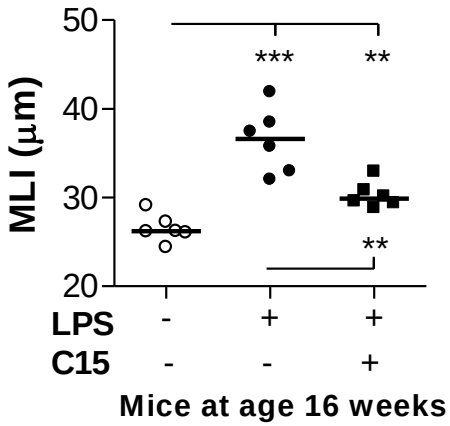

Figure 4-7: Pre-treatment with C15 attenuates the development of LPS-induced emphysema in older mice. 16 week old mice were administered C15 1 hour prior to exposure to aerosolised LPS in the 2 week model. Mean linear intercepts (MLI) of lung tissue was determined and compared to mice treated with vehicle or LPS only. n = 6 mice per group. ***P<0.0002, **P<0.005, Student's unpaired t-test.

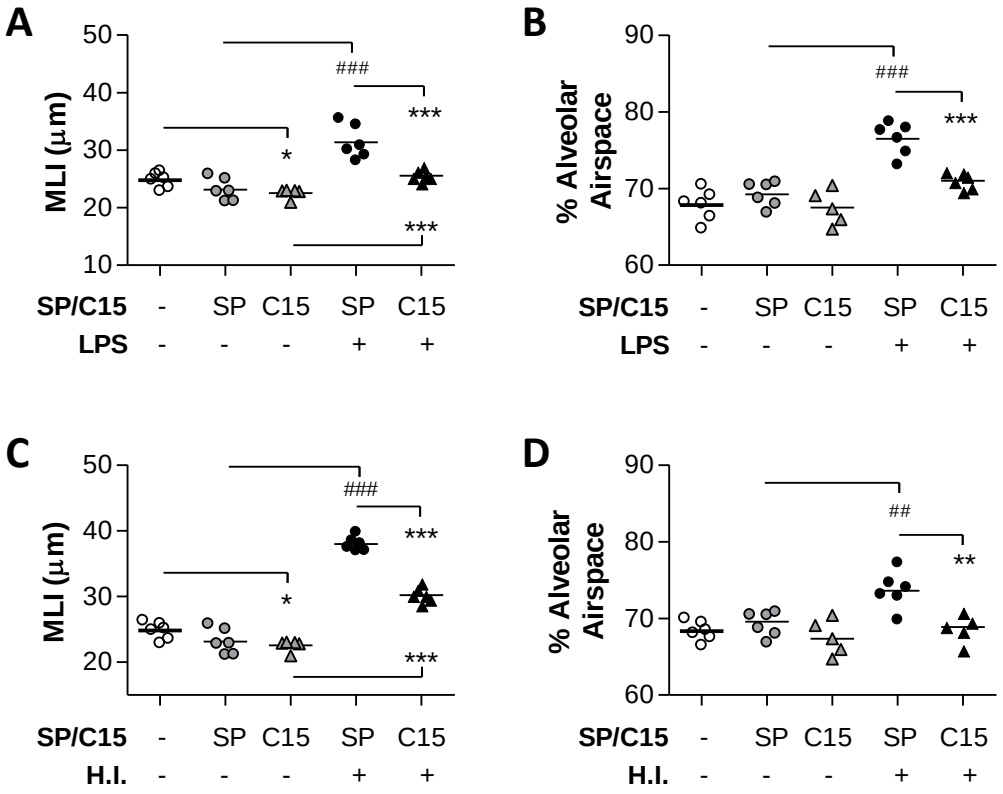

Figure 4-8: LPS and NTHi-induced emphysema is attenuated in mice pre-treated with chemerin-derived peptide (C15). Mice were administered SP (solid circles) or C15 (solid triangles) (2ng) 1 hour prior to the first exposure of LPS in the 2 week aerosol model (**A and B**) or 1 hour prior to the first NTHi challenge in the double challenge model (**C and D**). Control groups received vehicle (open circles), SP (grey circles), or C15 only (grey triangles). Mice were sacrificed 6 days after the last LPS exposure or 9 days after the last NTHi challenge. Lungs were prepared for morphometric analysis. n = 5-6 mice per group. H.I. = NTHi. *P<0.02, **/##P<0.005, ***/###P<0.0001, Student's unpaired t-test.

4.3.6 Effect of C15 and SP on lung volumes

In Chapters 1 and 2 we demonstrated that exposure to LPS or challenge with NTHi does not alter lung volume. Similarly, intravenous injection with SP or C15 alone does not affect lung volume in mice (**Figure 4-9**). These volumes are also comparable to observations in both Chapters 2 and 3.

4.3.7 Effect of C15 and SP on LPS- and NTHi-induced inflammation

We investigated whether treatment with C15 prior to exposure to LPS or challenge with NTHi would reduce the level of inflammation in the lungs. The number of neutrophils and macrophages in the lung tissue was determined by flow cytometry 24 hours after the final LPS exposure in the 2 week aerosol model, and 72 hours after the second NTHi challenge.

Pre-treatment with C15 significantly reduced the influx of both macrophages ($0.64 \pm 0.03 \times 10^6$ vs $0.98 \pm 0.024 \times 10^6$ cells; n = 6; $P<0.0001$) and neutrophils ($0.44 \pm 0.015 \times 10^6$ vs $0.66 \pm 0.023 \times 10^6$ cells; n = 6; $P<0.0001$) into the lungs of mice following exposure to LPS in a 2 week aerosol model compared to SP treated mice (**Figure 4-10A and B**). Similarly, pre-treatment with C15 significantly reduced the influx of macrophages into the lungs following NTHi challenge compared to SP treated group (**Figure 4-10C**) ($1.23 \pm 0.10 \times 10^6$ vs $2.32 \pm 0.14 \times 10^6$ cells; $P<0.0001$). However, pre-treatment with C15 did not have any significant effect on the number of neutrophils in the lungs compared to SP

treated mice (**Figure 4-10D**). This result is likely due to the time point (72 hours) investigated as neutrophils are most likely to have resolved back to baseline.

Treatment with C15 prior to exposure to LPS or challenge with NTHi can significantly reduce the level of inflammation within the lungs indicating the potential that a therapeutic blocking agent may be beneficial in preventing the progression of the development of emphysema-like lesions.

4.3.8 Effects of C15 on Chemerin expression and associated receptors

In our current mouse models, SP and C15 are administered in a prophylactic manner (i.e. before each LPS exposure, and before each NTHi exposure (including in between NTHi exposure)). Here we investigated whether treatment with C15 would alter the expression of chemerin as well as associated receptors ChemR23 and CCRL2. Both chemerin mRNA and protein levels were significantly up-regulated (approximately 25 fold) following exposure to LPS compared to unexposed control mice. Pre-treatment with C15 did not affect the LPS-induced changes in mRNA or protein levels of chemerin (**Figure 4-11A and B**).

While exposure to LPS induced a significant increase in mRNA expression for both ChemR23 and CCRL2, pre-treatment with C15 was only effective at reducing the expression of ChemR23 (**Figure 4-11C and D**) (10.38 ± 0.7609 vs 20.16 ± 1.716; n=5; $P<0.001$). There was no difference observed in CCRL2 expression levels between mice pretreated with C15 or scrambled peptide.

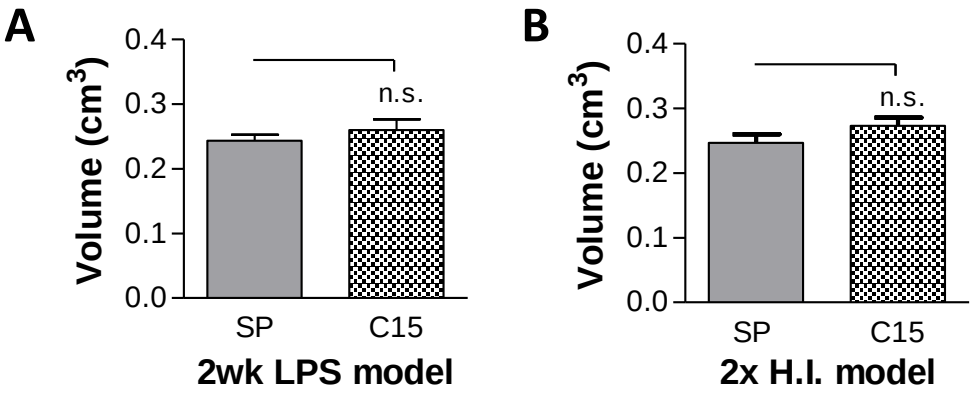

Figure 4-9: Lung volume of mice pre-treated with SP or C15 prior to LPS or NTHi exposure. Mice were pretreated with SP or C15 1 hour prior to LPS exposure (2 week aerosol model) **(A)** or NTHi challenge (double challenge model) **(B).** Mice were sacrificed 6 days after the last LPS exposure, or 9 days after the last NTHi challenge and their lung volume determined by liquid displacement. n = 6 mice per group. H.I. = NTHi. n.s. = not significant (P>0.05), Student's unpaired t-test.

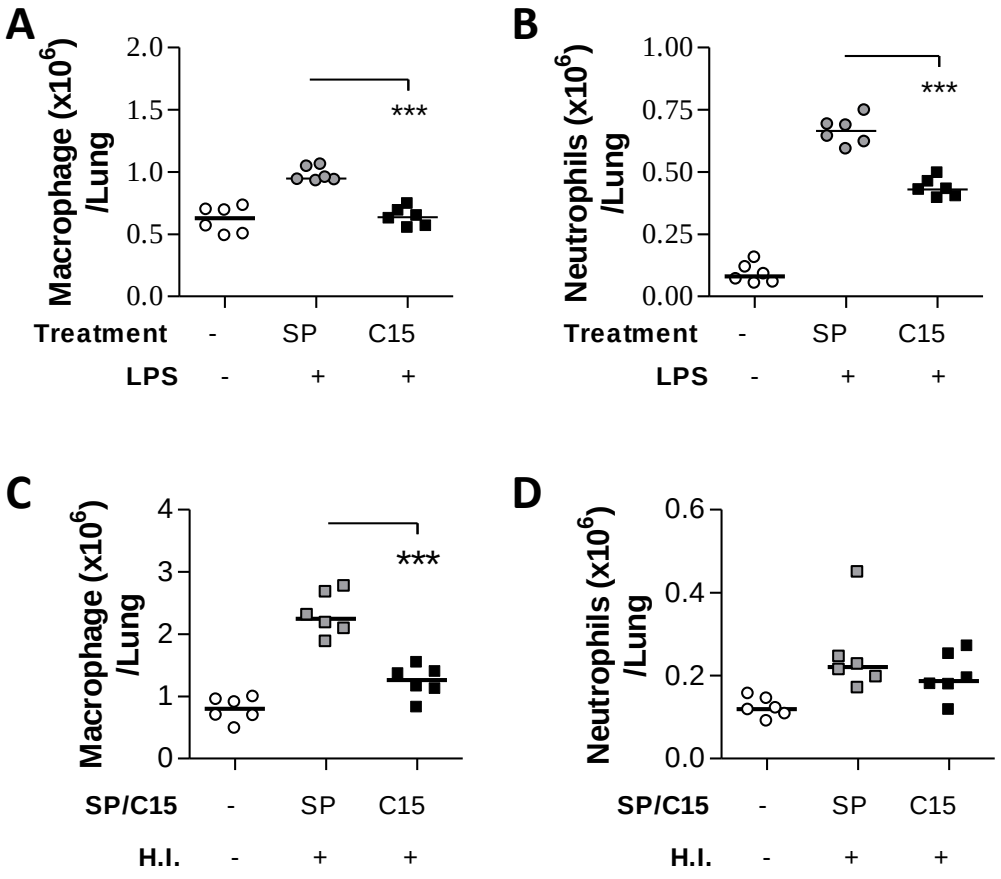

Figure 4-10: Pre-treatment with C15 attenuates LPS- or NTHi-induced inflammation in the lungs of mice. Mice were administered with SP (grey squares) or C15 (black squares) 1 hour prior to either LPS exposure or NTHi challenge. Macrophages and neutrophils within the lungs were enumerated by flow cytometry 24 hours after the last LPS exposure **(A and B)** or 72 hours after the last NTHi challenge **(C and D).** n = 6 mice per group. H.I. = NTHi. ***P<0.0001, Student's unpaired t-test.

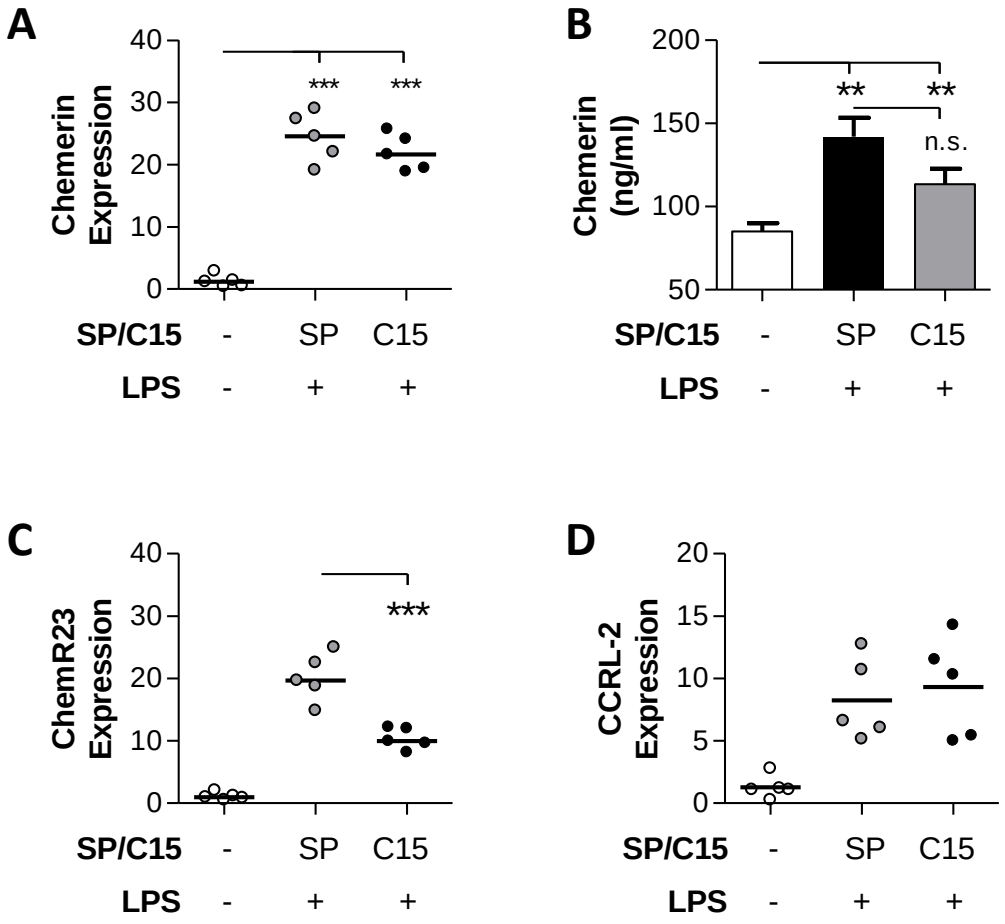

Figure 4-11: Prophylactic administration of C15 attenuates LPS-induced chemerin protein production and ChemR23 mRNA expression. Mice were exposed to vehicle only (open circles), SP+LPS (grey circles) or C15+LPS (solid circles) in a 2 week LPS aerosol model. Mice were sacrificed 48 hours after the last LPS exposure and mRNA or proteins levels of ChemR23 and CCRL2 in lung homogenates determined. mRNA levels were expressed as fold change over vehicle treated controls. Pre-treatment with C15 did not alter chemerin mRNA **(A)**, chemerin protein **(B)**, or CCRL2 mRNA levels **(D)**. However, mRNA levels of the ChemR23 were significantly reduced **(C)**. n= 5 mice per group. **P<0.005, ***P<0.001, Student's unpaired t-test.

4.3.9 Effect of C15 on LPS-induced proinflammatory chemokines

We next sought to determine the effects of C15 on the mRNA expression levels of the proinflammatory chemokines CCL3 (MiP-1α), MMP12, and HMGB-1 using qPCR. Both CCL3 and MMP-12 were measured in lung tissue obtained 48 and 72 hours after the last LPS exposure. HMGB1 was only measured in lung tissue taken 48 hours after the last LPS exposure.

C15 did not significantly reduce LPS-induced mRNA expression of chemokines CCL3, MMP-12 or HMGB-1 at 48 or 72 hours post final LPS exposure (although there is a slight trend for MMP-12 at 48 hours). However, the data did confirm our earlier prediction, that mRNA expression occurs earlier than 72 hours after LPS exposure (**Figure 4-12**).

4.3.10 Effect of C15 on NTHi-induced proinflammatory chemokines

We then proceeded to determine the effects of C15 on the mRNA expression levels of proinflammatory chemokines CCL3 (MiP-1α), and MMP12 following NTHi challenge. Pre-treatment with C15 significantly reduced NTHi-induced mRNA levels of MMP-12 (1.81 ± 0.30 vs 3.63 ± 0.44; n = 7-8; $P<0.006$), but not CCL3 (although a trend is observed) 72hours after the last NTHi challenge (**Figure 4-13A**). However, when we determined CCL3 protein levels by ELISA, the results indicated that C15 significantly reduces NTHi-induced CCL3 protein expression 72 hours after the last NTHi exposure compared to SP treated groups (**Figure 4-13B**) (935.9 ± 212.2ng vs 1806 ± 179.6ng; n = 5; $P<0.02$).

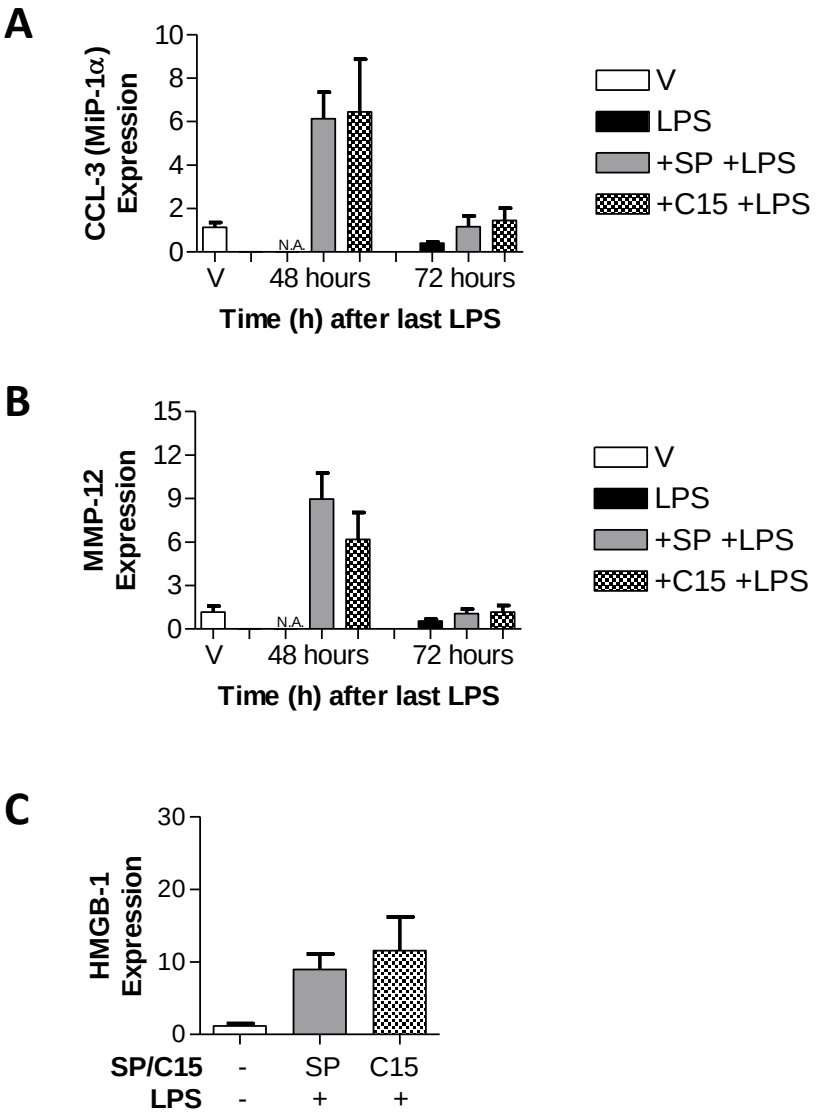

Figure 4-12: C15 has no significant effect on LPS-induced proinflammatory cytokine mRNA levels as determined 48 and 72 hours after the last LPS exposure. Mice were treated with SP or C15 1 hour prior to the first exposure to LPS in a 2 week aerosol model. Messenger RNA levels of CCL3 **(A)**, MMP-12 **(B)** and HMGB-1 **(C)** were determined by qPCR in lung tissue 48 and 72 hours after the last LPS exposure and expressed as a fold change over the control group. n = 5-6 mice per group. N.A. = Not Available.

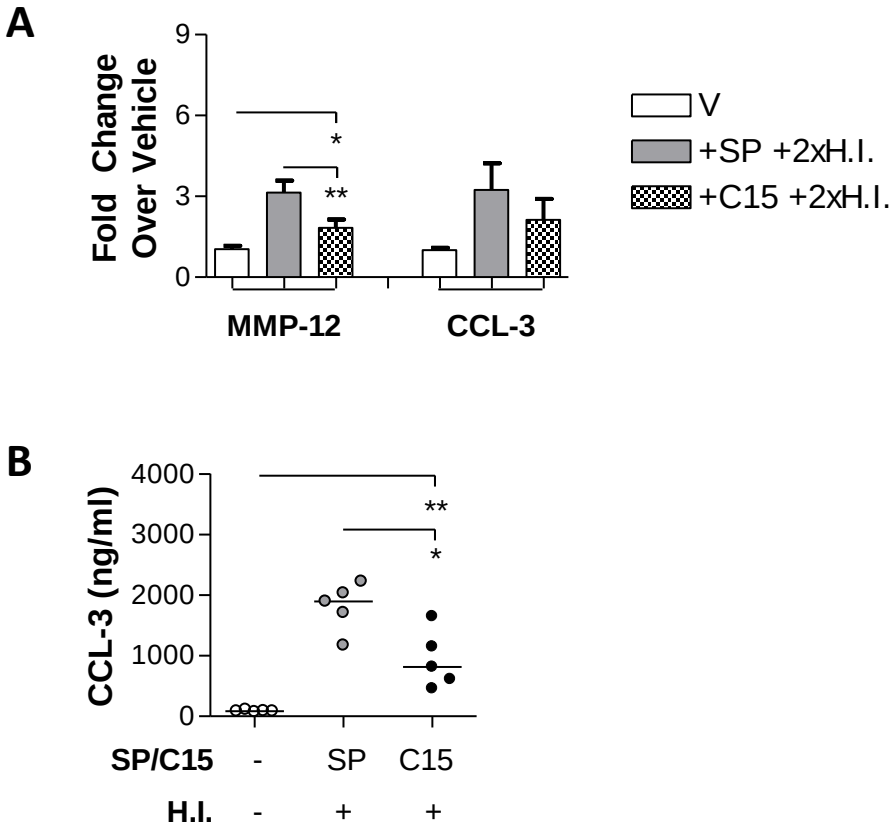

Figure 4-13 Prophylactic administration of C15 attenuates NTHi-induced proinflammatory chemokines. Mice were exposed to SP or C15 1 hour prior to each NTHi challenge. Mice were sacrificed 72 hours after the last challenge and mRNA levels of MMP-12 and CCL3, and protein levels of CCL3 in lung tissue determined. Pre-treatment with C15 significantly reduced the level of mRNA expression for MMP12, but not CCL3 **(A),** and significantly reduced the protein level of CCL3 **(B).** n= 5-8 mice per group. H.I. = NTHi. *P<0.03, **P<0.002.

4.3.11 Effect of C15 on LPS-induced enzymes associated with ceramide synthesis

Pre-treatment with C15 significantly reduced mRNA expression levels of ASmase by 24 (52.74 ± 4.00 vs 76.53 ± 5.12; n = 5; P<0.008) and 48 hours (262.7 ± 12.8 vs 330.2 ± 20.2; n = 5; P<0.03), but not 72 hours after the last LPS exposure (**Figure 4-14A**). Similarly, C15 treatment reduced mRNA expression levels of LASS-2 enzyme 48 hours (1.03 ± 0.1160 vs 2.02 ± 0.25; n = 5; P<0.008) but not 24 or 72 hours after the last LPS exposure (**Figure 4-14B**). However, there was no significant change in mRNA expression levels of NCdase following treatment with C15 (**Figure 4-14C**). Peak expression of ASmase and LASS-2 was observed 48 hours after the last LPS exposure, indicating that LPS exposure induces early activation of proinflammatory chemokines.

4.3.12 Effect of C15 on NTHi-induced enzymes associated with ceramide synthesis

Based on results from LPS treatment, we determined the effect that pre-treatment with C15 would have on NTHi-induced mRNA expression of enzymes involved with ceramide production. 48 hours after the last NTHi challenge, in response to prophylactic pre-treatment with C15, our results demonstrate a significant reduction in ASmase mRNA expression (**Figure 4-15A**) (248.0 ± 25.30 vs 432.9 ± 49.34; n = 5; P<0.02) but not LASS-2 (**Figure 4-15B**) (although a similar trend is observed) compared to controls.

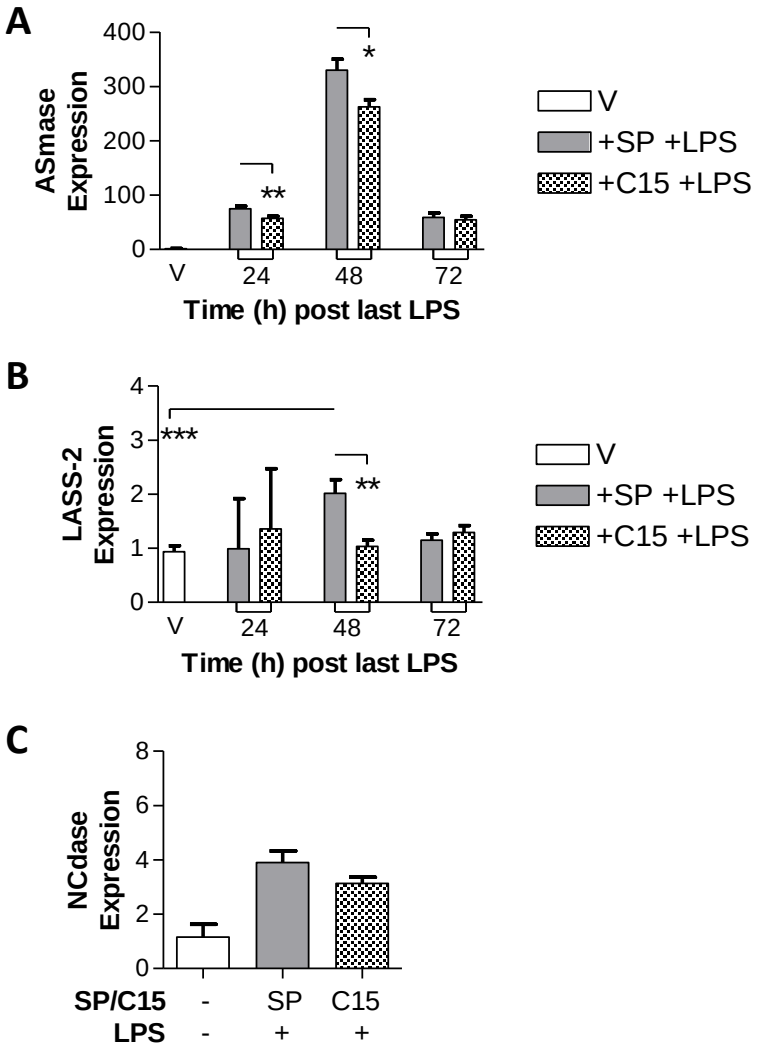

Figure 4-14: Prophylactic administration of C15 attenuates LPS-induced apoptosis related genes. Mice were treated with vehicle only (open bars), SP+LPS (grey bars), or C15+LPS (dotted bars) in a 2 week aerosol model and expression of mRNA of apoptosis related genes in lung tissue determined by qPCR. mRNA for ASmase **(A)** and LASS-2 **(B)** was determined in the lungs of mice 24, 48 and 72 hours after the last LPS exposure. mRNA for NCdase was determined in lungs of mice 48 hours after the last LPS exposure **(C)**. mRNA is expressed as fold change over the control group. n = 5 mice per group. *P<0.03, **P<0.008, ***P<0.0001, Student's unpaired t-test.

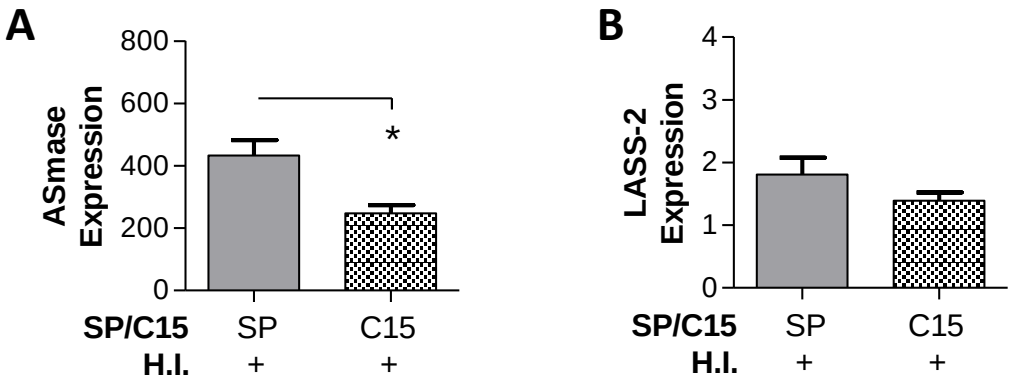

Figure 4-15: Prophylactic administration of C15 attenuates NTHi-induced apoptosis related genes. Mice were treated with C15 (dotted bars) or SP (grey bars), prior to challenge with NTHi. mRNA expression levels of the apoptosis related genes ASmase **(A)** and LASS-2 **(B)** were determined in the lung tissue by qPCR 48 hours after the last challenge. mRNA was expressed as a fold change over the control group. n = 5 mice per group. H.I. = NTHi. *P<0.02, Student's unpaired t-test.

4.3.13 Effect of C15 on LPS- or NTHi-induced ceramide levels in alveolar macrophages

Having demonstrated that treatment with C15 reduced mRNA expression levels of enzymes associated with ceramide production, we next sought to determine if ceramide levels in the LPS and NTHi models are also decreased. We used IHC to detect and semi-quantitate the average number of ceramide positive alveolar macrophages in the lung.

Cells staining positive for ceramide appear dark brown (**Figure 4-16A, left image**), while the cell nucleus stains blue (**Figure 4-16A, right image**). Mice pre-treated with C15 show low to no alveolar macrophages stained positive for ceramide compared to control mice.

C15 pre-treatment significantly reduced the average number of ceramide positive alveolar macrophages in both the LPS model (19.93 ± 2.00 vs 32.79 ± 1.50; n = 5; $P<0.001$) and NTHi model (15.44 ± 0.75 vs 29.47 ± 1.49, n = 5-6; $P<0.0001$) (**Figure 4-16B and C**) when compared to control groups pre-treated with SP.

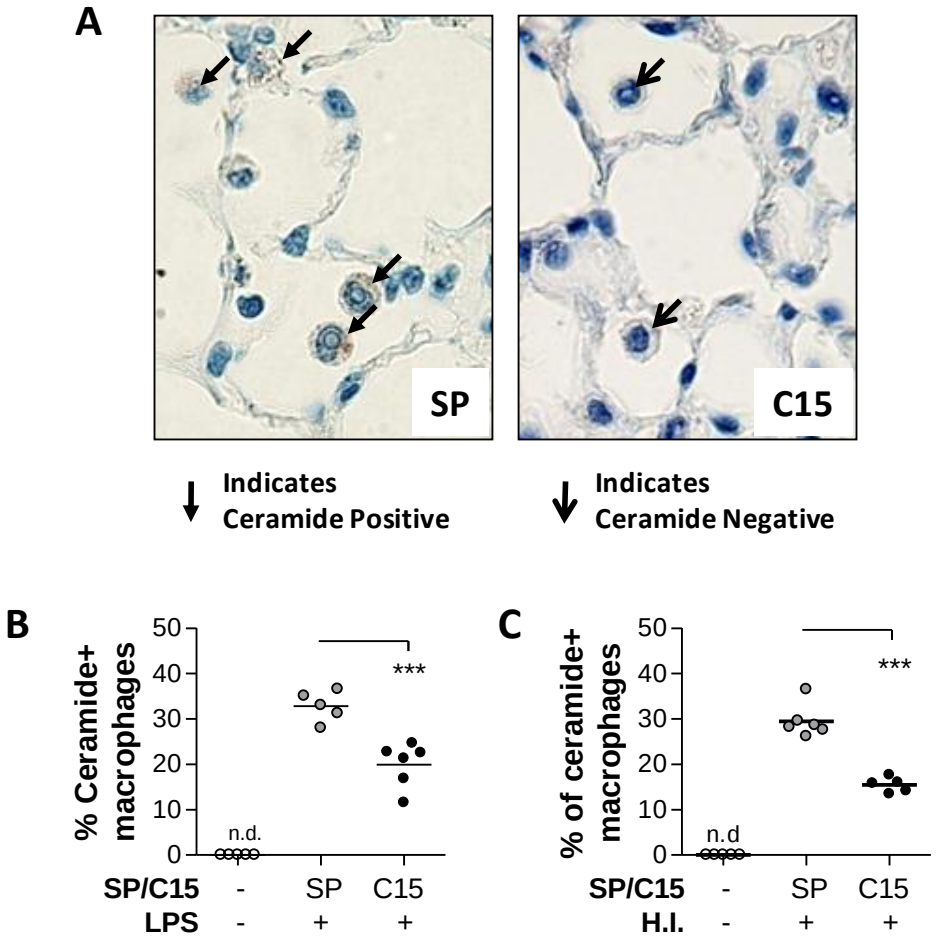

Figure 4-16: Prophylactic administration of C15 attenuates LPS and NTHi-induced ceramide production in alveolar macrophages. Mice were pre-treated with SP or C15 prior to LPS exposure or NTHi challenge in the respective models. Mice were sacrificed 6 or 9 days after the last LPS exposure or NTHi challenge respectively (when inflammation had resolved). IHC was used to identify ceramide positive alveolar macrophages in the lung. Representative images comparing macrophages stained positive for ceramide (left image) and macrophages stained negative for ceramide (right image) **(A)**. The Percentage of macrophages stained positive for ceramide was determined in mice treated in the 2 week LPS aerosol model **(B)** or in the NTHi challenge model **(C)**. n = 5-6 mice per group. Images are similar crops of 400x magnifications. H.I. = NTHi. ***P<0.001. n.d.= not detected, Student's unpaired t-test.

4.3.14 Effect of C15 on LPS- or NTHi-induced caspase-3 activity in the lung

We next sought to determine if prophylactic treatment with C15 can reduce LPS- or NTHi-induced caspase-3 activity in the lungs. Lung homogenates were collected 24 hours after the last LPS exposure and 72 hours after the last NTHi challenge and tested for caspase-3 activity.

Our data demonstrates that pre-treatment with C15 reduced the amount of LPS- (although insignificant, a trend is present, and P value of 0.051) and NTHi-induced caspase-3 activity (5.20 ± 0.73 vs 8.95 ± 1.21; n = 5; $P<0.03$) (**Figure 4-17A and B**).

4.3.15 Effect of C15 on bacterial clearance

We demonstrated that C15 protects mice from LPS- or NTHi-induced inflammation and related emphysematous lesion enlargement. We next sought to determined bacterial clearance 72 hours after the last NTHi challenge. Lung tissue was collected, homogenised and bacterial recovery determined.

Mice pre-treated with C15 had a higher bacterial load remaining in their lungs 72 hours after challenge compared to control treated animals (**Figure 4-18**), suggesting that the effect of the C15 on suppressing inflammation in the lungs also resulted in delayed bacterial clearance.

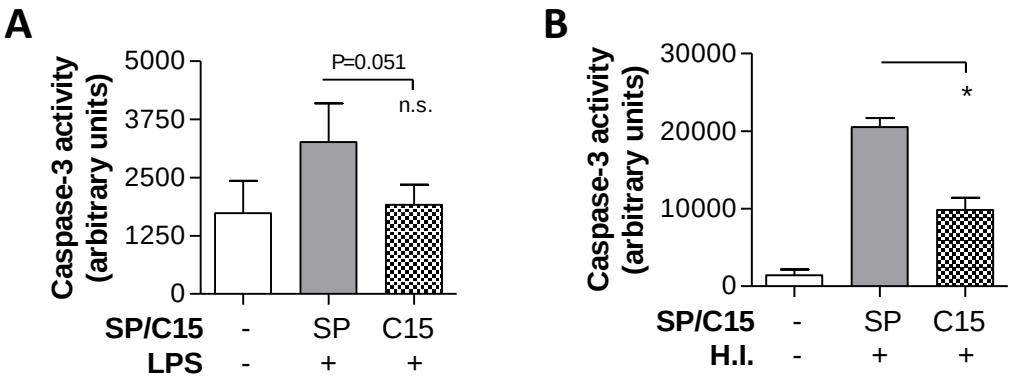

Figure 4-17: Prophylactic administration of C15 attenuates LPS and NTHi-induced caspase-3 activity. Mice were treated with prophylactic intravenous administration of SP or C15 in a 2 week LPS aerosol model or an NTHi challenge model. Mice were sacrificed 24 hours after the last LPS exposure **(A)** or 72 hours after the last NTHi challenge **(B)** and lung tissue homogenates analysed for caspase-3 activity. n = 5 mice per group. H.I. = NTHi. *P<0.03 , Student's unpaired t-test.

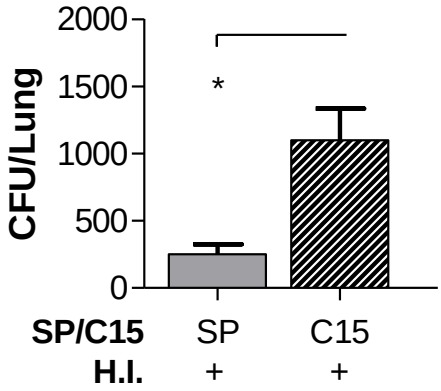

Figure 4-18: C15 treatment attenuates bacterial clearance in the NTHi challenge model. Mice pretreated with C15 prior to NTHi challenge were found to have a higher number of bacterial colony forming units remaining in their lungs 72 hours after the last challenge compared to SP (control) treated mice. n = 6 mice per group. H.I. = NTHi. *P<0.04, Student's unpaired t-test.

4.3.16 Effects of therapeutic administration of C15 on LPS and NTHi-induced emphysema

Data from the 1 week LPS model and the single NTHi challenge model suggest that there must be continuous exposure to stimuli (LPS or challenge) for emphysema to develop and this may arise from persistent and higher than normal levels of inflammation. Thus we questioned if the therapeutic administration of C15 could attenuate LPS- or NTHi-induced emphysema. Briefly, C15 or SP was administered intravenously only during the 2nd week of LPS exposure or NTHi challenge (as per models in **Figure 4-2**).

Therapeutic administration of C15 significantly protected mice from LPS-induced emphysema compared to SP treated mice. (**Figure 4-19A and B**) (**MLI:** 32.62 ± 0.79µm vs 37.14 ± 0.99µm; n = 5-6; P<0.006; **% alveolar airspace:** 67.73 ± 0.50**%** vs 75.10 ± 0.74**%**; n = 5-6; P<0.0001). SP or C15 only treated mice were used as negative controls. However, the protection conferred by therapeutic administration of C15 was not as great as observed in mice receiving prophylactic administration of C15. Similarly, therapeutic administration of C15 significantly protected mice from NTHi-induced emphysema (**Figure 4-19C and D**) (**MLI:** 29.70 ± 0.46µm vs 40.21 ± 1.76µm; n = 5-6; P=0.0001; **% alv airspace:** 70.36 ± 1.053**%** vs 76.84 ± 1.05**%**; n = 6; P<0.002). Again, the protection conferred by therapeutic administration of C15 was not as great as observed in mice receiving prophylactic administration of C15.

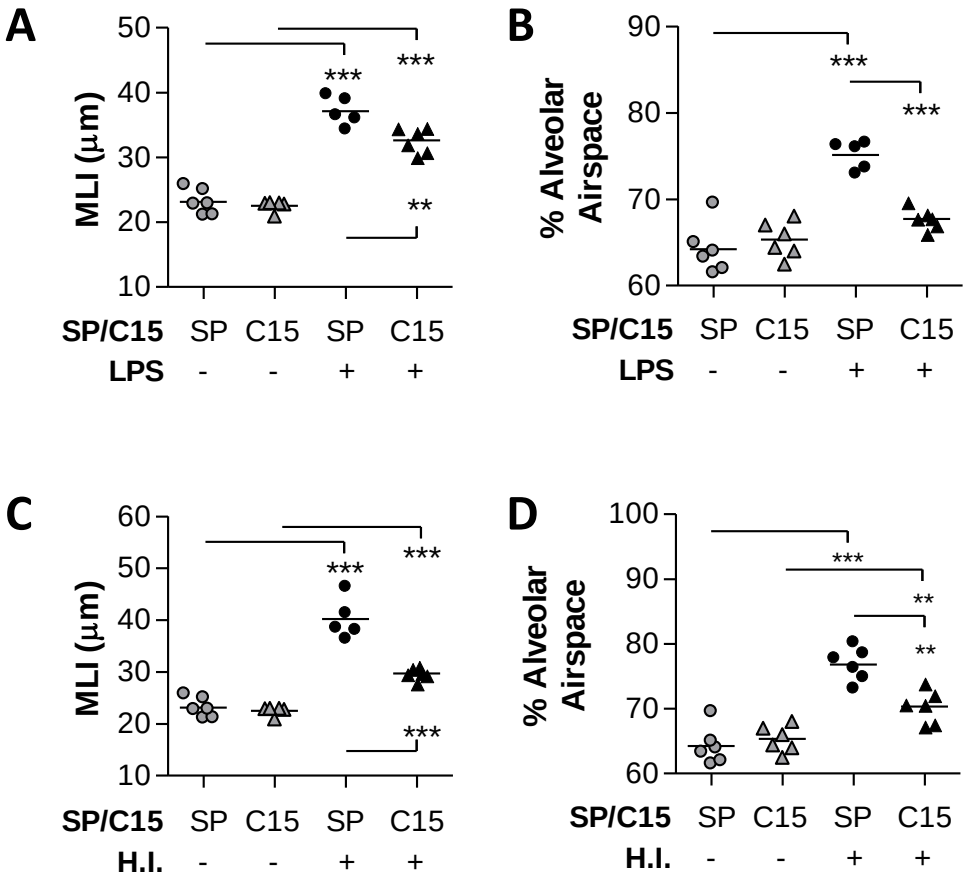

Figure 4-19: Therapeutic administration of C15 abrogated NTHi-induced emphysematous-like lesions. SP or C15 was administered *via* intravenous injection to mice only in the second week 1 hour prior to each aerosolised LPS exposure **(A & B)** or NTHi challenge **(C & D)**. Mice were sacrificed 6 or 9 days after the last LPS or NTHi challenge respectively. Lungs were processed and the MLI and percentage alveolar airspace determined. n = 5-6 mice per group. H.I. = NTHi. **P<0.006, ***P≤0.0001, Student's unpaired t-test.

4.3.17 Effect of therapeutic administration of C15 on ceramide production related enzymes in the 2 week LPS aerosol model

We next sought to determine the level of mRNA for ASmase and LASS-2, enzymes which drive the production of ceramide, which is in turn associated with apoptosis. We chose these 2 enzymes as they were the most prominent in response from our earlier observations (**Figure 4-14, 4-15**). Samples were collected 48 hours after the last LPS exposure based on previous results (which suggested peak expression did not occur 24 or 72 hours after last LPS exposure).

Therapeutic administration of C15 significantly reduced the mRNA expression levels of ASmase (**Figure 4-20A**) (107.3 ± 8.3 vs 176.3 ± 16.2; n = 5; $P<0.006$) and LASS-2 (1.20 ± 0.11 vs 1.79 ± 0.23; n = 5; $P<0.05$) (**Figure 4-20B**) enzymes.

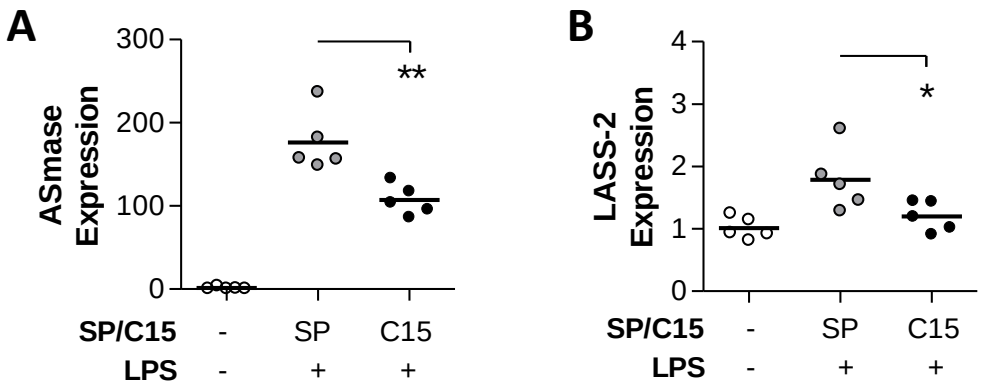

Figure 4-20: Therapeutic administration of C15 attenuated LPS-induced apoptosis related genes. SP or C15 was administered *via* intravenous injection to mice only in the second week, 1 hour prior to each LPS exposure. Lung tissue was collected 48 hours after the last LPS exposure and mRNA levels of ASmase **(A),** and LASS-2 **(B)** determined by qPCR. mRNA was expressed as a fold change over the control group. n = 5 mice per group. *P<0.05, **P<0.006, Student's unpaired t-test.

4.3.18 Effect of exposure to a combination of LPS and NTHi

We have shown that double exposure of LPS in the first week does not induce emphysema-like lesions in the lung (Chapter 2). We have also shown that a re-challenge with NTHi induces a more severe loss of parenchyma than a single challenge (Chapter 3). Here we determined the effects of exposing mice in the first week to LPS and then to NTHi in the second week (**Figure 4-21A**). This mouse model sought to demonstrate the patho-physiological effect of an opportunistic infection (bacterial) in the lung where the structure has previously been compromised.

Exposing mice to LPS in the first week (which does not in itself result in the development of emphysema-like lesions), followed by a single challenge with NTHi (which induces alveolar enlargement) resulted in an exaggerated loss of parenchyma (**Figure 4-21B**). The increase in MLI is also significantly higher (although low increase) than observed in the 2 week NTHi challenge model. This suggests that the initial LPS exposure (in the first week) may have primed the immune system to respond differently.

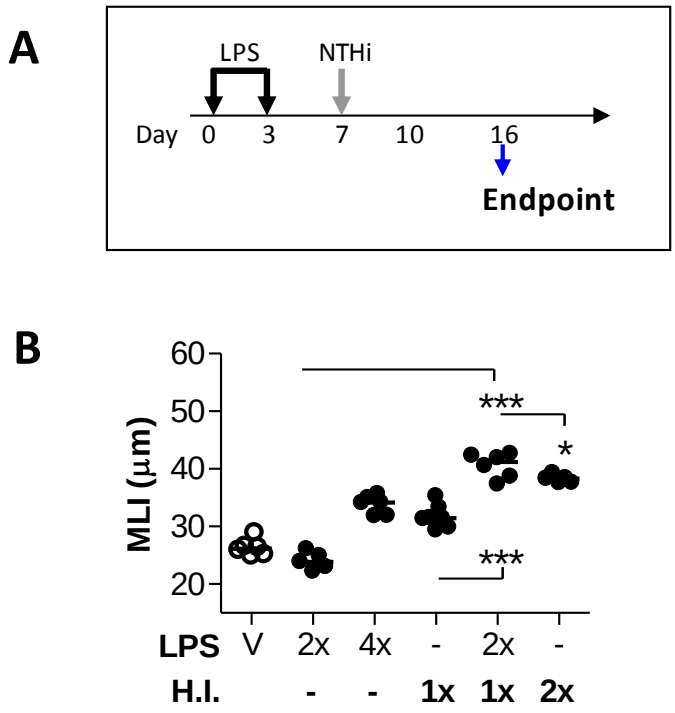

Figure 4-21: LPS and NTHi together further enhances emphysema development in mice. A model of LPS+NTHi induced emphysema **(A)**. Mice were exposed to aerosolised LPS in the first week while control mice were exposed to aerosolised vehicle. Mice were then infected once with $1x10^5$ CFU of NTHi in the second week, lung tissue was collected 9 days later and the MLI determined **(B)**. n = 5-7 mice per group. H.I. = NTHi. *P<0.05, ***P<0.0001, Student's unpaired t-test.

4.3.19 The role of alveolar macrophages in a mouse model of LPS-induced emphysema

While C15 demonstrated a general inhibition of inflammatory cells (notably neutrophils and macrophages), we next sought to determine if macrophages have a specific role in LPS-induced emphysema by depleting the lungs of alveolar macrophages *via* treatment with 2-chloroadenosine (2CA). We instilled 2CA to each mouse intratracheally, 1 hour prior to each LPS exposure in the 2 week model. Our preliminary tests demonstrated a significant depletion of alveolar macrophages in the lungs of mice instilled with 2CA compared to naive BALB/c WT mice (**Figure 4-22***).

Mice pre-treated with 2CA prior to LPS exposure (in the 2 week model) showed a significant reduction in the percentage of alveolar macrophages in the lungs compared to mice that were not pre-treated with 2CA before exposure to LPS (**Figure 4-22A**) (19.58 ± 0.32% vs 25.49 ± 1.41%; n = 5; $P<0.004$). Both of these groups had a higher number of total alveolar macrophages compared to control mice (treated only with vehicle). We did not determine for neutrophils (require different time point).

Caspase-3 activity in the lungs 72 hours after the last LPS exposure was also determined. The depletion of alveolar macrophages (though incomplete) significantly reduced the level of caspase-3 activity (**Figure 4-22B**), by approximately 50% compared to mice not treated with 2CA (6858 ± 854FU vs

3112 ± 125FU; n = 5; P<0.003). The level of caspase-3 activity in control mice (1081FU ± 245FU) was significantly lower than both LPS treated groups.

In a parallel experiment, mice were sacrificed 6 days after the last LPS exposure, and MLI and percentage alveolar airspace in the lungs determined (**Figure 4-22C and D**). Interestingly, our data indicated that treatment with 2CA significantly abrogated the effect of LPS-induced emphysema as both the MLI and percentage alveolar airspace were comparable to control mice (**MLI:** 23.88 ± 0.28μm vs 26.30 ± 0.59μm; n = 5 mice; P<0.0001; **% Alveolar Airspace:** 68.81 ± 0.56% vs 67.85 ± 0.82%; n = 5 mice; P<0.0001)

We also observed that vehicle treated control mice had a higher MLI compared to 2CA + LPS treated mice (**Figure 4-22C**). This was in accordance with our previous observation where intratracheal instillation of vehicle alone induced a slightly higher (significant) MLI value compared to mice exposed to aerosolised vehicle (Chapter 2, Figure 2-4).

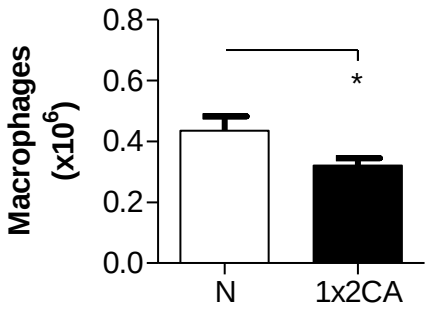

Figure 4-22*: Preliminary results of 2-Chloroadenosine on alveolar macrophages. Wildtype BALB/c mice were exposed to saline only (open bar) or 2CA (closed bar) and alveolar macrophages enumerated using flow cytometry. *P<0.05, Student's unpaired t-test.

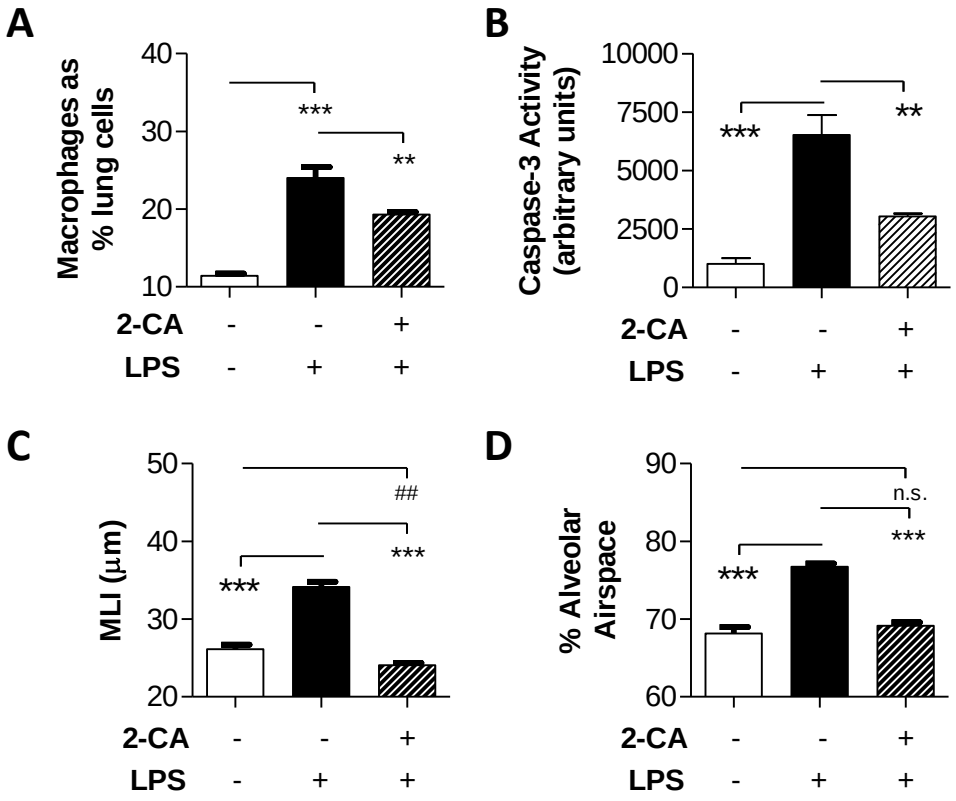

Figure 4-22: Depletion of alveolar macrophages by 2CA prevents LPS-induced emphysematous-like lesions and associated pathology. Mice were treated with 2CA 1 hour prior to each LPS exposure in a 2 week aerosol model. The percentage of macrophages in the lung was determined by flow cytometry 72 hours after the last LPS exposure **(A),** the level of Caspase-3 activity in lung homogenates determined 24 hours after the last LPS exposure **(B),** and MLI **(C)** and percentage alveolar airspace **(D)** in the lungs determined 6 days (day 16) after the last LPS exposure. Open bars represent vehicle treated control group. Solid bars represent groups treated with LPS only. Shaded bars represent groups pre-treated with 2CA before LPS exposure. **P<0.005, ***P≤0.0002, $^{\#\#}$P<0.001, n.s. = not significant. n = 5 mice per group. **/##P<0.004, ***P<0.0001, Student's unpaired t-test.

4.3.20 Chemerin levels in human patients

We also investigated chemerin levels in sputum patients diagnosed with COPD. Chemerin was significantly increased in COPD patients (n = 12) compared to healthy subjects (n = 19) (**Figure 4-23A and B**), ($P<0.05$). COPD patients with a history of smoking had higher levels of chemerin in the sputum compared to healthy patients with or without a history of smoking.

These results indicate that increased chemerin levels detected in sputum was positively correlated to the number of pack years (of cigarette smoking) **(C)** and the number of isolated neutrophils **(E)**, negatively correlated to FEV_1 %predicted **(D)**, and not correlated to changes in number of macrophages **(F)**.

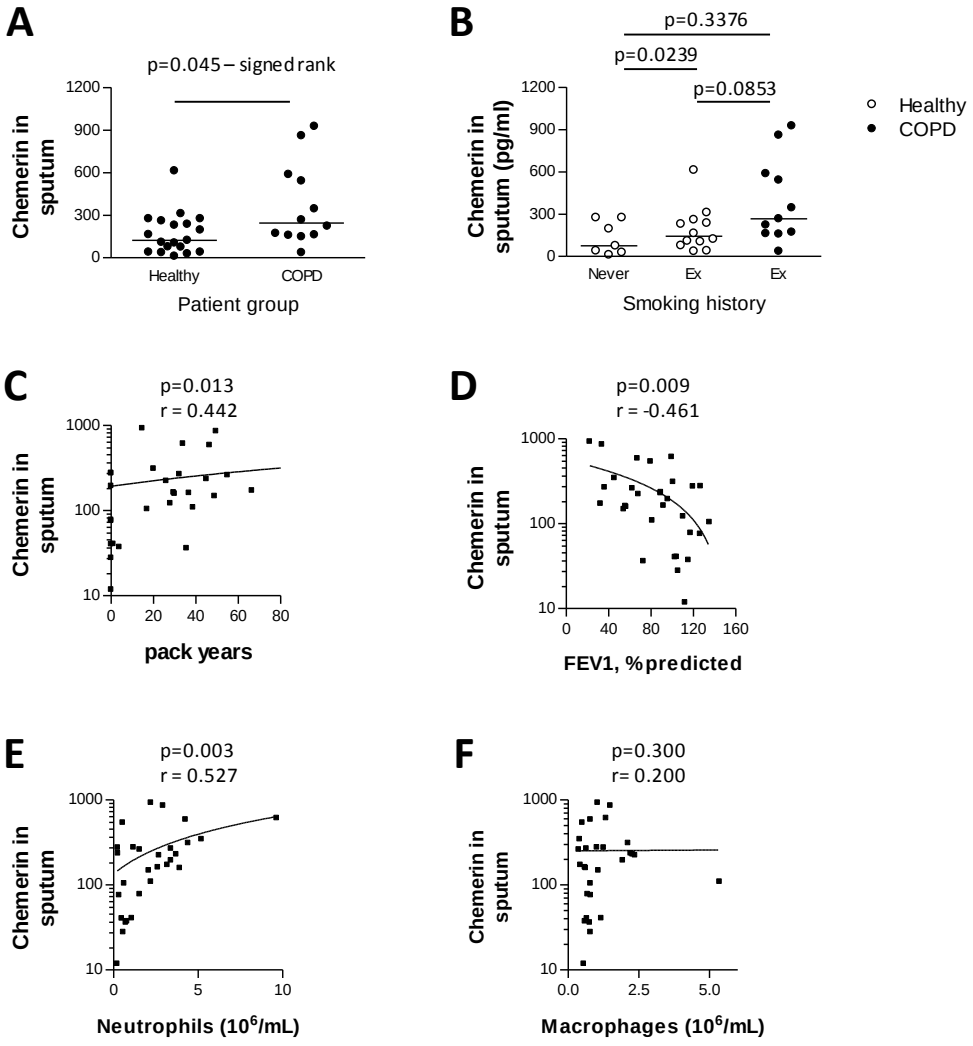

Figure 4-23: Chemerin production in human COPD patients and its correlation with markers of inflammation and lung function. (A and B) Chemerin was measured in human sputum samples taken from COPD patients or healthy controls. COPD patients were separated into those with a history of smoking and those without. Correlation of chemerin to pack years **(C)**, FEV1 % predicted **(D)**, number of neutrophils **(E)** and number of macrophages **(F)** was then determined. n = 7-12 patients per group.

4.4 Discussion

Cash *et al.,* (2008) demonstrated the relationship between chemerin and inflammation in a mouse model of emphysema. In their investigations, they showed that chemerin plays a proinflammatory role, but subsequent proteolytic cleavage of the active chemerin to smaller proteins may yield anti-inflammatory effects. We were intrigued by this novel finding and hence investigated whether similar observations would occur in our mouse models of emphysema. Specifically, we sought to determine whether administration of synthetic C15 peptide (a part of the full active chemerin protein), may attenuate LPS- or NTHi-induced hallmark features of emphysema, through inhibition of inflammatory cell influx to the lungs.

As pro-chemerin is ubiquitous and bioactive chemerin is only increased in concentration at inflammatory sites (after being cleaved by serine proteases) (Cash *et al.*, 2008; Yoshimura and Oppenheim, 2008), our initial experiments aimed to determine the levels of active chemerin protein present during the period of LPS exposure or NTHi challenge. Our results indicate that active chemerin is significantly increased in the lung from 6 hours after a single exposure to LPS until 72 hours later, peaking between 6 and 48 hours. A similar trend was observed when we investigated the concentration of chemerin present 24 and 48 hours after the last exposure to LPS in the 2 week aerosol model. In fact, the concentration of active chemerin detected is the same suggesting that

an increase in chemerin concentration may not be associated with continuous or repeated exposure to inflammatory stimuli. Chemerin was also shown to be significantly increased in the lung after challenge with NTHi. These data show that active chemerin is present and up-regulated in both of our mouse models of LPS- and NTHi-induced emphysema.

Cash *et al.* also demonstrated that C15 has very potent anti-inflammatory effects, and does not possess chemotactic activity (unlike chemerin). C15 was demonstrated to significantly reduce zymogen-induced peritoneal inflammation at picoMolar concentrations (optimum dose at 1pM) compared to the scrambled (control) peptide. Our initial experiments sought to determine whether the C15 peptide could inhibit LPS-induced inflammation (lung neutrophilia) in a dose dependent manner. However, initial observations indicated that the scrambled peptide also had an effect (Figure 4-1). Therefore the peptide was re-scrambled to avoid any common amino acid sequences.

The new scrambled peptide proved more suitable (Figure 4-5 and 4-6) as it did not induce any non-specific immune responses. We also determined that the optimal route of administration for SP or C15 was *via* an intravenous injection (Figure 4-6), as intraperitoneal administration resulted in a significant influx of inflammatory cells and intratracheal administration had no significant effect. A recent publication by Hart *et al* (2010) suggests that the effects of chemerin stems from within the blood capillaries giving rise to the chemoattractant

properties and movement of macrophages. This may suggest why our intratracheal administration route did not work as the C15 may not be able to pass the alveolar barrier to compete with active chemerin.

We then investigated whether treatment with C15 would attenuate LPS- or NTHi-induced emphysema. Mice treated with C15 had significantly reduced MLI, and percentage alveolar airspace compared to SP only treated mice (Figure 4-8). A similar result was observed in older mice confirming a key role in pathogenesis. Further, the lung volume between different groups was not significantly different, suggesting that a change in airway structure is not a result of an expanding or contracting lung.

We had previously shown that the number of macrophages in the lung increase over time during the 2 week aerosol model of LPS induced emphysema (Chapter 2, Figure 2-10B). We had also shown that neutrophils are transient in the lungs, peaking at 6 hours and resolving by 48 hours after the last LPS exposure. Thus, 24 hours after the last LPS exposure, we would expect to see elevated accumulation of macrophages and neutrophils. Indeed, treatment with C15 significantly attenuated the influx of macrophages and neutrophils into the lung following exposure to LPS (Figure 4-10A). We also determined the number of neutrophils and macrophages in the double NTHi challenge model 72 hours after the last challenge. Indeed, we once again saw a significant attenuation of

the number macrophages in the lungs of mice pre-treated with C15 (Figure 4-10B).

We now know that chemerin is up-regulated in LPS or NTHi treated mice. The cleaved by-product (as represented by C15), can inhibit LPS-induced inflammation and may be associated with attenuation of emphysema development. We next investigated the level of chemerin production and expression of its receptors in the lung. Both mRNA and protein expression for chemerin were increased following exposure to LPS, but were not significantly altered if mice were treated with C15 (Figure 4-11A and B). This suggests that expression and processing of pro-chemerin to active chemerin may be independent of the degree of inflammation

We also determined the mRNA level of the chemerin receptors ChemR23 and CCRL2. LPS-induced a significant increase in ChemR23 but was attenuated by approximately 50% following administration of C15. CCRL2 mRNA expression however, was not affected. While the reasons for these differences are not clear, it may be due to an overall decreased number of antigen presenting cells (such as macrophages) which are known to express ChemR23. CCRL2 has been shown to be up-regulated in macrophages upon stimulation but it is constitutively expressed on airway epithelial cells (Zabel *et al.*, 2008).

We then determined mRNA levels for LPS- or NTHi-induced proinflammatory cytokines. Lung tissue was collected 48 and 72 hours after the

last LPS exposure and mRNA expression levels for CCL3 (MiP-1α) and MMP-12 determined. mRNA for HMGB-1 was determined 48 hours after the final LPS exposure. While C15 had no apparent effect (Figure 4-12) we were able to show that mRNA levels for both MMP-12 and CCL3 were significantly higher at 48 hours compared to 72 hours after the last LPS exposure. These chemokines are therefore expressed prior to the peak of macrophage recruitment (72 hours after LPS exposure)

Surprisingly, there was a significant increase in the expression of MMP-12 mRNA 72 hours after final NTHi challenge (Figure 4-13A), which was significantly attenuated by pre-treatment with C15. Although C15 did not significantly reduce NTHi-induced CCL3 mRNA expression a trend to do so was observed. However, when we quantified CCL3 protein by ELISA, we observed a significant reduction in CCL3 protein in mice pre-treated with C15, compared to SP pre-treated mice. The attenuated CCL3 mRNA expression may have lead to the decreased influx of macrophages. The slight discrepancy in the level of significance could be due to the timing of mRNA and protein analysis (i.e. if we had the option of testing CCL-3 mRNA levels at an earlier time point, we may be able to observe C15 having a significant effect).

While it was unusual for C15 to have an effect in the NTHi model but not in the LPS model, the difference in observations could be attributed to the

different actual dose of LPS versus lipooligosaccharides on NTHi, and perhaps to an extent the method of delivery (aerosol vs intratracheal).

Having shown that C15 significantly attenuated LPS or NTHi-induced inflammation, up-regulation of proinflammatory cytokine mRNA expression and protein, as well as alveolar enlargement, we next sought to determine if C15 could attenuate LPS- or NTHi-induced apoptosis as described in Chapters 2 and 3. We initially investigated the mRNA expression levels for enzymes involved with ceramide production (e.g. ASmase, LASS-2, and NCdase) in the aerosol model of LPS-induced emphysema. Pre-treatment with C15 significantly attenuated LPS-induced ASmase mRNA expression as early as 24 hours after the final LPS exposure (Figure 4-14A) compared to mice pre-treated with SP. This was more apparent 48 hours but not 72 hours after LPS exposure. Again mRNA levels were observed to peaked at 48 hours.

It is of interest to note the increase in mRNA for ASmase compared to LASS-2 and NCdase. Both ASmase and LASS-2 are ceramide producing enzymes while NCdase breaks down ceramide. These enzymes amongst others in the ceramide synthesis pathway (described in Chapter 1, Figure 1) (Hannun and Obeid, 2008), act to keep the pathway in balance. Collectively, our data suggests that both LPS and NTHi induced a pro-ceramide profile where there is an over production of ceramide (increase in enzymes ASmases and LASS-2) which may push the system toward un-regulated apoptosis. Similarly, when C15 was

introduced prophylactically, there was a significant reduction of both ASmase and LASS-2 but no significant reduction of NCdase (Figure 4-14). This suggests that the balance for ceramide production may now be tipped back, resulting in decreasing ceramide levels and reducing the number of apoptotic cells.

Using IHC, we investigated the effects of C15 by semi-quantifying the number of ceramide positive macrophages in the lungs of mice first pre-treated with SP or C15, then exposed to LPS or NTHi. The lungs of mice pre-treated with C15 (Figure 4-16A, right image) had less alveolar macrophages stained positive for ceramide (dark brown stain) compared to mice pre-treated with SP. Results in Figure 4-16B and C show that C15 significantly attenuated the presence of ceramide positive macrophages in the parenchyma in both models of LPS- or NTHi-induced emphysema.

It is notable that there is a slight caveat here in that C15 inhibited the influx of macrophages which may contribute to the results observed. However, we are looking at the lungs 6 days after the last LPS exposure and 9 days after the last NTHi challenge. These time points were specifically chosen to allow time for the inflammatory response to resolve back to baseline.

We next determined the effect of C15 on LPS- or NTHi-induced caspase-3 activity in the lungs. Here we demonstrated that caspase-3 activity was elevated when mice were treated with LPS or NTHi, however this effect was attenuated if mice were pre-treated with C15. Interestingly, 24 hours after the last LPS

exposure or NTHi challenge, the level of caspase-3 activity detected in NTHi infected mice is an order of magnitude higher than mice exposed to LPS, suggesting the effects of recurrent bacterial exacerbations can indeed be highly detrimental to the integrity of the parenchyma. While C15 might not have a significant effect in reducing LPS-induced caspase-3 activity, there is an obvious trend nevertheless. Considering that NTHi treated mice have approximately 10 times the effect, it suggests that the difference in the LPS model could be significant if the dose of LPS is increased.

Collectively, we have now shown that C15 is effective in inhibiting LPS- or NTHi-induced emphysema, in part by inhibiting inflammatory cells infiltrating to the lungs (in particular neutrophils and macrophages). COPD and emphysema patients have difficulty in clearing bacterial infections as the bacteria have various methods of evading the host's immune system, either by hiding in the lower respiratory tract (Moller *et al.*, 1998), or altering surface constituents to evade the host's defense *via* mimicry (Pang *et al.*, 2008). It has also been demonstrated that clearance of NTHi from the mouse lung occurs within the first 4 days after infection (Toews *et al.*, 1984; Toews *et al.*, 1985; Pang *et al.*, 2008; Pang *et al.*, 2008). Thus, we sought to determine if bacterial clearance would be delayed in mice in which inflammation was inhibited due to treatment with C15. Our results indicated that by day 3, NTHi has almost been cleared in mice pre-treated with SP. In contrast, mice pre-treated with C15 still had approximately a 3 times higher bacterial load remaining in their lungs. The consequences of

decreased bacterial clearance may have consequences for use clinically (See general discussion).

The following experiments and data sets were undertaken as potential investigations to further study the effect of using C15 in variations of LPS- or NTHi-induced emphysema. COPD and especially emphysema are progressive diseases. Unfortunately, in most cases, disease is only identified after it has advanced to Stage II as per the GOLD standards. Exacerbations by infectious micro-organism continues to be rife and recurring, thus a continuous insult to the lung parenchyma occurs, driving disease progression.

Having established that prophylactic administration of C15 can attenuate LPS- or NTHi-induced emphysema, we next asked if therapeutic administration of C15 could also attenuate LPS or NTHi induced emphysema. The results demonstrated that administration of C15 only in the 2nd week of the 2 week LPS or NTHi models significantly attenuated induced alveolar enlargements (Figure 4-19). This data is promising, as it suggests that preventing or reducing the level of inflammation may potentially be beneficial in slowing disease progression.

We further evaluated our findings by determining the level of mRNA expression for enzymes related to ceramide production (ASmase, and LASS-2). The results demonstrated that therapeutic administration of C15 is also able to significantly attenuate LPS-induced increases in mRNA expression of ASmase and LASS-2, which reduces ceramide production and apoptosis.

In Chapter 2, we demonstrated that 1 week of LPS exposure does not induce emphysema, while in Chapter 3, we demonstrated a single exposure to NTHi is sufficient to induce emphysema of the same magnitude (MLI and percentage alveolar airspace) as that of the 2 week LPS aerosol model. Here, we attempt to mimic the conditions of an initial exposure to LPS, follow by a respiratory bacterial infection in a mouse model of experimental emphysema. Mice were exposed to aerosolised LPS in the first week, and then a single dose of NTHi in the second week. MLI measurements for the lung parenchyma were determined and the results indicated that a combined insult of LPS exposure followed by NTHi infection, induced significantly more damage to the parenchyma compared to LPS or NTHi alone (Figure 4-21).

We next sought to determine if specific inflammatory cell types were playing major roles. We had so far used C15 to inhibit the 2 major inflammatory cell types (neutrophils and macrophages). We asked if depletion of alveolar macrophages will protect mice from LPS-induced emphysema. We chose to deliver our drug of choice 2-chloroadenosine (2CA) intratracheally to the lungs of mice in a prophylactic manner (1 hour prior to each LPS exposure) (Kubota *et al.*, 1999; Takemura Y *et al.*, 2005). We then measured MLI, percentage alveolar airspace, macrophage depletion and caspase-3 activity from the lungs. Treatment with 2CA resulted in a reduction in alveolar macrophages by approximately 30%, a reduction in caspase-3 activity by approximately 50%, and abrogation of LPS-induced emphysema (Figure 4-22). The data overall suggests that alveolar

macrophages may be the pivotal cell to target in treatments aimed at slowing down the progression of emphysema. This is supported by findings in the literature that show a potential pathogenic role for macrophages in COPD ((Hautamaki *et al.*, 1997; Barnes, 2004; Minematsu *et al.*, 2011)

Chemerin levels in healthy human subjects were also compared to that of patients diagnosed with mild to severe COPD (patients sampled were generally at Stage II of the disease as per GOLD standards Chapter 1, Table 1-1. Some patients were at Stage 4 of the disease). Chemerin protein levels detected in the sputum of COPD patients were significantly higher compared to healthy controls (Figure 4-23). When the healthy subjects were split into those who had a history of smoking and those without, it was found that the healthy ex-smokers had significantly higher chemerin levels in the sputum compared to healthy non-smokers. This suggests that there were other factors involved with cigarette smoking which lead to a continued increase in the level of chemerin present.

The increase in the level of chemerin detected in sputum was also positively correlated with an increase in pack years (cigarette) and the number of neutrophils in the sputum (Figure 4-23). Increased chemerin was however negatively correlated with FEV_1 % predicted, a measurement of COPD onset (a lower FEV_1 % predicted, indicates a more severe case of COPD). There was however no significant correlation between Chemerin and the number of macrophages in the lung which differs from what is reported in the literature.

This may be due to our subject pool as these patients were from a neutrophilic asthma study where patients had a mild case of COPD (Stage II in general). This is seen in the FEV_1 % predicted data as most patients have more than 50% FEV_1, classified as COPD Stage II as per GOLD guidelines (GOLD, 2010).

In summary, we synthesised a 15 amino acid peptide (based on Cash and colleague's work), which was able to significantly attenuate LPS- or NTHi-induced hallmark features of emphysema in our mouse models. Our data collectively demonstrated that the development of LPS and NTHi-induced emphysema-like lesions occurs though increased inflammatory cells (neutrophils and macrophages), and this is associated with an increase in proinflammatory cytokines and chemokines associated with recruitment and activation of these inflammatory cells, in particular macrophages. The mechanisms responsible involve apoptosis as indicated by an increase in the expression of enzymes which drive ceramide production, increased ceramide detected in macrophages, as well as an increase in caspase-3 activity. These results (increased ceramide and caspase-3 activity) indicate that late phase apoptotic events are occurring. Interestingly, all studies demonstrated that C15 is effective and potent in low concentrations whether administered in a prophylactic or therapeutic manner.

Chapter 5

General Discussion and Conclusions

Chapter 5: General Discussion and Conclusions

Chronic obstructive pulmonary disease (COPD) is characterised by progressive and irreversible airway obstruction (Saetta *et al.*, 2001; Barnes, 2003). The disease is classified into four main stages based on the severity progression, and patient lung function (as determined by spirometry). Further specific characteristics of COPD separate it into 2 main categories of disease including (a) emphysema (enlargement of airspaces and destruction of lung parenchyma, loss of lung elasticity, and closure of small airways), and (b) chronic obstructive bronchitis (fibrosis and obstruction of small airways).

Emphysema is characterised by chronic inflammation and the destruction of the respiratory bronchioles, as well as the alveolar walls (Hogg, 2004). While multiple risk factors (such as host factors and environmental exposures) are associated with disease development, cigarette smoke has been shown to be one of the most significant risk factor (Taylor *et al.*, 2004). Yet cessation of smoking does not halt disease progression which gets worse as a person ages. In fact, emphysema is usually only diagnosed later in life (over the age of 40) and most patients, when first diagnosed are in Stage II of the disease already (GOLD, 2010).

COPD and emphysema patients have increased susceptibility to exacerbations from bacterial or viral infections (Moller *et al.*, 1998; Moghaddam *et al.*, 2008). Non-typeable *Haemophilus influenzae* (NTHi) is a common Gram negative bacteria isolated from COPD or emphysema patients suffering

exacerbations from bacterial infections. While the opportunistic NTHi causes no harm and resides in the upper airway of healthy adults, it colonises the lower respiratory airways in COPD and emphysema patients. The bacterium is thought to cause recurrent exacerbations. Studies in animal models suggests that once the bacteria colonise, they can alter their own surface molecules so as to inhibit bacterial clearance by the host's immune system (Sethi *et al.*, 2004; Pang *et al.*, 2008; Pang *et al.*, 2008; Moghaddam S.J. *et al.*, 2011). Gram negative bacteria produce endotoxins such as the common lipopolysaccharide (LPS) which can activate through Toll-like receptor 4 found on a variety of cell types (including epithelial cells and antigen presenting cells such as macrophages) (Miller *et al.*, 2009). LPS has also been detected in unusually high concentrations in the homes of smokers compared to non-smokers (Sebastian *et al.*, 2006).

The LPS expressed by NTHi is termed lipooligosacharride (LOS) and differs from common LPS in that it does not contain repeating 0-antigen units (Mandrell *et al.*, 1992). However, the common factor between LPS and LOS is active Lipid A, demonstrated to activate cells *via* the TLR4, MD-2 and CD14 complex (Poltorak *et al.*, 1998; Beutler and Poltorak, 2000; Park *et al.*, 2009). Activation of TLR4 by its ligand LPS had been demonstrated in multiple animal models to first signal through MyD88-Mal or TRIF-TRAM adaptor proteins, and then eventually activating the proinflammatory NF-κB pathway (Kawai *et al.*, 2001; Yamamoto *et al.*, 2002; Hoebe *et al.*, 2003; Yamamoto *et al.*, 2003). Activation of NF-κB leads to

the production of proinflammatory cytokines and chemokines involved with recruitment and activation of inflammatory cells.

In this thesis, we hypothesised that bacterial infections may be the driving force for the continued development of emphysema (even when external insults such as smoking have stopped). Specifically, LPS (or LOS) from gram-negative bacteria such as NTHi activates the immune system though TLR4, resulting in chronic inflammation, which may lead to the development of emphysema.

In Chapter 2, we developed a mouse model of LPS-induced emphysema. Based on the findings of Vernooy and colleagues (Vernooy *et al.*, 2002), we initially reproduced their results using intratracheal administration of LPS to mice. However, this model was time consuming and procedurally difficult. Thus, we generated a model which utilised aerosol delivery of LPS based on the works of Brass and colleagues (Brass *et al.*, 2004; Brass *et al.*, 2008). Hence, we repeated Vernooy's model using aerosolised LPS and demonstrated that the end results (enlargement of airways as determined by increased MLI) are comparable. We believe that the aerosol delivery technique is a closer representation of the exposure (inhalation) of humans to LPS from the environment (human breathes air and all included particulates). As Brass indicated, the dose of LPS administered through aerosol exposure approximates the amount of LPS inhaled from 25 cigarettes.

We next investigated the duration of LPS exposure required to induce pathological lesions in the lung. Surprisingly, while 1 week of exposure (mice were exposed twice) was not sufficient to induce significant changes to the MLI and percentage alveolar airspace, just 2 weeks of exposure (mice were exposed 4 times) was enough to induce the development of emphysematous-like lesions. The pathological changes we observed in the lung after 2 weeks exposure to LPS was comparable to that observed by Vernooy and colleagues after 8 weeks of exposure to LPS. This may not necessary exemplify the true inductive nature of emphysema in patients where the disease is progressive but it does provide a quantifiable endpoint of enlarged alveolar airspace and determination of pathogenic mechanisms. We also noted that the enlarged airspace was most likely due to a loss in parenchyma tissue rather than incomplete alveolarisation of the mouse lung at 8 weeks of age, as lung volumes did not change and 16 week old mice exhibited similar levels of enlargement. We also demonstrated other hallmark features of emphysema, including increased inflammation and irreversible loss of parenchyma.

LPS-induced inflammation was characterised by a rapid and sustained increase in lung neutrophils within 24 hours after the last LPS exposure. In contrast, alveolar macrophages peaked later, resulting in accumulation of the inflammatory cell in lung parenchyma. We also demonstrated that LPS-induced the down-regulation of CD11c on alveolar macrophages, an observation which

has not been reported previously in the literature. Further studies are required to determine whether these changes are permanent.

In Chapter 3, we developed a mouse model of NTHi-induced emphysema. There is virtually no published data available in relation to mouse models of NTHi-induced emphysema. The majority of studies looked at creating the condition (emphysema) through other means (such as administering elastase (Pang *et al.*, 2008)) to study the rate of bacterial clearance. The mouse model we generated was based on the 2 week LPS aerosol model (Chapter 2, section 2.2.2.2), and a re-infection model of NTHi-induced diseased (Chapter, 3, section 3.2.2.1). Mice were sacrificed at approximately the same age between the LPS and NTHi models for morphometric analysis of the lungs. We demonstrated that NTHi can induce emphysema in mice after just a single challenge (unlike LPS alone), however, our final model (that employed 2 challenges over 2 weeks) was more representative of recurring challenges.

Having established that both LPS and NTHi can induce the primary hallmark features of emphysema, i.e. alveolar enlargement, we then demonstrated that LPS-induced emphysema is an irreversible process, is MyD88-dependent (Chapter 2, Figure 2-7, 2-8), and that NTHi-induced emphysema is TLR4-dependent (Chapter 3, Figure 3-5). Collectively, we have shown that NTHi activates TLR4 and MyD88 to induce the loss of parenchymal tissue. However, our data also suggests that NTHi may induce emphysema through other

pathogen recognition receptors as TLR4 deficient mice were not completely protected from NTHi-induced disease, which agrees with investigations from other researchers (Wieland *et al.*, 2005; Månsson *et al.*, 2010; Moghaddam S.J. *et al.*, 2011).

In our studies in Chapter 3, we employed BALB/c TLR4$^{-/-}$ mice and age-matched BALB/c WT controls at 6 weeks of age instead of 8 weeks of age. This was because it had previously been demonstrated that TLR4 (and TLR2) play essential roles in alveolar structure maintenance (Taylor *et al.*, 2004; Zhang *et al.*, 2005; Williams *et al.*, 2007). In an interesting study of age-dependent onset of emphysema using C57BL/6 TLR-deficient mice, Lee and colleagues (2006) demonstrated that mice lacking TLR2, TLR4 or MyD88 (albeit to a lesser degree) develop emphysema spontaneously after the age of 8 weeks. The severity of disease worsened up to 16 weeks of age and was characterised by increased markers of oxidative stress in the lungs (Patty J. L. *et al.*, 2006). Our data in Figure 2-16 (Chapter 2) confirms similar findings in TLR-deficient mice on the BALB/c background. Both findings suggest that TLRs may play essential roles other than specific pathogen sensing and targeting them as a therapeutic approach may not be ideal.

After establishing our models of emphysema, we then investigated the underlying mechanisms responsible for the pathogenesis of COPD and emphysema and subsequent loss of lung parenchyma. Several possibilities have

been suggested and include 1) inflammation due to external factors (such as noxious particles from smoke); 2) a disruption of the balance between proteolytic and anti-proteolytic molecules that lead to the destruction of healthy lung parenchyma; 3) oxidative stress produced from excessive anti-oxidant defence mechanisms (or due to the loss of TLR functions as demonstrated by Patty Lee); and 4) disruption of the balance between apoptosis and replenishment of structural cells (Demedts *et al.*, 2006; Patty J. L. *et al.*, 2006).

The data presented in Chapters 2 and 3 outlines the presence of enhanced inflammation following LPS exposure or NTHi challenge, i.e. a significant influx of neutrophils and macrophages into the lungs, and an increase in proinflammatory cytokines (such as TNF-α, IL-1β, and IL-6) and macrophage specific chemokines (such as MMP-12, CCL3 (MiP-1α), and CCL-2 (MCP-1)) involved with recruitment and activation of these immune cells. Notably, mRNA expression of oxidative stress markers (Nox-3 and HMGB1) was not significantly altered between LPS or NTHi treated mice compared to control animals.

Given emerging literature and interest towards the idea of increased apoptosis in the lungs (Demedts *et al.*, 2006; Pierce *et al.*, 2007; Galani *et al.*, 2009) as well as new animal models of emphysema looking at stimulus induced apoptosis in the lungs (Kasahara *et al.*, 2000; Vernooy *et al.*, 2002; Petrache *et al.*, 2005; Brass *et al.*, 2008), we hypothesised that increased inflammation occurring during LPS- and NTHi-induced emphysema, may be driving an increase in

apoptotic events which causes the loss in parenchymal tissue. To determine this we investigated the presence of markers associated with apoptosis.

We looked at the production of ceramide and enzymes associated with its synthesis. Ceramide had been shown to play important regulatory roles in apoptosis, inflammation and angiogenesis (Hannun and Obeid, 2008), and has been shown to induce emphysema if administered to the lungs in mouse models (Petrache *et al.*, 2005). Enzymes involved in ceramide synthesis tightly regulate the pathway to maintain a balance required in normal conditions to get rid of dead or unwanted cells. However, a disruption or deregulation may allow disease states to form. Interestingly, while inflammatory cytokines such as TNF-α released by LPS stimulation can increase intracellular ceramide concentrations, it has also been shown to be negatively regulated by the same ceramide and ceramide 1-phosphate (Szczepan *et al.*, 2010).

On the other hand, TNF-α signals through different death ligand receptors such as TNF-R and TRAIL to induce apoptosis through activating different caspases such as caspase-8 and caspase-3. Caspase-3 finally activates caspase-activated DNAse which cleaves nuclear DNA content of cells undergoing full apoptosis (Tang and Kidd, 1998; Demedts *et al.*, 2006).

Our results from both Chapters 2 and 3 demonstrate that LPS- or NTHi-induced an increase in ceramide levels in macrophages (semi-quantified by IHC and confirmed by flow cytometry). qPCR studies also demonstrated that mRNA

expression of enzymes driving the production of ceramide in the synthesis pathway (ASmase and LASS-2) are increased. In particular, ASmase was increased up to 300 fold when compared to control mice, while neutral ceremidase, an enzyme which breaks down ceramide as a negative regulator is only mildly up-regulated. Caspase-3 activity was also found to be increased in mice exposed to LPS or NTHi. Together, these data suggest that the over-production of ceramide is responsible for an increase in apoptosis.

Cigarette smoking has been demonstrated to induce strong inflammatory responses and is one of the multiple factors inducing the onset of COPD and emphysema. However, even with cessation of smoking, the disease continues to progress relentlessly, exacerbated by recurring infections from bacteria and viruses, amongst other microorganisms. Current treatments aimed to reduce exacerbations include cessation of smoking (as mentioned), pulmonary rehabilitation, oxygen therapy, inhaler therapy, antibiotics and lung volume reduction surgery (GOLD, 2010). With regard to inhibiting the inflammatory response in human COPD and emphysema, inhaled corticosteroids are frequently the therapy of choice, as they are with asthma patients despite the fact that their success rate is low. This is because unlike asthma, inflammation in late stages of COPD is not suppressed even with high doses, especially for inflammation involving neutrophils (Barnes, 2003).

Studies on human emphysema, as well as from the multitude of animal models of emphysema induced through exposure to stimuli such as cigarette smoke, smoke extract, LPS, bacterial- or viral infection, and other substances (ceramide, elastase, VEGF inhibitors), have all demonstrated a common overly enhanced inflammatory response involving at least neutrophils and macrophages that leads to features of emphysema (Hautamaki *et al.*, 1997; Kasahara *et al.*, 2000; Vernooy *et al.*, 2002; Petrache *et al.*, 2005; Marwick *et al.*, 2006; Brass *et al.*, 2008). While no current treatments have been shown to slow the progression of COPD, these studies again strongly suggest that blocking inflammation may be beneficial for the treatment or delay of emphysema development. Clearly, a need for a broad-spectrum anti-inflammatory suppressant that induces few side effects is required.

In 2008, an interesting study by Cash and colleagues suggested an important role for chemerin in inflammation (Cash *et al.*, 2008). Chemerin was first identified and characterised as the natural ligand to its orphan G-protein-coupled receptor ChemR23 in 2003 (Wittamer *et al.*, 2003). However, since its identification, there has been little focus on chemerin and its role in inflammation, with the literature instead focusing on the origins of chemerin, which is from adipocytes. However, the study by Cash, which demonstrated strong chemotactic activities from active chemerin, and then strong anti-inflammatory properties of (theorised) cleaved by-products of chemerin, led to a huge increase in studies looking at the association between chemerin and

inflammatory responses. In their study, Cash and colleagues synthesised a peptide of 15 amino acids long (C15) that represents a part of the parent product, chemerin. The difference between Chemerin and C15 was that C15 was devoid of the chemotactic properties which chemerin exhibited. Instead, C15 had very potent anti-inflammatory properties, blocking the very cells that chemerin acts to draw to the site of inflammation. In particular, C15 successfully attenuated the influx of zymogen-induced neutrophils and macrophages.

This data demonstrated the potential of C15 to act as a broad spectrum anti-inflammatory treatment. In Chapter 4, we investigated whether the administration of C15 could attenuate LPS- or NTHi-induced emphysema through the inhibition of inflammation. We administered C15 in a prophylactic manner, prior to each LPS or NTHi exposure and found that C15 could indeed successfully attenuate (not fully inhibit) both LPS- or NTHi-induced influx of neutrophils and macrophages. More importantly, this treatment appeared to have reduced all the hallmark features of emphysema including preventing an increase in MLI and percentage alveolar airspace, inhibiting ceramide production (positively stained macrophages), reducing caspase-3 activity, and inhibiting the expression of enzymes that drive ceramide production (ASmase and LASS-2). Surprisingly, C15 treatment did not alter (i.e. lower) the expression of NCdase, the enzyme that breaks down ceramide to other by-products. This reverse in the balance of products in the ceramide synthesis pathway may be the main reason for the lower production of ceramide and hence less apoptosis occurring.

Further investigations into therapeutic administration of C15 yielded even more interesting results. From the LPS studies, we observed that a single week of exposure is insufficient to induce emphysema, and administration of C15 further attenuated inflammation in the second week. Observations made with our NTHi model are very exciting because we already know that a single exposure to NTHi will induce significant alveolar enlargement. However, therapeutic administration of C15 seemed not only able to protect mice from further damage by subsequent infections, but may also halt disease progression from the initial exposure. An article published (post thesis submission) by Churg et al (2011) cemented the need for treatments to be commenced not just at the start of the model, but as well as midway through a disease model in mice especially if it is meant as a model after human disease (Andrew C. *et al.*, 2011).

The C15 studies however pose some further questions. Attenuation of the inflammatory response (due to C15 treatment) resulted in delayed bacterial clearance following NTHi challenge. This may or may not be beneficial in patients and will require further investigations into any repercussions posed by the remaining bacteria. However, the benefits of retarding or stopping disease progression may be more worthwhile in the long term. It should still be noted that C15 did not fully abrogate the inflammatory response as there was still a significant increase in the number of neutrophils and macrophages in the lung, and these may play a potential role in bacterial clearance, albeit at a slower rate. The possibility of combined therapy such as uses of antibiotics that target

bacterial biosynthesis and or suppression of pro-inflammatory mediators (eg macrolides) (Duranti, 2010) would definitely be advantageous.

The final aim of these studies was to specifically target alveolar macrophages to determine their role in LPS-induced emphysema (Chapter 4). Clodronate is typically reported in the literature as the mechanism to deplete alveolar macrophages (or blood macrophages), however, for this to be effective the clodronate must be packaged into liposomes for delivery to the target macrophages. 2-chloroadenosine (2CA) however, is easily dissolved in saline, is effective in depleting macrophages, and has successfully been administered *via* different delivery methods (Kubota *et al.*, 1999; Kumar *et al.*, 2010) making it an easier treatment option. In our experiments, the prophylactic administration of 2CA successfully depleted alveolar macrophages (albeit incompletely). The effects of 2CA treatment were impressive as caspase-3 activity was reduced by half, and LPS-induced alveolar enlargement was completely abrogated (measured as MLI and percentage alveolar airspace).

We next investigated the signalling pathways activated as a result of C15 treatment. Initial reports regarding chemerin detailed activation *via* the ChemR23 receptor (Cash *et al.*, 2008; Yoshimura and Oppenheim, 2008), however this was soon superseded by the discovery of additional receptors for chemerin, termed CCRL2 and GPCR1 (Zabel *et al.*, 2008). It was demonstrated that the anti-inflammatory effects of C15 occur *via* the chemerin receptor,

ChemR23, suggesting that there would likely be competitive binding between Chemerin and C15 for their common receptor (Cash *et al.*, 2008; Cash *et al.*, 2010). Zabel's studies (2008) describe CCRL2 as a non-functional receptor which acts as a sink to concentrate chemerin at the site of inflammation, and may increase its chemo-attractant properties. These studies together provide a link between CCLR2, ChemR23, chemerin and inflammation. More recent findings by Cash and colleagues have shed more light on the pathways and interaction between chemerin, C15 and the receptors ChemR23 and CCRL2. They demonstrated that chemerin peptide (C15) can enhance phagocytosis by macrophages in a ChemR23- and Syk-dependent manner (Cash *et al.*, 2010). Their study also outlines potential roles neutrophils play in stimulus-induced apoptosis, as well as macrophages ingesting these apoptotic cells. Further studies from Hart and Greaves characterised the mechanism of how chemerin contributes to macrophage migration to sites of inflammation (Hart and Greaves, 2010). Figure 5-2 are suggestions on how (A) chemerin and (B) C15 may be interacting with macrophages and neutrophils, and signalling through ChemR23 and CCRL2 in the lung environment to induce or attenuate LPS-induced emphysema.

Collectively, these studies have resulted in the development of mouse models of acute LPS- or NTHi-induced emphysema, which can be further utilised for investigations into the mechanisms underlying the development of emphysema in humans. While certain human features may not be induced in the

LPS model (e.g.loss in lung function (we tried to measure lung function via the flexivent system but found no consistent data to support otherwise in our earlier/preliminary studies and decided not to further run lung function tests), increased lung volume, or continued loss of parenchymal tissue), other important hallmark features were observed, including increased alveolar enlargement (which is irreversible), increased inflammation, and increased markers of apoptosis (ceramide and active caspase-3). There were also typical increases in proinflammatory cytokines and chemokines involved with recruitment and activation of neutrophils, macrophages and other cells, as well as enzymes involved with ceramide synthesis. Furthermore, we were able to demonstrate that the novel peptide C15 (derived from the major proinflammatory protein chemerin), is devoid of chemotactic abilities, and has extremely potent and broad ranging anti-inflammatory properties. Both prophylactic and therapeutic administration of C15 was demonstrated to reduce LPS- and NTHi-induced inflammation, including a reduction in markers of apoptosis and emphysema development. This strongly suggests that C15 has immense potential perhaps as a form of anti-inflammatory therapy. However, further rigorous testing is required.

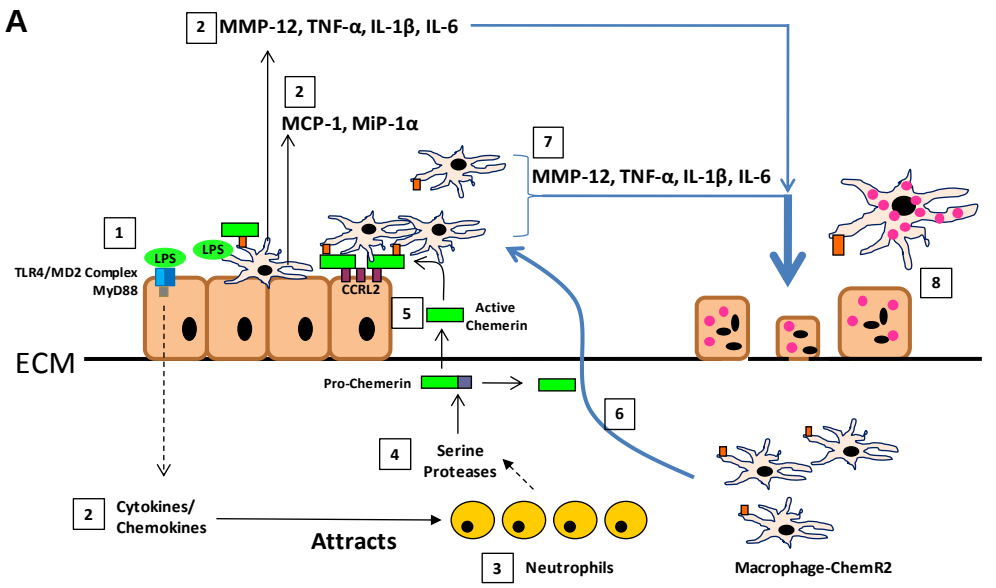
A
2 MMP-12, TNF-α, IL-1β, IL-6
2
MCP-1, MiP-1α
7
MMP-12, TNF-α, IL-1β, IL-6
1
LPS
LPS
TLR4/MD2 Complex
MyD88
CCRL2
5
Active
Chemerin
8
ECM
Pro-Chemerin
6
4
Serine
Proteases
2
Cytokines/
Chemokines
Attracts
3 Neutrophils
Macrophage-ChemR2

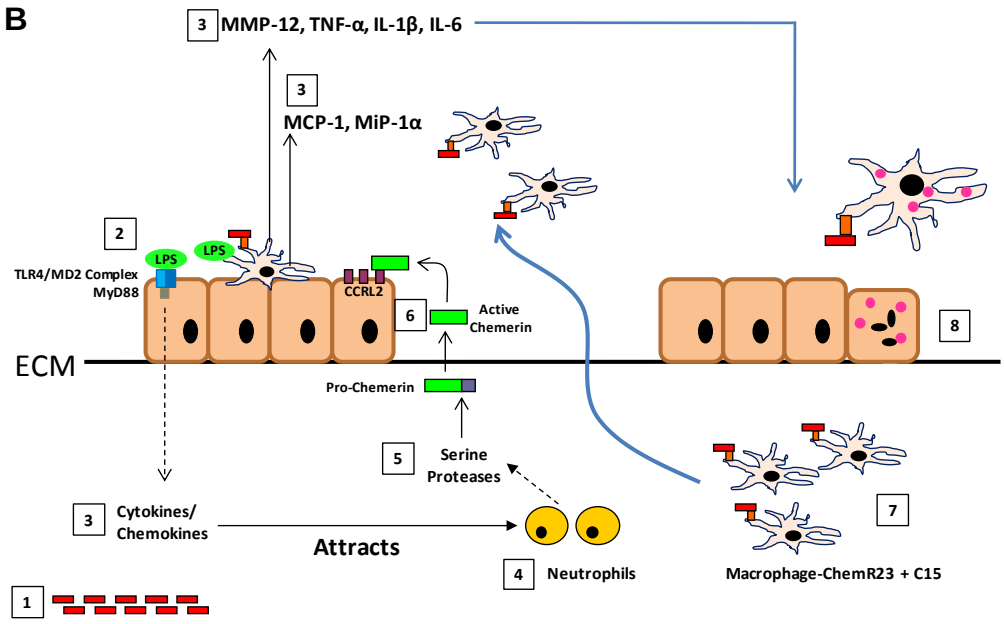
B
3 MMP-12, TNF-α, IL-1β, IL-6
3
MCP-1, MiP-1α
2
LPS
LPS
TLR4/MD2 Complex
MyD88
CCRL2
6
Active
Chemerin
8
ECM
Pro-Chemerin
5
Serine
Proteases
3
Cytokines/
Chemokines
Attracts
4 Neutrophils
7
Macrophage-ChemR23 + C15
1

FIGURE 5-2: Theorised interactions between chemerin, C15 and associated receptors.

(A) Model of LPS-induced lung inflammation. [1] Aerosolised LPS enters the lung and triggers TLR4-MD2 complex on TLR4 expressing cells (epithelial cells and alveolar macrophages). [2] Cytokines and chemokines that recruit and activate neutrophils and macrophages (MiP-1α, MCP-1, MMP-12, TNF-α, IL-1β, IL-6) are released from epithelial cells and alveolar macrophages. [3] Neutrophil activation occurs rapidly (within the first 24 hours) resulting in the release of serine proteases. [4] Serine proteases cleave ubiquitous inactive pro-chemerin into active chemerin. [5] Active chemerin binds to alveolar macrophages *via* ChemR23, or on CCRL-2 expressed by epithelial cells creating a region of high concentration. [6] Circulating monocytes or macrophages are attracted by proinflammatory chemokines (eg MiP-1α, MCP-1) which cross the extracellular matrix (ECM), possibly promoted by active chemerin (Hart and Greaves, 2010). Macrophages then migrate to epithelial/airway regions concentrated with chemerin due to the presence of ChemR23. [7] The proximity of macrophages and subsequent LPS stimulus triggers a further increase in cytokine production (eg MMP-12, TNF-α, IL-1β, IL-6) which is sufficient to induce apoptosis of the airway cells. [8] Cell debris from apoptosis are phagocytosed and cleared by alveolar macrophages (stained pink if using APAAP system to detect ceramide).

(B) Mechanism of action of C15-induced inhibition of inflammation [1] 2ng of C15 was first administered intravenously *via* the tail vein. C15 binds to the surface of cells expressing ChemR23. [2] Mice are exposed to LPS which activates the TLR4 signalling pathway in cells of the airway and proinflammatory cytokines and chemokines are released [3]. [4] The mechanisms of how C15 restricts or limits the influx of neutrophils is

unclear at this stage. [5] Serine proteases are released (presumably lesser quantities) and inactive pro-chemerin is cleaved to active chemerin which can now only bind to CCRL2. Presumably C15 has blocked ChemR23 on alveolar macrophages [6]. [7] Inflammatory macrophages and monocytes are attracted by proinflammatory cytokines but are not aided to cross the ECM by chemerin as the ChemR23 should also have been blocked by C15. Moreover, these infiltrated macrophages have been suggested to not remain at sites (lack of chemerin interactions) or concentrate on chemerin-CCRL2 sites (Hart and Greaves, 2010). This potentially decreases the impact of inflammatory macrophages. [8] Lowered apoptotic events leads to less loss of alveolar tissue.

References

References

Abramoff, M. D., P. J. Magelhaes and S. J. Ram (2004). "Image Processing with ImageJ." Biophotonics International **11**(7): 36-42.

Akira, S. and T. K. (2004). "Functions of toll-like receptors: lessons from KO mice." Comptes Rendus Biologies **327**(6): 581-589.

Andrew C., Don D.S. and J. L. Wright (2011). "Everything Prevents Emphysema: Are animal Models of Cigarette Smoke-Induced COPD Any Use?" Am. J. Respir. Cell Mol. Biol.

Atochina-Vasserman, E. N., M. F. Beers, H. Kadire, Y. Tomer, A. Inch, P. Scott, C. J. Guo and A. J. Gow (2007). "Selective inhibition of inducible NO Synthase activity in vivo reverses inflammatory abnormalities in surfactant protein D-deficient mice." The Journal of Immunology **179**(12): 8090-8097.

Bang BR, Chun E, Shim EJ, Lee HS, Lee SY, Cho SH, Min KU, Kim YY and P. HW. (2011). "Alveolar macrophages modulate allergic inflammation in a murine model of asthma." Exp Mol Med.: [Epub ahead of print].

Barnes, P. (2004). "Alveolar macrophages as orchestrators of COPD." COPD **1**: 59-70.

Barnes, P. J. (2003). "New concepts in Chronic Obstructive Pulmonary Disease." Annual Review of Medicine **54**: 113-129.

Beutler, B. and A. Poltorak (2000). "Review: The search for Lps: 1993—1998." Journal of Endotoxin Research **6**(4): 269-293.

Bhalla, D. K., F. Hirata, A. K. Rishi and C. G. Gairola (2009). "Cigarette smoke, inflammation, and lung injury: A Mechanistic Perspective." Journal of Toxicology and Environmental Health, Part B: Critical Reviews **12**(1): 45-64.

Bozaoglu, K., K. Bolton, J. McMillan, P. Zimmet, J. Jowett, G. Collier, K. Walder and D. Segal (2007). "Chemerin is a novel adipokine associated with obesity and Metabolic Syndrome." Endocrinology **148**(10): 4687-4694.

Bracke, K. R., A. I. D'hulst, T. Maes, K. B. Moerloose, I. K. Demedts, S. Lebecque, G. F. Joos and G. G. Brusselle (2006). "Cigarette smoke-induced pulmonary inflammation and emphysema are attenuated in CCR6-deficient Mice." The Journal of Immunology **177**(7): 4350-4359.

Brass, D. M., J. W. Hollingsworth, M. Cinque, Z. Li, E. Potts, E. Toloza, W. M. Foster and D. A. Schwartz (2008). "Chronic LPS inhalation causes emphysema-like changes in mouse lung that are associated with apoptosis." Am. J. Respir. Cell Mol. Biol. **39**(5): 584-590.

Brass, D. M., J. D. Savov, G. S. Whitehead, A. B. Maxwell and D. A. Schwartz (2004). "LPS binding protein is important in the airway response to inhaled endotoxin." Journal of Allergy and Clinical Immunology **114**(3): 586-592.

BRF-JCSMR-ANU (2008). "Peptide Synthesis." from http://brf.jcs.anu.edu.au/services/Peptidesynthesis/pepsynthmain.php.

Campbell, E. L., N. A. Louis, S. E. Tomassetti, G. O. Canny, M. Arita, C. N. Serhan and S. P. Colgan (2007). "Resolvin E1 promotes mucosal surface clearance of neutrophils: a new paradigm for inflammatory resolution." The FASEB Journal **21**(12): 3162-3170.

Cash, J. L., A. R. Christian and D. R. Greaves (2010). "Chemerin peptides promote phagocytosis in a ChemR23- and Syk-dependent manner." The Journal of Immunology **184**(9): 5315-5324.

Cash, J. L., R. Hart, A. Russ, J. P. C. Dixon, W. H. Colledge, J. Doran, A. G. Hendrick, M. B. L. Carlton and D. R. Greaves (2008). "Synthetic chemerin-derived peptides suppress inflammation through ChemR23." The Journal of Experimental Medicine **205**(4): 767-775.

Chin, C. L., L. J. Manzel, E. E. Lehman, A. L. Humlicek, L. Shi, T. D. Starner, G. M. Denning, T. F. Murphy, S. Sethi and D. C. Look (2005). "Haemophilus influenzae from patients with Chronic Obstructive Pulmonary Disease exacerbation induce more inflammation than colonizers." Am. J. Respir. Crit. Care Med. **172**(1): 85-91.

Claycombe, K. J., D. Wu, M. Nikolova-Karakashian, A. B. H. Palmer, K. E. Paulson and S. N. Meydani (2002). "Ceramide mediates age-associated increase in macrophage cyclooxygenase-2 expression." J Biol Chem **277**(34): 30784-30791.

Covert, M. W., T. H. Leung, J. E. Gaston and D. Baltimore (2005). "Achieving stability of lipopolysaccharide-induced NF-kappaB activation." Science. **309**(5742): 1854-1857.

Cua, D. J., J. Sherlock, Y. Chen, C. A. Murphy, B. Joyce, B. Seymour, L. Lucian, W. To, S. Kwan, T. Churakova, S. Zurawski, M. Wiekowski, S. A. Lira, D. Gorman, R. A. Kastelein and J. D. Sedgwick (2003). "Interleukin-23 rather than interleukin-12 is the critical cytokine for autoimmune inflammation of the brain." Nature **421**(6924): 744-748.

D'hulst, A. I., K. R. Bracke, T. Maes, J. L. De Bleecker, R. A. Pauwels, G. F. Joos and G. G. Brusselle (2006). "Role of tumour necrosis factor-α receptor p75 in cigarette smoke-induced pulmonary inflammation and emphysema." European Respiratory Journal **28**(1): 102-112.

Daheshia, M. (2005). "Therapeutic inhibition of matrix metalloproteinases for the treatment of chronic obstructive pulmonary disease (COPD)." Curr Med Res Opin. **21**(4): 587-594.

Daley, J. M., A. A. Thomay, M. D. Connolly, J. S. Reichner and J. E. Albina (2008). "Use of Ly6G-specific monoclonal antibody to deplete neutrophils in mice." Journal of Leukocyte Biology **83**(1): 64-70.

De Yang, Gonzalo de la R., Poonam T. and J. J. Oppenheim (2009). "Alarmins link neutrophils and dendritic cells." Trends Immunol **30**(11): 531-537.

DeMaria, T., M. Apicella, W. Nichols and E. Leake (1997). "Evaluation of the virulence of nontypeable Haemophilus influenzae lipooligosaccharide htrB and rfaD mutants in the chinchilla model of otitis media." Infect. Immun. **65**(11): 4431-4435.

Demedts, I., T. Demoor, K. Bracke, G. Joos and G. Brusselle (2006). "Role of apoptosis in the pathogenesis of COPD and pulmonary emphysema." Respiratory Research **7**(1): 53.

Diebold SS, Kaisho T, Hemmi H, Akira S. and R. e. S. C (2004). "Innate antiviral responses by means of TLR7-mediated recognition of single-stranded RNA." Science **303**(5663): 1529-1531.

Doggrell, S. A. (2006). "Ceramide as a target in emphysema." Expert Opinion on Therapeutic Targets **10**(1): 191-194.

Doz, E., N. Noulin, E. Boichot, I. Guénon, L. Fick, M. Le Bert, V. Lagente, B. Ryffel, B. Schnyder, V. F. J. Quesniaux and I. Couillin (2008). "Cigarette smoke-induced pulmonary inflammation is TLR4/MyD88 and IL-1R1/MyD88 signaling dependent." The Journal of Immunology **180**(2): 1169-1178.

Duranti, R. (2010). "Long-Term Treatment with Macrolides - Light in the Darkness of COPD Therapy?" Respiration. **80**(6): 441-442.

E.M. Pålsson-McDermott and L. A. J. O'Neill. (2007). "Building an immune system from nine domains." Biochemical Society Transactions **35**(6): 1437–1444.

Ferwerda, G., F. Meyer-Wentrup, B.-J. Kullberg, M. G. Netea and G. J. Adema (2008). "Dectin-1 synergizes with TLR2 and TLR4 for cytokine production in human primary monocytes and macrophages." Cellular Microbiology **10**(10): 2058-2066.

Galani, V., E. Tatsaki, M. Bai, P. Kitsoulis, M. Lekka, G. Nakos and P. Kanavaros (2009). "The role of apoptosis in the pathophysiology of Acute Respiratory Distress Syndrome (ARDS): An up-to-date cell-specific review." Pathology - Research and Practice **206**(3): 145-150.

Galdiero, M., M. Galdiero, E. Finamore, F. Rossano, M. Gambuzza, M. R. Catania, G. Teti and a. G. M. A. Midiri (2004). "Haemophilus influenzae porin induces Toll-like receptor 2-mediated cytokine production in human monocytes and mouse macrophages. ." Infect. Immun.(72): 1204–1209.

GOLD (2005). "GOLD Report 2005." from http://www.goldcopd.org/.

GOLD (2010). "GOLD Report 2010." from http://www.goldcopd.org/.

Guillot, L., S. Medjane, K. Le-Barillec, V. Balloy, C. Danel, M. Chignard and M. Si-Tahar (2003). "Response of human pulmonary epithelial cells to LPS involves toll-like receptor 4 (TLR4)-dependent signaling pathways:Evidence for an intracellular compartmentalization of TLR4." J Biol Chem **279**(4): 2712-2718.

Hannun, Y. A. and L. M. Obeid (2008). "Principles of bioactive lipid signalling: lessons from sphingolipids." Nat Rev Mol Cell Biol **9**(2): 139-150.

Hansen, M. J., R. C. Gualano, S. Bozinovski, R. Vlahos and G. P. Anderson (2006). "Therapeutic prospects to treat skeletal muscle wasting in COPD (chronic obstructive lung disease)." Pharmacol Ther. **109**(1-2): 162-172.

Hart, R. and D. R. Greaves (2010). "Chemerin contributes to inflammation by promoting macrophage adhesion to VCAM-1 and fibronectin through clustering of VLA-4 and VLA-5." The Journal of Immunology **185**(6): 3728-3739.

Hasday, J. D., R. Bascom, J. J. Costa, T. Fitzgerald and W. Dubin (1999). "Bacterial endotoxin is an active component of cigarette smoke." Chest **115**(3): 829-835.

Hautamaki, R. D., D. K. Kobayashi, R. M. Senior and S. D. Shapiro (1997). "Requirement for macrophage elastase for cigarette smoke-induced emphysema in mice." Science **277**(5334): 2002-2004.

Hillier J, G. C. (2004). "Anaesthesia for lung volume reduction surgery." Anaesthesia **59**(4): 409.

Hoebe, K., X. Du, P. Georgel, E. Janssen, K. Tabeta, S. O. Kim, J. Goode, P. Lin, N. Mann, S. Mudd, K. Crozat, S. Sovath, J. Han and B. Beutler (2003). "Identification of Lps2 as a key transducer of MyD88-independent TIR signalling." Nature **424**(6950): 743-774.

Hogg, J. C. (2004). "Pathophysiology of airflow limitation in chronic obstructive pulmonary disease." The Lancet **364**(9435): 709-721.

Hogg, J. C., F. Chu, S. Utokaparch, R. Woods, W. M. Elliott, L. Buzatu, R. M. Cherniack, R. M. Rogers, F. C. Sciurba, H. O. Coxson and P. D. Pare (2004). "The nature of small-airway obstruction in chronic obstructive pulmonary disease." N Engl J Med **350**(26): 2645-2653.

Horvat, J. C., M. R. Starkey, R. Y. Kim, K. W. Beagley, J. A. Preston, P. G. Gibson, P. S. Foster and P. M. Hansbro (2010). "Chlamydial respiratory infection during allergen sensitization drives neutrophilic allergic airways disease." The Journal of Immunology **184**(8): 4159-4169.

Imler, J.-L. and L. B. Zheng (2004). "Biology of Toll receptors: lessons from insects and mammals." J Leukoc Biol **75**(1): 18-26.

Ismail, H. F., P. Fick, J. Zhang, R. G. Lynch and D. J. Berg (2003). "Depletion of neutrophils in IL-10-/- mice delays clearance of gastric Helicobacter infection and decreases the Th1 immune response to Helicobacter." The Journal of Immunology **170**(7): 3782-3789.

J. T. Rosenbaum and R. B. Mandell (1983). "The effect of endotoxin and endotoxin tolerance on inflammation induced by mycobacterial adjuvant." Yale J Biol Med. **56**(4): 293–301.

Jeffery, P. K. (1998). "Structural and inflammatory changes in COPD: a comparison with asthma." Thorax **53**(2): 129-136.

Jiang, D., J. Liang, J. Fan, S. Yu, S. Chen, Y. Luo, G. D. Prestwich, M. M. Mascarenhas, H. G. Garg, D. A. Quinn, R. J. Homer, D. R. Goldstein, R. Bucala, P. J. Lee, R. Medzhitov and P. W.

Noble (2005). "Regulation of lung injury and repair by Toll-like receptors and hyaluronan." Nature Medicine **11**(11): 1173-1179.

Jiang, D., J. Liang and P. W. Noble (2007). "Hyaluronan in tissue injury and repair." Annual Review of Cell and Developmental Biology **23**(1): 435-461.

Jiang, D., J. Liang and P. W. Noble (2011). "Hyaluronan as an immune regulator in human diseases." Physiological Reviews **91**(1): 221-264.

Kambris, Z., Hoffmann J.A., I. Jean-Luc. and C. M. (2002). "Tissue and stage-specific expression of the Tolls in Drosophila embryos." Gene Expression Patterns **2**(3-4): 311-317.

Kasahara, Y., R. M. Tuder, L. Taraseviciene-Stewart, T. D. Le Cras, S. Abman, P. K. Hirth, J. Waltenberger and N. F. Voelkel (2000). "Inhibition of VEGF receptors causes lung cell apoptosis and emphysema." The Journal of Clinical Investigation **106**(11): 1311-1319.

Kawai, T., O. Takeuchi, T. Fujita, J. Inoue, P. F. Muhlradt, S. Sato, K. Hoshino and S. Akira (2001). "Lipopolysaccharide stimulates the MyD88-independent pathway and results in activation of IFN-regulatory factor 3 and the expression of a subset of lipopolysaccharide-inducible genes." J Immunol. **167**(10): 5887-5894.

Keatings, V. M., P. D. Collins, D. M. Scott and P. J. Barnes (1996). "Differences in interleukin-8 and tumor necrosis factor-alpha in induced sputum from patients with chronic obstructive pulmonary disease or asthma." Am. J. Respir. Crit. Care Med. **153**(2): 530-534.

Kubota, Y., Y. Iwasaki, H. Harada, I. Yokomura, M. Ueda, S. Hashimoto and M. Nakagawa (1999). "Depletion of alveolar macrophages by treatment with 2-Chloroadenosine aerosol." Clin. Diagn. Lab. Immunol. **6**(4): 452-456.

Kumar Mangalam, A., A. Aggarwal and S. Naik (2002). "Gold sodium thiomalate (GSTM) inhibits lipopolysaccharide stimulated tumor necrosis factor-alpha through ceramide pathway." Cell Immunol. **219**(1): 1-10.

Kumar, V., K. Harjai and S. Chhibber (2010). "2-Chloroadenosine (2-CADO) treatment modulates the pro-inflammatory immune response to prevent acute lung inflammation in BALB/c mice suffering from Klebsiella pneumoniae B5055-induced pneumonia." International Journal of Antimicrobial Agents **35**(6): 599-602.

Lazou, A., A. B. I., A. Egesten and K. Riesbeck. (2001). "Lipopolysaccharide-binding protein increases toll-like receptor 4-dependent activation by nontypeable Haemophilus influenzae." J. Infect. Dis. **184**(7): 926–930.

Li, P., D. Nijhawan, I. Budihardjo, S. M. Srinivasula, M. Ahmad, E. S. Alnemri and X. Wang (1997). "Cytochrome c and dATP-Dependent Formation of Apaf-1/Caspase-9 Complex Initiates an Apoptotic Protease Cascade." Cell **91**(4): 479-489.

Lindberg, A., B. Eriksson, L.-G. Larsson, E. Rönmark, T. Sandström and B. Lundbäck (2006). "Seven-Year Cumulative Incidence of COPD in an Age-Stratified General Population Sample*." Chest **129**(4): 879-885.

Maes, T., K. Bracke, K. Vermaelen, I. Demedts, G. Joos, R. Pauwels and G. Brusselle (2006). "Murine TLR4 Is Implicated in Cigarette Smoke-Induced Pulmonary Inflammation." Int Arch Allergy Immunol **141**: 354 - 368.

Mandrell, R. E., R. McLaughlin, Y. Aba Kwaik, A. Lesse, R. Yamasaki, B. Gibson, S. M. Spinola and M. A. Apicella (1992). "Lipooligosaccharides (LOS) of some Haemophilus species mimic human glycosphingolipids, and some LOS are sialylated." Infect. Immun. **60**(4): 1322-1328.

Månsson, A., J. Bogefors, A. Cervin, R. Uddman and L. O. Cardell (2010). "NOD-like receptors in the human upper airways: a potential role in nasal polyposis." Allergy **66**(5): 621-628.

Marwick, J. A., C. S. Stevenson, J. Giddings, W. MacNee, K. Butler, I. Rahman and P. A. Kirkham (2006). "Cigarette smoke disrupts VEGF165-VEGFR-2 receptor signaling complex in rat lungs and patients with COPD: morphological impact of VEGFR-2 inhibition." Am J Physiol Lung Cell Mol Physiol **290**(5): L897-908.

Medzhitov, R., P. Preston-Hurlburt and J. C. A. Janeway (1997). "A human homologue of the Drosophila Toll protein signals activation of adaptive immunity." Nature **388**(6640): 394-397.

Miller, Y. I., S.-H. Choi, L. Fang and R. Harkewicz (2009). "Toll-Like Receptor-4 and Lipoprotein Accumulation in Macrophages." Trends in Cardiovascular Medicine **19**(7): 227-232.

Minematsu, N., A. Blumental-Perry and S. D. Shapiro (2011). "Cigarette Smoke Inhibits Engulfment of Apoptotic Cells by Macrophages through Inhibition of Actin Rearrangement." Am. J. Respir. Cell Mol. Biol. **44**(4): 474-482.

Moghaddam S.J., Cesar E Ochoa, Sanjay Sethi and B. F. Dickey (2011). "Nontypeable Haemophilus influenzae in chronic obstructive pulmonary disease and lung cancer." Int J Chron Obstruct Pulmon Dis(6): 113–123.

Moghaddam, S. J., C. G. Clement, M. M. De la Garza, X. Zou, E. L. Travis, H. W. J. Young, C. M. Evans, M. J. Tuvim and B. F. Dickey (2008). "Haemophilus influenzae Lysate Induces Aspects of the Chronic Obstructive Pulmonary Disease Phenotype." Am. J. Respir. Cell Mol. Biol. **38**(6): 629-638.

Moller, Lieke V. M., W. I. M. Timens, W. I. M. van der Bij, K. O. R. Kooi, B. O. B. de Wever, J. Dankert and L. van Alphen (1998). "Haemophilus Influenzae in Lung Explants of Patients with End-stage Pulmonary Disease." Am. J. Respir. Crit. Care Med. **157**(3): 950-956.

Moran, A. P., M. M. Prendergast and B. J. Appelmelk (1996). "Molecular mimicry of host structures by bacterial lipopolysaccharides and its contribution to disease." FEMS Immunology & Medical Microbiology **16**(2): 105-115.

Mund, S. I., M. Stampanoni and J. C. Schittny (2008). "Developmental alveolarization of the mouse lung." Developmental Dynamics **237**(8): 2108-2116.

Murphy, T. F. and S. S. (1992). "Bacterial infection in chronic obstructive pulmonary disease." Am Rev Respir Dis. **146**(4): 1067-1083.

Murray, C. J. and A. D. Lopez. (1996). "Evidence-based health policy--lessons from the Global Burden of Disease Study." Science **274**(5288): 740-743.

Nagase, H., Okugawa S., Ota Y., Yamaguchi M., Tomizawa H., Matsushima K., Ohta K., Y. K. and H. K. (2003). "Expression and Function of Toll-Like Receptors in Eosinophils: Activation by Toll-Like Receptor 7 Ligand." J Immunol **171**(8): 3977-3982.

Nagase, H., Okugawa S., Ota Y., Yamaguchi M., Tomizawa H., Matsushima K., Ohta K., Yamamoto K. and Hirai K. (2003). "Expression and Function of Toll-Like Receptors in Eosinophils: Activation by Toll-Like Receptor 7 Ligand " J Immunol **171**(8): 3977-3982.

Napolitani, G., A. Rinaldi, F. Bertoni, F. Sallusto and A. Lanzavecchia (2005). "Selected Toll-like receptor agonist combinations synergistically trigger a T helper type 1-polarizing program in dendritic cells." Nat Immunol **6**(8): 769-776.

Noble, P. W. and D. Jiang (2006). "Matrix Regulation of Lung Injury, Inflammation, and Repair: The Role of Innate Immunity." Proc Am Thorac Soc **3**(5): 401-404.

O'Byrne P, M. and D. S. Postma (1999). "The many faces of airway inflammation. Asthma and chronic obstructive pulmonary disease. Asthma Research Group." Am. J. Respir. Crit. Care Med. **159**(5 Pt 2): S41-63.

O'Neill, L. A., K. A. Fitzgerald and A. G. Bowie (2003). "The Toll-IL-1 receptor adaptor family grows to five members." Trends Immunol. **24**(6): 286-290.

Pang, B., W. Hong, S. L. West-Barnette, N. D. Kock and W. E. Swords (2008). "Diminished ICAM-1 Expression and Impaired Pulmonary Clearance of Nontypeable Haemophilus influenzae in a Mouse Model of Chronic Obstructive Pulmonary Disease/Emphysema." Infect. Immun. **76**(11): 4959-4967.

Pang, B., D. Winn, R. Johnson, W. Hong, S. West-Barnette, N. Kock and W. E. Swords (2008). "Lipooligosaccharides Containing Phosphorylcholine Delay Pulmonary Clearance of Nontypeable Haemophilus influenzae." Infect. Immun. **76**(5): 2037-2043.

Park, B. S., D. H. Song, H. M. Kim, B.-S. Choi, H. Lee and J.-O. Lee (2009). "The structural basis of lipopolysaccharide recognition by the TLR4-MD-2 complex." Nature **458**(7242): 1191-1195.

Patty J. L., Xuchen Zhang, Peiying Shan, Ge Jiang and Lauren Cohn (2006). "Toll-like receptor 4 deficiency causes pulmonary emphysema." J Clin Invest **116**(11): 3050–3059.

Petrache, I., V. Natarajan, L. Zhen, T. R. Medler, A. T. Richter, C. Cho, W. C. Hubbard, E. V. Berdyshev and R. M. Tuder (2005). "Ceramide upregulation causes pulmonary cell apoptosis and emphysema-like disease in mice." Nat Med **11**(5): 491-498.

Pewzner-Jung, Y., S. Ben-Dor and A. H. Futerman (2006). "When Do Lasses (Longevity Assurance Genes) Become CerS (Ceramide Synthases)?" Journal of Biological Chemistry **281**(35): 25001-25005.

Pierce, J. D. D., ARNP, CCRN, J. M. PIERCE, RN, CNP, S. B. R. STREMMING, M. B. FAKHARI and R. L. P. CLANCY (2007). "The Role of Apoptosis in Respiratory Diseases." Clinical Nurse Specialist **21**(1): 22-28.

Poltorak, A., I. Smirnova, X. He, M.-Y. Liu, C. Van Huffel, D. Birdwell, E. Alejos, M. Silva, X. Du, P. Thompson, E. K. L. Chan, J. Ledesma, B. Roe, S. Clifton, S. N. Vogel and B. Beutler

(1998). "Genetic and Physical Mapping of theLpsLocus: Identification of the Toll-4 Receptor as a Candidate Gene in the Critical Region." Blood Cells, Molecules, and Diseases **24**(3): 340-355.

Rao, R. V., E. Hermel, S. Castro-Obregon, G. del Rio, L. M. Ellerby, H. M. Ellerby and D. E. Bredesen (2001). "Coupling Endoplasmic Reticulum Stress to the Cell Death Program." Journal of Biological Chemistry **276**(36): 33869-33874.

Robbesom, A. A., E. M. M. Versteeg, J. H. Veerkamp, J. H. J. M. van Krieken, H. J. Bulten, H. T. J. Smits, L. N. A. Willems, C. L. A. van Herwaarden, P. N. R. Dekhuijzen and T. H. van Kuppevelt (2003). "Morphological Quantification of Emphysema in Small Human Lung Specimens: Comparison of Methods and Relation with Clinical Data." Mod Pathol **16**(1): 1-7.

Roh, S.-g., S.-H. Song, K.-C. Choi, K. Katoh, V. Wittamer, M. Parmentier and S.-i. Sasaki (2007). "Chemerin--A new adipokine that modulates adipogenesis via its own receptor." Biochemical and Biophysical Research Communications **362**(4): 1013-1018.

Roth, M. (2008). "Pathogenesis of COPD. Part III. Inflammation in COPD [State of the Art Series. Chronic obstructive pulmonary disease in high- and low-income countries. Edited by G. Marks and M. Chan-Yeung. Number 3 in the series]." The International Journal of Tuberculosis and Lung Disease **12**: 375-380.

Saetta, M., G. Turato, P. Maestrelli, C. E. Mapp and L. M. Fabbri (2001). "Cellular and Structural Bases of Chronic Obstructive Pulmonary Disease." Am. J. Respir. Crit. Care Med. **163**(6): 1304-1309.

Samson, M., A. L. Edinger, P. Stordeur, J. Rucker, V. Verhasselt, M. Sharron, C. Govaerts, C. Mollereau, G. Vassart, R. W. Doms and M. Parmentier (1998). "ChemR23, a putative chemoattractant receptor, is expressed in monocyte-derived dendritic cells and macrophages and is a coreceptor for SIV and some primary HIV-1 strains." European Journal of Immunology **28**(5): 1689-1700.

Sarir, H., E. Mortaz, K. Karimi, A. Kraneveld, I. Rahman, E. Caldenhoven, F. Nijkamp and G. Folkerts (2009). "Cigarette smoke regulates the expression of TLR4 and IL-8 production by human macrophages." Journal of Inflammation **6**(1): 12.

Schipper, P. H., B. F. Meyers, R. J. Battafarano, T. J. Guthrie, G. A. Patterson and J. D. Cooper (2004). "Outcomes after resection of giant emphysematous bullae." The Annals of Thoracic Surgery **78**(3): 976-982.

Schnare M, Holt AC, Takeda K, A. S and M. R. (2000). "Recognition of CpG DNA is mediated by signaling pathways dependent on the adaptor protein MyD88." Current Biology **10**(18): 1139-1142.

Schweda, E. K. H., P.-E. Jansson, E. R. Moxon and A. A. Lindberg (1995). "Structural studies of the saccharide part of the cell envelope lipooligosaccharide from Haemophilus influenzae strain galEgalK." Carbohydrate Research **272**(2): 213-224.

Sean E. Hesselbacher, Robert Ross, Matthew B. Schabath, E. O'Brian Smith, Sarah Perusich, Nadia Barrow, Pamela Smithwick, Manoj J. Mammen, Harvey Coxson, Natasha Krowchuk, David B. Corry and F. Kheradmand (2011). "Cross-Sectional Analysis of the Utility of Pulmonary Function Tests in Predicting Emphysema in Ever-Smokers." Int J Environ Res Public Health. **8**(5): 1324-1340.

Sebastian, A., C. Pehrson and L. Larsson (2006). "Elevated concentrations of endotoxin in indoor air due to cigarette smoking." Journal of Environmental Monitoring **8**(5): 519-522.

Sethi, S., J. Maloney, L. Grove, C. Wrona and C. S. Berenson (2006). "Airway Inflammation and Bronchial Bacterial Colonization in Chronic Obstructive Pulmonary Disease." Am. J. Respir. Crit. Care Med. **173**(9): 991-998.

Sethi, S., C. Wrona, B. J. B. Grant and T. F. Murphy (2004). "Strain-specific Immune Response to Haemophilus influenzae in Chronic Obstructive Pulmonary Disease." Am. J. Respir. Crit. Care Med. **169**(4): 448-453.

Shapiro, S. D. and E. P. Ingenito (2005). "The pathogenesis of chronic obstructive pulmonary disease: advances in the past 100 years." Am. J. Respir. Cell Mol. Biol. **32**(5): 367-372.

Shinohara, M., K.-i. Hirata, T. Yamashita, T. Takaya, N. Sasaki, R. Shiraki, T. Ueyama, N. Emoto, N. Inoue, M. Yokoyama and S. Kawashima (2007). "Local Overexpression of Toll-Like Receptors at the Vessel Wall Induces Atherosclerotic Lesion Formation: Synergism of TLR2 and TLR4." Arterioscler Thromb Vasc Biol **27**(11): 2384-2391.

Shuto, T., H. Xu, B. Wang, J. Han, H. Kai, X. X. Gu, T. F. Murphy, D. J. Lim and J. D. Li. (2001). "Activation of NF-kappa B by nontypeable Hemophilus [sic] influenzae is mediated by toll-like receptor 2-TAK1-dependent NIKIKK alpha /beta-I kappa B alpha and MKK3/6-p38 MAP kinase signaling pathways in epithelial cells." Proc. Natl. Acad. Sci. USA **98**(15): 8774-8779.

Slee, E. A., M. T. Harte, R. M. Kluck, B. B. Wolf, C. A. Casiano, D. D. Newmeyer, H.-G. Wang, J. C. Reed, D. W. Nicholson, E. S. Alnemri, D. R. Green and S. J. Martin (1999). "Ordering the Cytochrome c–initiated Caspase Cascade: Hierarchical Activation of Caspases-2, -3, -6, -7, -8, and -10 in a Caspase-9–dependent Manner." The Journal of Cell Biology **144**(2): 281-292.

Sozzani, S., P. Allavena, G. D'Amico, W. Luini, G. Bianchi, M. Kataura, T. Imai, O. Yoshie, R. Bonecchi and A. Mantovani (1998). "Cutting Edge: Differential Regulation of Chemokine Receptors During Dendritic Cell Maturation: A Model for Their Trafficking Properties." The Journal of Immunology **161**(3): 1083-1086.

Szczepan, J., M. Czerkies, A. Łukasik, A. Bielawska, J. Bielawski, K. Kwiatkowska and A. Sobota (2010). "Ceramide and Ceramide 1-Phosphate Are Negative Regulators of TNF-α Production Induced by Lipopolysaccharide." The Journal of Immunology **185**(11): 6960-6973.

Szegezdi, E. V. A., U. N. A. Fitzgerald and A. Samali (2003). "Caspase-12 and ER-Stress-Mediated Apoptosis." Annals of the New York Academy of Sciences **1010**(1): 186-194.

Takemura Y, Iwasaki Y, Nagata K, Yokomura I, Tando S, Fushiki S and M. H. (2005). "Influence of depletion of alveolar macrophages on apoptosis in Candida-induced acute lung injury." Exp Lung Res. **31**(3): 307-321.

Tang, D. and V. J. Kidd (1998). "Cleavage of DFF-45/ICAD by Multiple Caspases Is Essential for Its Function during Apoptosis." Journal of Biological Chemistry **273**(44): 28549-28552.

Taylor, K. R., J. M. Trowbridge, J. A. Rudisill, C. C. Termeer, J. C. Simon and R. L. Gallo (2004). "Hyaluronan Fragments Stimulate Endothelial Recognition of Injury through TLR4

10.1074/jbc.M310859200." J. Biol. Chem. **279**(17): 17079-17084.

Toews, G. B., D. A. Hart and E. J. Hansen (1985). "Effect of systemic immunization on pulmonary clearance of Haemophilus influenzae type b." Infect. Immun. **48**(2): 343-349.

Toews, G. B., S. Viroslav, D. A. Hart and E. J. Hansen (1984). "Pulmonary clearance of encapsulated and unencapsulated Haemophilus influenzae strains." Infect. Immun. **45**(2): 437-442.

van de Veerdonk, F. L., B. J. Kullberg, J. W. M. van der Meer, N. A. R. Gow and M. G. Netea (2008). "Host-microbe interactions: innate pattern recognition of fungal pathogens." Current Opinion in Microbiology **11**(4): 305-312.

Vernooy, J. H. J., M. A. Dentener, R. J. van Suylen, W. A. Buurman and E. F. M. Wouters (2001). "Intratracheal Instillation of Lipopolysaccharide in Mice Induces Apoptosis in Bronchial Epithelial Cells . No Role for Tumor Necrosis Factor-{alpha} and Infiltrating Neutrophils." Am. J. Respir. Cell Mol. Biol. **24**(5): 569-576.

Vernooy, J. H. J., M. A. Dentener, R. J. van Suylen, W. A. Buurman and E. F. M. Wouters (2002). "Long-Term Intratracheal Lipopolysaccharide Exposure in Mice Results in Chronic Lung Inflammation and Persistent Pathology." Am. J. Respir. Cell Mol. Biol. **26**(1): 152-159.

Vuillemenot, B. R., J. F. Rodriguez and G. W. Hoyle (2004). "Lymphoid tissue and emphysema in the lungs of transgenic mice inducibly expressing tumor necrosis factor-alpha." Am. J. Respir. Cell Mol. Biol. **30**(4): 438-448

Warburton, D., J. Gauldie, S. Bellusci and W. Shi (2006). "Lung Development and Susceptibility to Chronic Obstructive Pulmonary Disease." Proc Am Thorac Soc **3**(8): 668-672.

Werner, S. L., D. Barken and A. Hoffmann (2005). "Stimulus specificity of gene expression programs determined by temporal control of IKK activity." Science **309**(5742): 1857-1861.

West, A. P., A. A. Koblansky and S. Ghosh (2006). "Recognition and Signaling by Toll-Like Receptors." Annual Review of Cell and Developmental Biology **22**(1): 409-437.

Wieland, C. W., S. Florquin, N. A. Maris, K. Hoebe, B. Beutler, K. Takeda, S. Akira and T. van der Poll (2005). "The MyD88-Dependent, but Not the MyD88-Independent, Pathway of TLR4 Signaling Is Important in Clearing Nontypeable Haemophilus influenzae from the Mouse Lung." J Immunol **175**(9): 6042-6049.

Wikén, M., J. Grunewald, A. Eklund and J. Wahlström (2009). "Higher Monocyte Expression of TLR2 and TLR4, and Enhanced Pro-inflammatory Synergy of TLR2 with NOD2 Stimulation in Sarcoidosis." Journal of Clinical Immunology **29**(1): 78-89.

Williams, A., S.-Y. Leung, P. Nath, N. Khorasani, P. Bhavsar, R. Issa, J. Mitchell, I. Adcock and K. Chung (2007). "Role of TLR2, TLR4 and MyD88 in ozone-induced airway hyperresponsiveness and neutrophilia." J Appl Physiol **103**: 1189 - 1195.

Wittamer, V., B. Bondue, A. Guillabert, G. Vassart, M. Parmentier and D. Communi (2005). "Neutrophil-Mediated Maturation of Chemerin: A Link between Innate and Adaptive Immunity." The Journal of Immunology **175**(1): 487-493.

Wittamer, V., J.-D. Franssen, M. Vulcano, J.-F. Mirjolet, E. Le Poul, I. Migeotte, S. Brézillon, R. Tyldesley, C. Blanpain, M. Detheux, A. Mantovani, S. Sozzani, G. Vassart, M. Parmentier and D. Communi (2003). "Specific Recruitment of Antigen-presenting Cells by Chemerin, a Novel Processed Ligand from Human Inflammatory Fluids." The Journal of Experimental Medicine **198**(7): 977-985.

Yamamoto, M., S. Sato, H. Hemmi, H. Sanjo, S. Uematsu, T. Kaisho, K. Hoshino, O. Takeuchi, M. Kobayashi, T. Fujita, K. Takeda and S. Akira (2002). "Essential role for TIRAP in activation of the signalling cascade shared by TLR2 and TLR4." Nature **420**(6913): 324-329.

Yamamoto, M., S. Sato, H. Hemmi, S. Uematsu, K. Hoshino, T. Kaisho, O. Takeuchi, K. Takeda and S. Akira (2003). "TRAM is specifically involved in the Toll-like receptor 4-mediated MyD88-independent signaling pathway." Nat Immunol. **4**(11): 1144-1150

Yoneyama, M., M. Kikuchi, T. Natsukawa, N. Shinobu, T. Imaizumi, M. Miyagishi, K. Taira, S. Akira and T. Fujita (2004). "The RNA helicase RIG-I has an essential function in double-stranded RNA-induced innate antiviral responses." Nat Immunol **5**(7): 730-737.

Yoshimura, T. and J. J. Oppenheim (2008). "Chemerin reveals its chimeric nature." The Journal of Experimental Medicine **205**(10): 2187-2190.

Yoshimura, T. and J. J. Oppenheim (2011). "Chemokine-like receptor 1 (CMKLR1) and chemokine (C-C motif) receptor-like 2 (CCRL2); Two multifunctional receptors with unusual properties." Experimental Cell Research **317**(5): 674-684.

Zabel, B. A., S. J. Allen, P. Kulig, J. A. Allen, J. Cichy, T. M. Handel and E. C. Butcher (2005). "Chemerin Activation by Serine Proteases of the Coagulation, Fibrinolytic, and Inflammatory Cascades." Journal of Biological Chemistry **280**(41): 34661-34666.

Zabel, B. A., S. Nakae, L. Zúñiga, J.-Y. Kim, T. Ohyama, C. Alt, J. Pan, H. Suto, D. Soler, S. J. Allen, T. M. Handel, C. H. Song, S. J. Galli and E. C. Butcher (2008). "Mast cell–expressed orphan receptor CCRL2 binds chemerin and is required for optimal induction of IgE-mediated passive cutaneous anaphylaxis." The Journal of Experimental Medicine **205**(10): 2207-2220.

Zhang, X., P. Shan, S. Qureshi, R. Homer, R. Medzhitov, P. Noble and P. Lee (2005). "Cutting edge: TLR4 deficiency confers susceptibility to lethal oxidant lung injury." J Immunol **175**: 4834 - 4838.

Zou, H., W. J. Henzel, X. Liu, A. Lutschg and X. Wang (1997). "Apaf-1, a Human Protein Homologous to C. elegans CED-4, Participates in Cytochrome c Dependent Activation of Caspase-3." Cell **90**(3): 405-413.

ZuWallack, R., C. F. Donner and R. Dahl (2005). "On the cutting edge of clinical pulmonary medicine in COPD." Respir Med **99**(Suppl B): S1-2 Epub.